



DOCTORAL PROGRAMME IN ELECTRONIC ENGINEERING DOCTORAL THESIS

“Machine Health Monitoring for Welding Guns: Early Detection
of Performance Issues in Resistance Welding”

Author:

Daniel Ibáñez Bordallo

Supervisor:

Dr.Eng. Jesús Soret Medel

Dr.Eng. Julio Martos Torres

Dr.Eng. Eduardo García Magraner

Universitat de València (UV)

Department of Electronic
Engineering

Valencia, Spain – December 2023

DECLARATION

D. Jesús Soret Medel , Doctor en Ingeniería Electrónica, Profesor Titular del Departamento de Ingeniería Electrónica de la Escola Tècnica Superior d'Enginyeria de la Universitat de València

D. Julio Martos Torres , Doctor en Ingeniería Electrónica, Profesor Titular del Departamento de Ingeniería Electrónica de la Escola Tècnica Superior d'Enginyeria de la Universitat de València

Y

D. Eduardo García Magraner, Doctor en Ingeniería Industrial y Producción Computacional , Manufacturing Manager Body & Stamping en Ford Motor Company

HACEN CONSTAR QUE:

D. Daniel Ibáñez Bordallo, Graduado en Ingeniería Electrónica Industrial y Máster en Ingeniería Electrónica, ha realizado bajo su dirección el trabajo titulado “Machine Health Monitoring for Welding Guns: Early Detection of Performance Issues in Resistance Welding”, que se presenta en esta memoria para optar al grado de Doctor por la Universitat de València. Y para que así conste a los efectos oportunos, y dando su conformidad para la presentación de este trabajo delante del Tribunal de Tesis Doctoral que corresponda, firma el presente certificado, en Valencia, a 15 de diciembre de 2023.

		<i>Eduardo García Magraner</i>
Fdo. D. Jesús Soret Medel	Fdo. D. Julio Martos Torres	Fdo. D. Eduardo García Magraner

NOTE TO THE READER

According to the regulations of the University of Valencia on doctoral studies, "Reglament sobre dipòsit, avaluació i defensa de la tesi doctoral. 31 d'octubre de 2017. (ACGUV 245/2017)," this PhD dissertation is presented as a compilation of at least three international scientific articles that show the results of the work developed. Additionally, in accordance with the aforementioned regulations and in order to facilitate the understanding of this PhD dissertation, it begins with an extended summary in the co-official languages of the University of Valencia (Spanish and Valencian). Therefore, this PhD dissertation begins on page one with a short abstract in English followed by the research context, motivation, objectives, theoretical fundamentals, methodology, results, conclusion, and future work.

RESUMEN

1. CONTEXTO DE LA INVESTIGACIÓN Y MOTIVACIÓN

La optimización de los procesos de producción se ha convertido en uno de los pilares fundamentales de la industria moderna. La búsqueda constante de reducción de costos, tanto en términos económicos como energéticos, así como la mejora de la calidad del producto final, ha llevado a una constante evolución y mejora de los procesos de producción en diversos sectores industriales. En este contexto, el análisis y la optimización de los procesos de producción son clave, a través de la identificación de factores críticos y el diseño de soluciones para mejorar la eficiencia y efectividad de dichos procesos. En este sentido, la soldadura por resistencia, uno de los procesos de unión más utilizados en la industria, es un área de gran interés para la optimización y la investigación de procesos.

Además, la creciente digitalización de los procesos de producción en la industria está permitiendo una mayor optimización y oportunidades de investigación en los procesos. La gran cantidad de datos generados en los procesos de producción, gracias al uso de sensores y sistemas de control, permite una mayor visibilidad y control de los procesos, así como la recopilación de datos en tiempo real que pueden ser analizados posteriormente. En este contexto, la soldadura por resistencia es un área de investigación que se beneficia enormemente de la digitalización, ya que permite una mejor monitorización del proceso y una mayor capacidad de análisis de datos. En este sentido, este estudio de doctorado se centra en la aplicación de técnicas avanzadas de análisis de datos para mejorar la eficiencia y la calidad de los procesos de soldadura por resistencia en la industria.

Por lo general, la investigación en el campo de la soldadura por resistencia se ha centrado en pruebas de laboratorio para encontrar parametrizaciones óptimas, métodos avanzados de predicción de

problemas de calidad, correlación entre parámetros y problemas de calidad, entre otros aspectos. Sin embargo, el principal obstáculo de estos estudios es que difícilmente se pueden implementar en una fábrica de alta producción debido a la falta de capacidad para la extracción y el análisis de datos, y la alta variabilidad en el proceso, en contraste con los estudios de laboratorio.

Dado este marco de referencia en este estudio de doctorado busca abordar un problema existente en la industria, que es el mantenimiento de los equipos utilizados en la soldadura por resistencia. Específicamente, se basa en la premisa de que, si el equipo está generando una soldadura correcta con una parametrización establecida, y el proceso no cambia, la calidad no debería cambiar. Sin embargo, los equipos utilizados en la soldadura por resistencia, como las pinzas de soldadura, tienen una vida útil, se desgastan y sufren averías. Por lo tanto, este estudio se centra en la detección de los desgastes que pueden aparecer en los equipos de soldadura a fin de detectar de manera precoz el fin de la vida útil del equipo, contribuyendo así a la mejora de la eficiencia y calidad en la producción industrial.

Por último, cabe señalar que este tesis doctoral ha sido desarrollado en un entorno industrial, utilizando datos adquiridos de líneas de producción reales. Todos los algoritmos y modelos matemáticos han sido desarrollados y validados utilizando datos de la industria

2. OBJETIVOS

En base al contexto y la motivación de investigación presentados en la sección anterior, el objetivo principal es mejorar la eficiencia y calidad de los procesos de soldadura por resistencia en la industria mediante la aplicación de técnicas avanzadas de análisis de datos. Específicamente, se busca detectar el final de la vida útil y el desgaste del equipo de soldadura antes de que causen problemas de calidad,

contribuyendo a la mejora de la eficiencia y calidad en la producción industrial.

El objetivo de investigación principal se puede subdividir en metas o hitos específicos que se espera lograr a lo largo del desarrollo de esta tesis doctoral. Estas metas específicas, también conocidas como "objetivos específicos", son esenciales para alcanzar el objetivo general de la investigación y sirven como una hoja de ruta para guiar el proceso de investigación. Las metas específicas de este trabajo de doctorado son las siguientes:

- O.E1.** Analizar y comprender más profundamente los parámetros que afectan la calidad de la soldadura y cómo estos se relacionan con problemas mecánicos comunes en las pinzas de soldadura. Esto nos permitirá comprender mejor el comportamiento de las líneas de producción basándonos en la experiencia de los operadores.
- O.E2.** Identificar las variables que están más influenciadas por el desgaste del electrodo para que, a través del análisis y monitoreo de estas variables, podamos determinar el estado de desgaste de los electrodos. El objetivo final es establecer un método para detectar variaciones en el desgaste del electrodo a través del análisis de datos.
- O.E3.** El desarrollo de un sistema de patrones para detectar el desalineamiento de electrodos en pinzas de soldadura utilizando modelos de simulación nos permitirá determinar cómo el desalineamiento afecta las magnitudes físicas que se ven modificadas por ello, como el campo magnético generado. Esto se validará mediante simulación.
- O.E4.** A partir de los hallazgos de **O.E3**, el objetivo es desarrollar un método y un dispositivo capaces de medir el estado de desalineamiento en las líneas de producción de soldadura. Esto

permitirá la implementación de los resultados obtenidos en **O.E3**.

- O.E5.** Analizando el comportamiento de la pinza de soldadura y el circuito de potencia de esta, determinar la existencia de puntos de pérdida de energía y, por lo tanto, desgaste en la pinza de soldadura. En última instancia, el objetivo es desarrollar un método para prevenir paradas en la línea y problemas de calidad causados por el desgaste de la pinza de soldadura.

3. METODOLOGÍA

Esta tesis doctoral se basa en un conjunto de publicaciones científicas sometidas a revisión por pares internacionales. En el cuerpo de la tesis se presentan un total de tres artículos publicados en revistas indexadas en el Journal Citation Reports (JCR) y tres artículos publicados en congresos internacionales. Cada uno de estos artículos muestra la investigación realizada para alcanzar los objetivos específicos enunciados en la sección anterior. La metodología de esta tesis doctoral se desarrolla en tres capítulos después de realizar una introducción a los conceptos clave de este tema (**Capítulo 2**). En primer lugar, en el **Capítulo 3** se presenta la primera publicación científica en revista y en el **Capítulo 4** se presenta la segunda publicación científica en revista, junto con las dos publicaciones en congresos que sirven de antecedentes a la publicación científica. Finalmente, se aborda la investigación publicada en el tercer artículo científico publicado en revista, junto con la contribución al congreso que sirve de antecedente a este tercer artículo científico (**Capítulo 5**).

Capítulo 3. Detection of poor electrode milling by means of unsupervised classification

En este capítulo se presenta el primer artículo científico sobre un nuevo método de clasificación no supervisado para detectar problema de fresado de los electrodos en la soldadura por puntos de resistencia,

dando respuesta al **O.E2**. El mal fresado de los electrodos puede causar problemas significativos de calidad al alterar la geometría de la cara activa del electrodo, afectando la entrega de energía al punto de soldadura y la distribución de fuerza. El método propuesto ofrece una solución a este problema al permitir la detección temprana del desgaste del electrodo, facilitando acciones correctivas oportunas y mejorando el control de calidad. Este capítulo detalla la metodología y los resultados del estudio, demostrando la efectividad del enfoque de clasificación no supervisado en la detección del desgaste del electrodo.

Los electrodos de pinzas de soldadura por resistencia son componentes críticos en las operaciones de soldadura, y su calidad es esencial para garantizar el éxito del proceso. Uno de los problemas significativos asociados con los electrodos de pinzas de soldadura es su desgaste debido al uso constante, lo que lleva a cambios en la geometría del electrodo. Como resultado, la uniformidad de la distribución de fuerza y corriente se ve afectada, lo que conduce a una disminución en la calidad de las soldaduras producidas. Por lo tanto, es esencial mantener la geometría del electrodo mediante un fresado adecuado para evitar estos problemas.

Garantizar un fresado adecuado es fundamental, ya que tiene un impacto directo en la geometría del electrodo y, en consecuencia, en la calidad de las soldaduras. Una geometría constante del electrodo garantiza una distribución uniforme de fuerza y corriente, lo que conduce a soldaduras de alta calidad. Sin embargo, un fresado inadecuado puede resultar en superficies de electrodo desiguales, lo que lleva a una distribución desigual de fuerza y corriente, resultando en soldaduras de mala calidad. Por lo tanto, para mantener una geometría constante del electrodo, es crucial garantizar un buen fresado.

Para detectar la calidad de los fresados de los electrodos de pinzas de soldadura por resistencia, se desarrolló un método de detección no supervisado. El método implica la recolección de datos de tensión y corriente de los electrodos después de cada fresado. Los datos

recopilados se someten a extracción de características para reducir el número de variables de entrada, y las variables finales de extracción de características se utilizan como entradas para el algoritmo K-means. La salida del algoritmo K-means se clasifica en tres grupos: 'ok', 'alarma' y 'pre-alarma'.

El grupo 'ok' indica que la calidad del fresado está dentro del rango aceptable, y no se requiere ninguna acción adicional. El grupo 'pre-alarma' indica que la calidad del fresado está por debajo del rango aceptable, y se requiere mantenimiento. Por último, el grupo 'alarm' indica que la calidad del fresado del electrodo se está deteriorando y se requiere mantenimiento de manera urgente

Capítulo 4. Real-time monitoring of electrode alignment

En este capítulo se presenta la investigación realizada para la de detección de desalineación de electrodos en la soldadura por resistencia puntual (RSW). La desalineación de los electrodos es un problema mecánico común que causa problemas de calidad, como soldaduras de tamaño insuficiente y uniones no redondeadas. En este capítulo se presentan dos contribuciones a congresos científicos y finalmente un artículo científico que muestran el trabajo desarrollado en esta línea de investigación.

La primera contribución presenta una propuesta inicial de un nuevo método para detectar la desalineación a través del análisis del campo magnético generado por los electrodos en cortocircuito. Este artículo proporciona un punto de partida para la investigación al discutir la importancia de la desalineación de electrodos como factor mecánico en la RSW y los problemas que causa, incluyendo el aumento de costos debido a reparaciones manuales. El artículo propone una solución novedosa para detectar la desalineación a través de la medición del campo magnético generado por los electrodos. El método se valida mediante simulación y se prueba en una línea de producción de automóviles.

La segunda contribución profundiza en la optimización del método y examina la robustez del campo magnético en los electrodos de soldadura mediante simulaciones. Este segundo artículo profundiza en el estudio del método propuesto mediante el análisis de la robustez del análisis del campo magnético en diferentes escenarios típicos de pinza de soldadura. El objetivo es determinar si otros problemas mecánicos en la pinza de soldadura podrían causar falsos positivos en la detección de la desalineación y hasta qué punto pueden ser detectados.

Finalmente, el artículo científico presenta una solución implementable para la detección de desalineaciones en líneas de producción industrial reales. El tercer artículo presenta una solución práctica para la detección de la desalineación de electrodos en un entorno industrial. El método para monitorear la alineación de los electrodos se desarrolla en base a investigaciones anteriores, que mostraron la relación entre la desalineación y el campo magnético generado por electrodos en cortocircuito. Se crea un dispositivo para medir el campo magnético y se implementa un sistema para la detección en tiempo real de desalineaciones. Este sistema establece umbrales de comportamiento basados en experimentación y permite el monitoreo de las condiciones después de cada ciclo de soldadura.

En general, los tres artículos contribuyen al avance de la comprensión y la solución del problema de la desalineación de electrodos en la RSW dando respuesta a los **O.E3** y **O.E4**. A través de esta investigación, se propone, prueba y demuestra una solución valiosa para la industria mediante un enfoque novedoso para detectar la desalineación.

Capítulo 5. Virtual sensor for the detection of wear in the secondary circuit of the welding gun

Este capítulo se presenta un nuevo método desarrollado para la detección del desgaste en el circuito secundario de las pinzas de soldadura por resistencia. En este capítulo se muestra la evolución de la investigación para llegar a una solución final a través de una contribución

a congreso internacional y un artículo científico. En primer lugar, se muestra la primera aproximación a la detección del desgaste a través del análisis del ciclo de trabajo del circuito de potencia del control de soldadura. El segundo artículo va más allá al agregar las variables de las resistencias secundarias mediante un sensor virtual, permitiendo la detección temprana del desgaste que ocurre en las pinzas de soldadura.

La detección del desgaste secundario de las pinzas de soldadura es fundamental para mantener la eficiencia y calidad de las operaciones de soldadura. La parte secundaria, que es la encargada de transferir la energía eléctrica desde el transformador al electrodo, está sujeta a un desgaste constante debido al calor y la presión que experimenta durante el proceso de soldadura. Por lo tanto, la detección del desgaste secundario es esencial para evitar posibles problemas como el aumento del consumo de energía, la disminución de la calidad y los frecuentes tiempos de inactividad.

Una de las principales razones para detectar el desgaste secundario es el impacto en el consumo de energía. A medida que el secundario se desgasta, la resistencia de contacto entre el electrodo y el secundario aumenta, lo que conduce a un mayor consumo de energía. Esto no solo aumenta los costes de producción, sino que también afecta al medio ambiente al producir más emisiones de carbono. Además, el desgaste secundario puede provocar una mala calidad de soldadura, lo que genera costes de reparación de los posibles defectos. De igual manera, una detección temprana del desgaste del secundario permite realizar los mantenimientos correctivos de forma programada, lo que reduce los paros de producción y retrasos en la producción.

Durante esta investigación, se han desarrollado dos artículos para explorar la importancia de detectar el desgaste en el secundario de las pinzas de soldadura. El primer artículo busca enfatizar la importancia de monitorear el desgaste secundario, destacando la importancia de mantener registros precisos del desgaste secundario y reemplazarlos cuando sea necesario para evitar tiempos de inactividad inesperados.

Este artículo muestra en primer lugar la correlación entre el desgaste secundario y el ciclo de trabajo del circuito de potencia del control de soldadura mediante la simulación del circuito eléctrico. Una vez establecida esta correlación, se propone un método inicial para la detección del desgaste secundario mediante la monitorización continua de la variable de control de los IGBT.

El segundo artículo se enfoca en optimizar el primer método para que se pueda detectar el desgaste de forma temprana, tratando de tener una detección lo antes posible del desgaste. En este artículo, partimos de la variable de control de los IGBTs para implementar un sensor virtual de las resistencias secundarias. Esto permite un análisis de la distancia de Mahalanobis entre ambas variables. Este nuevo método puede predecir el desgaste del operador secundario y alertar antes de que surja cualquier problema importante. Esta mejora puede ayudar a reducir el tiempo de inactividad y los costos al predecir cuándo es necesario reemplazar el secundario.

En conclusión, ambos un método real probado en una línea de producción para la detección del desgaste del electrodo en tiempo real, lo que permite reducir los costos de fabricación, evitando paradas y problemas de calidad, dando así respuesta al **O.E5**.

4. CONCLUSIÓN

Durante este estudio de doctorado, se desarrollaron diferentes líneas de investigación centradas en el monitoreo continuo de los diferentes parámetros que podrían afectar la calidad de la soldadura. Específicamente, la premisa fue que, en los procesos de producción, una variación en las condiciones de la máquina conduce a un aumento de problemas con la calidad del producto final. En el caso de la soldadura por resistencia, las pinzas de soldadura son responsables de realizar la unión soldada. Por lo tanto, los estudios realizados se centraron en detectar y reducir la variabilidad en el proceso, evitar el desgaste y detectar anomalías en el comportamiento.

Durante el estudio de doctorado, se desarrollaron principalmente tres líneas de investigación para lograr el objetivo establecido de optimizar el proceso de soldadura por resistencia. El **Capítulo 3** presenta la primera línea de investigación, que se centra en reducir la variabilidad que existe en el proceso de fresado, causando principalmente problemas en la calidad del punto de soldadura. Esta investigación presenta un método novedoso para detectar problemas de fresado y desgaste de electrodos utilizando métodos de agrupamiento no supervisados. A lo largo del artículo, se describe la relación entre los datos de resistencia en serie y la variación de las propiedades mecánicas de los electrodos. A pesar de trabajar con series de tiempo, se realizó la extracción de características para reducir la dimensionalidad, lo que permitió reducir el número de entradas para el algoritmo de agrupamiento. Esto también permitió escalar los datos de entrada para que no fueran influenciados por las diferencias de resistencia existentes en cada pinza de soldadura. Los principales avances obtenidos de esta investigación son: un método para detectar la relación entre las variables de soldadura y el estado de fresado, un sistema de alarma que establece estados de pre-alarma y operación correcta según la salida del algoritmo de agrupamiento, proporcionando una respuesta satisfactoria a la **O.E2**, y un sistema de recopilación de datos en una línea de soldadura que permite el análisis de datos en tiempo real, tanto para esta investigación como para las siguientes líneas de investigación. Esta línea de investigación también permitió la primera publicación en revistas científicas de alto impacto, como se muestra en el capítulo.

La segunda línea de investigación, presentada en el **Capítulo 4**, también se centró en detectar problemas mecánicos que generan problemas de calidad y paradas en las líneas de soldadura. Específicamente, la segunda línea de investigación tuvo como objetivo detectar el alineamiento de los electrodos. A lo largo de los tres artículos presentados en este capítulo, se ve la evolución tanto del método como del dispositivo capaz de aplicar el método en una línea de soldadura dura

real. Los tres artículos muestran el proceso seguido desde la idea inicial hasta la solución final implementada en una línea de soldadura real.

Esta línea de investigación logró relacionar la alineación de los electrodos y el campo magnético generado por las pinzas de soldadura para detectar defectos mecánicos en las líneas de producción de juntas soldadas mediante soldadura por resistencia. El estudio encontró que la desalineación de los electrodos causaba variaciones en el área de contacto y el campo magnético, que puede ser medido de manera fiable y económica. También se propuso un protocolo para enviar alarmas a través de LoRa al software de análisis de datos, con umbrales de alarma establecidos para determinar la desalineación.

En general, el artículo presenta una solución real al problema de las desalineaciones en las líneas de producción, con un método para la detección en tiempo real e integración fácil en la industria, cumpliendo los objetivos **O.E3** y **O.E4**.

Además, se destaca que este método propuesto de detección representa una mejora respecto a aquellos basados actualmente en visión, ya sea a través de la observación por parte de los operadores o utilizando sistemas de visión artificial. Esto se debe a que el método de detección propuesto tiene un costo de implementación más bajo y no está influenciado por la suciedad ambiental típica de la línea de soldadura. Esto hace que este método sea más preciso y confiable, ya que se basa en la medición directa del campo magnético generado por las pinzas de soldadura.

Finalmente, el **Capítulo 5** muestra la última de las líneas de investigación, que busca detectar otro problema mecánico como el desgaste en el circuito secundario de las pinzas de soldadura, es decir, el desgaste en los brazos de la pinza de soldadura. Esta línea de investigación se dividió en dos fases, representadas en los dos artículos publicados. En el primer artículo, se presenta un método efectivo para detectar el desgaste en el circuito secundario de las pinzas de soldadura por resistencia, lo que puede causar una disminución en la calidad de la

soldadura y un aumento en el consumo de energía en los procesos de soldadura por resistencia. Se ha demostrado a través de la simulación electrónica cómo el cambio en la relación entre la corriente y el ángulo de control es fácilmente demostrable. A partir de esta relación, se ha asumido que si se lleva a cabo un análisis histórico de los datos, se puede determinar un aumento en el desgaste en el circuito de soldadura. Este método se ha aplicado en una fábrica real, adaptando el estudio para la reducción de datos y simplificando el análisis y el envío de alarmas al personal de mantenimiento. A partir de los datos reales adquiridos en las líneas de producción, se ha validado que este método es viable y confiable para detectar problemas de desgaste en las líneas de soldadura a través del análisis del control del ángulo de cambio. Como continuación de este primer artículo, se presenta el segundo artículo como una mejora sobre el primero. Este artículo muestra un sistema que utiliza un sensor virtual que convierte las señales de corriente, voltaje y ciclo de trabajo en valores de soldadura y resistencia. Luego, se calcula la distancia de Mahalanobis entre ambas resistencias, y se envían alarmas a los operadores en función de esos valores.

El sistema fue probado en un estudio real en una fábrica de automóviles en la que se probaron 650 pinzas de soldadura. Los resultados mostraron que el sistema es capaz de detectar el desgaste incipiente de manera precisa y oportuna tanto en los brazos de la pinza como en la parte responsable de la soldadura (electrodos, portaelectrodos, etc.), lo que permite alcanzar el objetivo de **O.E5**.

Las principales ventajas obtenidas de esta línea de investigación presentada en el Capítulo 5 son que, en comparación con otros métodos de detección de desgaste, este método no depende de inspecciones visuales o mediciones realizadas por los operadores, por lo que no es necesario tener personal encargado de realizar estas acciones. Además, se basa en datos accesibles, lo que facilita su implementación en las fábricas. En segundo lugar, permite la detección de desgaste en tiempo real, lo que permite intervenir antes de que se produzcan fallas en las

pinzas de soldadura, a diferencia de los sistemas actuales basados en el mantenimiento periódico.

En conclusión, este estudio de doctorado presenta tres líneas de investigación destinadas a optimizar el proceso de soldadura por resistencia mediante la reducción de la variabilidad y la detección de problemas mecánicos que afectan la calidad del producto final. La primera línea de investigación se centra en la reducción de la variabilidad en el proceso de fresado mediante la detección de problemas de fresado y el desgaste del electrodo mediante métodos de clustering no supervisados. La segunda línea de investigación tiene como objetivo detectar el desalineamiento del electrodo, y la tercera línea de investigación se centra en la detección del desgaste en el circuito secundario de las pinzas de soldadura por resistencia.

Las principales contribuciones de este estudio de doctorado son el desarrollo de nuevos métodos para la detección de problemas mecánicos y la reducción de la variabilidad en el proceso de soldadura por resistencia. Estos métodos se han aplicado con éxito en entornos reales y han dado lugar a una mejora de la calidad de las juntas soldadas, una reducción del consumo de energía y un aumento de la eficiencia. Los métodos propuestos se basan en datos accesibles, lo que permite su fácil implementación en las fábricas, y permiten la detección en tiempo real de problemas mecánicos, lo que permite la intervención antes de que se produzcan fallas en las pinzas de soldadura. En general, este estudio de doctorado realiza importantes contribuciones al campo de la soldadura por resistencia y proporciona soluciones prácticas para mejorar la calidad y eficiencia de las líneas de producción.

RESUM

1. CONTEXT DE LA INVESTIGACIÓ I MOTIVACIÓ

L'optimització dels processos de producció s'ha convertit en un dels pilars fonamentals de la indústria moderna. La recerca constant de reducció de costos, tant en termes econòmics com energètics, així com la millora de la qualitat del producte final, ha portat a una constant evolució i millora dels processos de producció en diversos sectors industrials. En aquest context, l'anàlisi i l'optimització dels processos de producció són clau, a través de la identificació de factors crítics i el disseny de solucions per a millorar l'eficiència i efectivitat d'aquests processos. En aquest sentit, la soldadura per resistència, un dels processos d'unió més utilitzats en la indústria, és una àrea de gran interès per a l'optimització i la recerca de processos.

A més, la creixent digitalització dels processos de producció en la indústria està permetent una major optimització i oportunitats de recerca en els processos. La gran quantitat de dades generades en els processos de producció, gràcies a l'ús de sensors i sistemes de control, permet una major visibilitat i control dels processos, així com la recopilació de dades en temps real que poden ser analitzades posteriorment. En aquest context, la soldadura per resistència és una àrea de recerca que es beneficia enormement de la digitalització, ja que permet una millor monitorització del procés i una major capacitat d'anàlisi de dades. En aquest sentit, aquest estudi de doctorat es centra en l'aplicació de tècniques avançades d'anàlisi de dades per a millorar l'eficiència i la qualitat dels processos de soldadura per resistència en la indústria.

Per regla general, la recerca en el camp de la soldadura per resistència s'ha centrat en proves de laboratori per a trobar parametritzacions òptimes, mètodes avançats de predicció de problemes de qualitat, correlació entre paràmetres i problemes de qualitat, entre altres aspectes. No obstant això, l'obstacle principal d'aquests estudis és que

diffícilment es poden implementar en una fàbrica d'alta producció a causa de la falta de capacitat per a l'extracció i l'anàlisi de dades, i l'alta variabilitat en el procés, en contrast amb els estudis de laboratori.

En aquest context, aquest estudi de doctorat busca abordar un problema existent en la indústria, que és el manteniment dels equips utilitzats en la soldadura per resistència. Específicament, es basa en la premisa que si l'equip està generant una soldadura correcta amb una parametrització establerta, i el procés no canvia, la qualitat no hauria de canviar. No obstant això, els equips utilitzats en la soldadura per resistència, com les pinces de soldadura, tenen una vida útil, s'esgasten i pateixen avaries. Per tant, Aquest estudi es centra en la detecció dels desgastes que poden aparèixer en els equips de soldadura per a detectar de manera precoç el final de la vida útil de l'equip, contribuint així a la millora de l'eficiència i qualitat en la producció industrial.

Finalment, cal assenyalar que aquest estudi de doctorat s'ha desenvolupat en un entorn industrial, utilitzant dades adquirides de línies de producció reals. Tots els algorismes i models matemàtics han estat desenvolupats i validats utilitzant dades de la indústria.

2 OBJECTIUS

Basant-nos en el context i la motivació de la investigació presentats a la secció anterior, l'objectiu principal és millorar l'eficiència i qualitat dels processos de soldadura per resistència en la indústria mitjançant l'aplicació de tècniques avançades d'anàlisi de dades. Específicament, es busca detectar el final de la vida útil i l'ús dels equips de soldadura abans que causen problemes de qualitat, contribuint a la millora de l'eficiència i qualitat en la producció industrial.

L'objectiu de la investigació principal es pot subdividir en metes o fites específiques que s'espera aconseguir al llarg del desenvolupament de l'estudi de doctorat. Aquestes metes específiques, també conegudes com "objectius específics", són essencials per assolir l'objectiu general de la

investigació i serveixen com una guia per al procés d'investigació. Les metes específiques d'aquest estudi de doctorat són les següents:

- O.E1.** Analitzar i comprendre més profundament els paràmetres que afecten la qualitat de la soldadura i com aquests es relacionen amb problemes mecànics comuns en les pinces de soldadura. Això ens permetrà comprendre millor el comportament de les línies de producció basant-nos en l'experiència dels operadors.
- O.E2.** Identificar les variables que estan més influenciades per l'ús de l'elèctrode perquè, mitjançant l'anàlisi i monitoratge d'aquestes variables, puguem determinar l'estat d'ús dels electrods. L'objectiu final és establir un mètode per detectar variacions en l'ús de l'elèctrode mitjançant l'anàlisi de dades.
- O.E3.** El desenvolupament d'un sistema de patrons per detectar el desalineament d'elèctrodes en pinces de soldadura utilitzant models de simulació ens permetrà determinar com el desalineament afecta les variables físiques que es veuen modificades per ell, com el camp magnètic generat. Això es validarà mitjançant simulació.
- O.E4.** A partir dels resultats de **O.E3**, l'objectiu és desenvolupar un mètode i un dispositiu capaços de mesurar l'estat de desalineament en les línies de producció de soldadura. Això permetrà la implementació dels resultats obtinguts a **O.E3**.
- O.E5.** Analitzant el comportament de la pinza de soldadura i el circuit de potència de la mateixa, determinar l'existència de punts de pèrdua d'energia i, per tant, desgast en la pinza de soldadura. En última instància, l'objectiu és desenvolupar un mètode per a prevenir parades en la línia i problemes de qualitat causats pel desgast de la pinza de soldadura.

3 METODOLOGIA

Aquesta tesi doctoral es basa en un conjunt de publicacions científiques internacionals sotmeses a revisió per parells. En el cos de la tesi s'hi presenten un total de tres articles publicats en revistes indexades en el Journal Citation Reports (JCR) i tres articles publicats en congressos internacionals. Cadascun d'aquests articles mostra la investigació realitzada per assolir els objectius específics enunciats en la secció anterior. La metodologia d'aquesta tesi doctoral es desenvolupa en tres capítols després de realitzar una introducció als conceptes clau d'aquest tema (**Capítol 2**). En primer lloc, en el **Capítol 3** es presenta la primera publicació científica en revista i en el **Capítol 4** es presenta la segona publicació científica en revista, juntament amb les dues publicacions en congressos que serveixen d'antecedents a la publicació científica. Finalment, s'aborda la investigació publicada en el tercer article científic publicat en revista, juntament amb la contribució al congrés que serveix d'antecedent a aquest tercer article científic (**Capítol 5**).

Capítol 3. Detection of poor electrode milling by means of unsupervised classification

En aquest capítol es presenta el primer article científic sobre un nou mètode de classificació no supervisada per detectar problemes de fresat dels electrods en la soldadura per punts de resistència, donant resposta a l'**O.E2**. El mal fresat dels electrods pot causar problemes significatius de qualitat en alterar la geometria de la cara activa de l'elèctrode, afectant la entrega d'energia al punt de soldadura i la distribució de força. El mètode proposat ofereix una solució a aquest problema al permetre la detecció primerenca de l'ús de l'elèctrode, facilitant accions correctives oportunes i millorant el control de qualitat. Aquest capítol detalla la metodologia i els resultats de l'estudi, demostrant l'efectivitat de l'enfocament de classificació no supervisada en la detecció de l'ús de l'elèctrode.

Els electrods de pinces de soldadura per resistència són components crítics en les operacions de soldadura, i la seva qualitat és

essencial per garantir l'èxit del procés. Un dels problemes significatius associats als electrodos de pinces de soldadura és el seu deteriorament degut a l'ús constant, el que porta a canvis en la geometria de l'elèctrode. Com a resultat, la uniformitat de la distribució de força i corrent es veu afectada, el que condueix a una disminució en la qualitat de les soldadures produïdes. Per tant, és essencial mantenir la geometria de l'elèctrode mitjançant un fresat adequat per evitar aquests problemes

Garantir un fresat adequat és fonamental, ja que té un impacte directe en la geometria de l'elèctrode i, en conseqüència, en la qualitat de les soldadures. Una geometria constant de l'elèctrode garanteix una distribució uniforme de força i corrent, la qual cosa condueix a soldadures d'alta qualitat. No obstant això, un fresat inadequat pot resultar en superfícies d'elèctrode desiguals, la qual cosa porta a una distribució desigual de força i corrent, resultant en soldadures de mala qualitat. Per tant, per mantenir una geometria constant de l'elèctrode, és crucial garantir un bon fresat.

Per detectar la qualitat dels fresats dels electrodos de pinces de soldadura per resistència, es va desenvolupar un mètode de detecció no supervisat. El mètode implica la recollida de dades de tensió i corrent dels electrodos després de cada fresat. Les dades recopilades es sotmeten a extracció de característiques per reduir el nombre de variables d'entrada, i les variables finals d'extracció de característiques s'utilitzen com a entrades per a l'algorisme K-means. La sortida de l'algorisme K-means es classifica en tres grups: 'ok', 'alarma' i 'pre-alarma'.

El grup 'ok' indica que la qualitat del fresat està dins del rang acceptable, i no es requereix cap acció addicional. El grup 'pre-alarma' indica que la qualitat del fresat està per sota del rang acceptable, i es requereix manteniment. Finalment, el grup 'alarma' indica que la qualitat del fresat de l'elèctrode s'està deteriorant i es requereix manteniment de manera urgent.

Capítol 4. Real-time monitoring of electrode alignment

En aquest capítol es presenta la investigació realitzada per a la detecció de desalineació d'elèctrodes en la soldadura per punts de resistència (RSW). La desalineació dels electrods és un problema mecànic comú que causa problemes de qualitat, com soldadures de mida insuficient i unions no arrodonides. En aquest capítol es presenten dues contribucions a congressos científics i finalment un article científic que mostren el treball desenvolupat en aquesta línia d'investigació.

La primera contribució presenta una proposta inicial d'un nou mètode per a detectar la desalineació a través de l'anàlisi del camp magnètic generat pels elèctrodes en curtcircuit. Aquest article proporciona un punt de partida per a la investigació en discutir la importància de la desalineació d'elèctrodes com a factor mecànic en la RSW i els problemes que causa, incloent-hi l'augment de costos a causa de reparacions manuals. L'article proposa una solució novedosa per a detectar la desalineació a través de la mesura del camp magnètic generat pels elèctrodes. El mètode es valida mitjançant simulació i es prova en una línia de producció d'automòbils.

La segona contribució aprofundeix en l'optimització del mètode i examina la robustesa del camp magnètic en els elèctrodes de soldadura mitjançant simulacions. Aquest segon article aprofundeix en l'estudi del mètode proposat mitjançant l'anàlisi de la robustesa de l'anàlisi del camp magnètic en diferents escenaris típics de pinza de soldadura. L'objectiu és determinar si altres problemes mecànics en la pinza de soldadura podrien causar falsos positius en la detecció de la desalineació i fins a quin punt poden ser detectats.

Finalment, l'article científic presenta una solució implementable per a la detecció de desalineacions en línies de producció industrial reals. El tercer article presenta una solució pràctica per a la detecció de la desalineació d'elèctrodes en un entorn industrial. El mètode per a monitorar l'alineació dels elèctrodes es desenvolupa en base a investigacions

anteriors, que van mostrar la relació entre la desalineació i el camp magnètic generat per elèctrodes en curtcircuit. Es crea un dispositiu per a mesurar el camp magnètic i s'implementa un sistema per a la detecció en temps real de desalineacions. Aquest sistema estableix llindars de comportament basats en experimentació i permet el monitoratge de les condicions després de cada cicle de soldadura.

En general, els tres articles contribueixen a l'avanç de la comprensió i la solució del problema de la desalineació d'elèctrodes en la RSW donant resposta als **O.E3** i **O.E4**. A través d'aquesta investigació, es proposa, prova i es demostra una solució valuosa per a la indústria mitjançant un enfocament nou per a detectar la desalineació.

Capítol 5. Virtual sensor for the detection of wear in the secondary circuit of the welding gun

En aquest capítol es presenta un nou mètode desenvolupat per a la detecció de l'ús en el circuit secundari de les pinces de soldadura per resistència. Es mostra l'evolució de la investigació per arribar a una solució final a través d'una contribució a un congrés internacional i un article científic. En primer lloc, es presenta la primera aproximació a la detecció de l'ús a través de l'anàlisi del cicle de treball del circuit de potència del control de soldadura. El segon article va més enllà en afegir les variables de les resistències secundàries mitjançant un sensor virtual, permetent la detecció primerenca de l'ús que es produeix en les pinces de soldadura.

La detecció del desgast secundari de les pinces de soldadura és fonamental per mantenir l'eficiència i qualitat de les operacions de soldadura. La part secundària, que és l'encarregada de transferir l'energia elèctrica del transformador a l'elèctrode, està subjecta a un constant desgast a causa del calor i la pressió que experimenta durant el procés de soldadura. Per tant, la detecció de l'ús secundari és essencial per evitar possibles problemes com l'augment del consum d'energia, la disminució de la qualitat i els freqüents temps d'inactivitat. Una de les principals raons per detectar desgast secundari és l'impacte en el consum d'energia. A mesura que el secundari s'usa, la resistència de contacte entre l'elèctrode

i el secundari augmenta, el que condueix a un major consum d'energia. Això no només augmenta els costos de producció, sinó que també afecta al medi ambient produint més emissions de carboni. A més, desgast secundari pot provocar una mala qualitat de soldadura, el que genera costos de reparació dels possibles defectes. De la mateixa manera, una detecció primerenca del desgast del secundari permet realitzar les mantencions correctives de forma programada, el que redueix les parades de producció i els retards en la producció.

Durant aquesta investigació, s'han publicat dos articles per a explorar la importància de detectar el desgast en el secundari de les pines de soldadura. El primer article busca posar l'èmfasi en la importància de monitoritzar el desgast secundari, destacant la importància de mantenir registres precisos del desgast secundari i reemplaçar-los quan siga necessari per a evitar temps d'inactivitat inesperats. Aquest article mostra en primer lloc la correlació entre el desgast secundari i el cicle de treball del circuit de potència del control de soldadura mitjançant la simulació del circuit elèctric. Una vegada establerta aquesta correlació, es proposa un mètode inicial per a la detecció del desgast secundari mitjançant la monitorització contínua de la variable de control dels IGBT.

El segon article es centra a optimitzar el primer mètode perquè es puga detectar el desgast de forma precoç, tractant d'aconseguir una detecció el més aviat possible del desgast. En aquest article, partim de la variable de control dels IGBT per a implementar un sensor virtual de les resistències secundàries. Això permet un anàlisi de la distància de Mahalanobis entre ambdues variables. Aquest nou mètode pot predir el desgast de l'operador secundari i alertar abans que sorgeixca qualsevol problema important. Aquesta millora pot ajudar a reduir el temps d'inactivitat i els costos al predir quan és necessari reemplaçar el secundari.

En conclusió, ambdós articles proporcionen un mètode real provat en una línia de producció per a la detecció del desgast de l'elèctrode en

temps real, la qual cosa permet reduir els costos de fabricació, evitant parades i problemes de qualitat, donant així resposta a l'O.E5.

4. CONCLUSIÓ

Durant aquest treball de doctorat, es van desenvolupar diferents línies d'investigació centrades en el monitoratge continu dels diferents paràmetres que podrien afectar la qualitat de la soldadura. Específicament, la premisa va ser que, en els processos de producció, una variació en les condicions de la màquina condueix a un augment de problemes amb la qualitat del producte final. En el cas de la soldadura per resistència, les pinces de soldadura són responsables de realitzar la unió soldada. Per tant, els estudis realitzats es van centrar en detectar i reduir la variabilitat en el procés, evitar el desgast i detectar anomalies en el comportament.

Durant l'estudi de doctorat, es van desenvolupar principalment tres línies d'investigació per aconseguir l'objectiu establert d'optimitzar el procés de soldadura per resistència. El **Capítol 3** presenta la primera línia d'investigació, que es centra en reduir la variabilitat que existeix en el procés de fresat, causant principalment problemes en la qualitat del punt de soldadura. Aquesta investigació presenta un mètode innovador per detectar problemes de fresat i desgast d'elèctrodes utilitzant mètodes d'agrupament no supervisats. Al llarg de l'article, es descriu la relació entre les dades de resistència en sèrie i la variació de les propietats mecàniques dels electrodos. Malgrat treballar amb sèries de temps, es va realitzar l'extracció de característiques per reduir la dimensionalitat, el que va permetre reduir el nombre d'entrades per a l'algorisme d'agrupament. Això també va permetre escalar les dades d'entrada perquè no fossin influenciades per les diferències de resistència existents en cada pinza de soldadura. Els principals avenços obtinguts d'aquesta investigació són: un mètode per detectar la relació entre les variables de soldadura i l'estat de fresat, un sistema d'alarma que estableix estats de prealarma i operació correcta segons la sortida de l'algorisme d'agrupament, proporcionant una resposta satisfactòria a l'O.E2, i un sistema de recopilació de dades en una

línia de soldadura que permet l'anàlisi de dades en temps real, tant per a aquesta investigació com per a les següents línies d'investigació. Aquesta línia d'investigació també va permetre la primera publicació en revistes científiques d'alt impacte, com es mostra en el capítol.

La segona línia d'investigació, presentada en el **Capítol 4**, també es va centrar en detectar problemes mecànics que generen problemes de qualitat i parades en les línies de soldadura. Específicament, la segona línia d'investigació va tenir com a objectiu detectar l'aliniament dels elèctrodes. Al llarg dels tres articles presentats en aquest capítol, es veu l'evolució tant del mètode com del dispositiu capaç d'aplicar el mètode en una línia de soldadura real. Els tres articles mostren el procés seguit des de la idea inicial fins a la solució final implementada en una línia de soldadura real.

Aquesta línia d'investigació va aconseguir relacionar l'aliniament dels elèctrodes i el camp magnètic generat per les pinces de soldadura per detectar defectes mecànics en les línies de producció de juntes soldades mitjançant soldadura per resistència. L'estudi va trobar que la desalineació dels elèctrodes causava variacions en l'àrea de contacte i el camp magnètic, que podien mesurar-se mitjançant un dispositiu capaç de mesurar el camp magnètic. També es va proposar un protocol per enviar alarmes a través de LoRa al programari d'anàlisi de dades, amb llindars d'alarma establerts per determinar la desalineació.

En general, l'article presenta una solució real al problema de les desalineacions en les línies de producció, amb un mètode per a la detecció en temps real i integració fàcil en la indústria, complint els objectius **O.E3** i **O.E4**.

A més, es destaca que aquest mètode proposat de detecció representa una millora respecte a aquells basats actualment en visió, ja siga a través de l'observació per part dels operadors o utilitzant sistemes de visió artificial. Això es deu a que el mètode de detecció proposat té un cost d'implementació més baix i no està influenciat per la brutícia ambiental típica de la línia de soldadura. Això fa que aquest mètode siga més precís

i fiable, ja que es basa en la mesura directa del camp magnètic generat per les pinces de soldadura.

Finalment, el **Capítol 5** mostra l'última de les línies d'investigació, que busca detectar un altre problema mecànic com el desgast en el circuit secundari de les pinces de soldadura, és a dir, el desgast en els braços de la pinza de soldadura. Aquesta línia d'investigació es va dividir en dues fases, representades en els dos articles publicats. En el primer article, es presenta un mètode efectiu per a detectar el desgast en el circuit secundari de les pinces de soldadura per resistència, el que pot causar una disminució en la qualitat de la soldadura i un augment en el consum d'energia en els processos de soldadura per resistència. S'ha demostrat a través de la simulació electrònica com el canvi en la relació entre la corrent i l'angle de control és fàcilment demostrable.

A partir d'aquesta relació, s'ha assumit que si es porta a terme una anàlisi històrica de les dades, es pot determinar un augment en el desgast en el circuit de soldadura. Aquest mètode s'ha aplicat en una fàbrica real, adaptant l'estudi per a la reducció de dades i simplificant l'anàlisi i l'enviament d'alarms al personal de manteniment. A partir de les dades reals adquirides en les línies de producció, s'ha validat que aquest mètode és viable i fiable per a detectar problemes de desgast en les línies de soldadura a través de l'anàlisi del control de l'angle de control. Com a continuació d'aquest primer article, es presenta el segon article com una millora sobre el primer. Aquest article mostra un sistema que utilitza un sensor virtual que converteix les senyals de corrent, voltatge i cicle de treball en valors de soldadura i resistència. Llavors, es calcula la distància de Mahalanobis entre ambdues resistències, i s'envien alarmes als operadors en funció d'aquests valors.

El sistema va ser provat en un estudi real en una fàbrica d'automòbils en la qual es van provar 650 pinces de soldadura. Els resultats van mostrar que el sistema és capaç de detectar el desgast incipient de manera precisa i oportuna tant en els braços de la pinza com en la part responsable de la

soldadura (elèctrodes, portaelèctrodes, etc.), el que permet assolir l'objectiu d'**O.E5**.

Les principals avantatges obtinguts d'aquesta línia d'investigació presentada en el **Capítol 5** són que, en comparació amb altres mètodes de detecció de desgast, aquest mètode no depèn d'inspeccions visuals o mesures realitzades pels operadors, per la qual cosa no és necessari tenir personal encarregat de realitzar aquestes accions. A més, es basa en dades accessibles, el que facilita la seua implementació en les fàbriques. En segon lloc, permet la detecció de desgast en temps real, el que permet intervenir abans que es produeixin fallades en les pinces de soldadura, a diferència dels sistemes actuals basats en el manteniment periòdic.

En conclusió, aquest estudi de doctorat presenta tres línies d'investigació destinades a optimitzar el procés de soldadura per resistència mitjançant la reducció de la variabilitat i la detecció de problemes mecànics que afecten la qualitat del producte final. La primera línia d'investigació se centra en la reducció de la variabilitat en el procés de fresat mitjançant la detecció de problemes de fresat i el desgast de l'elèctrode mitjançant mètodes de clustering no supervisats. La segona línia d'investigació té com a objectiu detectar la desalineació de l'elèctrode, i la tercera línia d'investigació se centra en la detecció del desgast en el circuit secundari de les pinces de soldadura per resistència.

Les principals contribucions d'aquest estudi de doctorat són el desenvolupament de nous mètodes per a la detecció de problemes mecànics i la reducció de la variabilitat en el procés de soldadura per resistència. Aquests mètodes s'han aplicat amb èxit en entorns reals i han donat lloc a una millora de la qualitat de les unions soldades, una reducció del consum d'energia i un augment de l'eficiència. Els mètodes proposats es basen en dades accessibles, el que permet la seua fàcil implementació en les fàbriques, i permeten la detecció en temps real de problemes mecànics, el que permet la intervenció abans que es produeixin fallades en les pinces de soldadura. En general, aquest estudi de doctorat realitza importants contribucions al camp de la soldadura per resistència i

proporciona solucions pràctiques per a millorar la qualitat i eficiència de les línies de producció.

ABSTRACT

Currently, it is of vital importance in productive systems to maintain the quality of manufactured products. In this sense, it is essential to establish controls or systems capable of detecting changes in production patterns, which would allow for cost reduction and increased quality of manufactured products. Within productive systems, the resistance welding process is widely used in the metallurgical industry for joining metals without the use of additional material. This process is of great importance in the automotive industry, being the most commonly used method for joining metal parts of the body.

Although the welding process has been extensively researched over the years, the increase in industrial process digitalization has led to an increase in research conducted in industrial settings, moving away from laboratory solutions and proposing solutions applicable to real problems in the industry. Within this context, this research has developed three lines of investigation with a single objective: to maintain the quality of welded joints.

Usually, studies developed around the resistance welding process have focused on determining which parameters influence the quality of the welding nugget and then developing predictive methods to determine or predict the quality of weld points. However, this doctoral thesis starts from a different premise: if a welding gun is capable of generating weld points with acceptable quality, this means that quality problems arise from variations in the process, usually due to variations in the mechanical conditions of the equipment. From this assertion, each of the lines of investigation of this doctoral thesis was born, based on the detection of faults, problems, and wear in welding guns.

First, an exploration of a novel unsupervised classification method was carried out to determine the state of electrode milling, in order to obtain a functional system capable of detecting their wear. To do this, an alarm system was implemented that would inform operators in real-time about the state of the milling.

Second, research was conducted to determine the alignment state of the electrodes from the magnetic field generated by them. Based on simulations, the correlation between both variables could be verified. These results allowed for the development of a device capable of detecting changes in the magnetic field generated by the electrodes and, therefore, detecting misalignment. This device was integrated into production lines so that operators could be aware of the alignment state of the electrodes at all times.

Finally, the wear of the secondary circuit of the welding gun was investigated, that is, the mechanical elements located in that circuit. To do this, control monitoring of the IGBTs of the welding control power circuit was used to monitor the resistances of the elements of the secondary circuit through a virtual resistance sensor. From the analysis of the resistances using the Mahalanobis distance, it was determined that it was possible to detect the wear of the secondary circuit incipiently.

These three lines of investigation allowed for a global view of the state of the welding gun, making it possible to ensure that if these three methods provide a correct result, the quality of welding should remain constant.

Keywords: Resistance Spot Welding (RSW), Condition Monitoring, Wear Detection, Quality, Unsupervised classification, Mechanical conditions

ACKNOWLEDGEMENTS

Firstly, I would like to express my sincere gratitude to professors Julio Martos Torres and Jesús Soret, from the Department of Electronic Engineering at the University of Valencia, for their dedication. Their guidance has been essential in achieving each of the proposed objectives, and I also appreciate the trust they have placed in me. Likewise, I extend my gratitude to the University of Valencia for providing me with the necessary knowledge throughout the years since my Bachelor's degree in Electronic Engineering and my Official Master's degree in Electronic Engineering, which allowed me to carry out this doctoral thesis.

Similarly, I would like to thank Eduardo García for giving me the opportunity to develop my doctoral thesis in the context of Ford. His experience and knowledge about applied research in an industrial environment have been crucial to understand the needs and focus the research lines in order to propose real solutions. I appreciate his commitment to research and his unconditional support during these years.

Secondly, I would like to express my gratitude to my colleagues and collaborators at Ford, who have contributed significantly to this research, providing not only valuable information, resources, and technical support at all times, but also support in the most complicated moments of the research.

I also thank the Foundation for Development and Innovation (FDI) for the financial support to carry out this doctoral thesis. This research work has been made possible thanks to the funding, in accordance with the “Specific collaboration agreement between the Foundation for Development and Innovation and the University of Valencia for the development of a doctoral program in the framework of Industry 4.0 (Ford Spain) - Improvement of quality in welding lines”. FDI has shown a great commitment to continuous collaboration between universities and industries related to the automation sector in the Valencian Community,

allowing the development of this doctoral thesis in an industrial environment. For all this, my gratitude to the FDI for their support and commitment to this project.

Thirdly, I would like to express my gratitude to my parents, for the education they have provided me since my childhood. Their help and guidance have been essential in achieving my goals and fulfilling my dreams. I could not have done it without their constant support and motivation. I am deeply grateful to have them in my life and for everything they have done for me. I also extend my gratitude to my siblings for their presence throughout the years.

Finally, I want to thank my wife and children for being the motivation and unconditional support during all this time dedicated to research. Their understanding, patience, and love have been fundamental in achieving the objectives of this doctoral thesis. Their presence in my life has made this process more bearable and less arduous. I am deeply grateful for everything they do for me and for being my greatest source of motivation.

AGRADECIMIENTOS

En primer lugar, deseo expresar mi más sincero agradecimiento a los profesores Julio Martos y Jesús Soret, pertenecientes al Departamento de Ingeniería Electrónica de la Universidad de Valencia, por su dedicación. Su guía ha sido esencial en la consecución de cada uno de los objetivos propuestos, y agradezco también la confianza depositada en mí. Asimismo, extendiendo mi gratitud a la Universidad de Valencia por brindarme los conocimientos necesarios a lo largo de los años desde mis estudios de Grado en Ingeniería Electrónica y Máster Oficial en Ingeniería Electrónica, lo que me permitió llevar a cabo esta Tesis Doctoral.

Igualmente, deseo agradecer a Eduardo García por haberme brindado la oportunidad de desarrollar mi tesis doctoral en el ámbito de Ford. Su experiencia y conocimientos sobre la investigación aplicada en un entorno industrial han sido cruciales para entender las necesidades y enfocar las líneas de investigación con el fin de proponer soluciones reales. Agradezco su compromiso con la investigación y su apoyo incondicional durante estos años.

En segundo lugar, quisiera expresar mi agradecimiento a mis compañeros de trabajo y colaboradores en Ford, quienes han contribuido significativamente a esta investigación, brindando no solo información valiosa, recursos y apoyo técnico en todo momento, sino también apoyo en los momentos más complicados de la investigación.

También agradezco la Fundación para el Desarrollo y la Innovación (FDI). Este trabajo de investigación ha sido posible gracias a su financiación, en conformidad con el "Convenio específico de colaboración entre la Fundación para el Desarrollo y la Innovación y la Universitat de Valencia para el desarrollo de un programa de doctorado en el marco de la Industria 4.0 (Ford España)- Mejora de la calidad en las líneas de soldadura". FDI ha demostrado un gran compromiso con la colaboración continua entre las universidades y las industrias relacionadas con el sector de la automatización en la Comunidad

Valenciana permitiendo el desarrollo de esta tesis doctoral en un entorno industrial. Por todo ello, mi agradecimiento a la FDI por su apoyo y compromiso con este proyecto.

En tercer lugar, deseo expresar mi agradecimiento a mis padres, por la educación que me han brindado desde mi infancia. Su ayuda y guía han sido esenciales para alcanzar mis metas y cumplir mis sueños. No podría haberlo logrado sin su apoyo y motivación constante. Estoy profundamente agradecido por tenerlos en mi vida y por todo lo que han hecho por mí. También extendo mi agradecimiento a mis hermanos por su presencia a lo largo de los años.

Por último, quiero agradecer a mi esposa e hijos por ser la motivación y el apoyo incondicional durante todo este tiempo dedicado a la investigación. Su comprensión, paciencia y amor han sido fundamentales para poder cumplir con los objetivos de esta tesis doctoral. Su presencia en mi vida ha hecho que este proceso sea más llevadero. Estoy profundamente agradecido por todo lo que hacen por mí y por ser mi mayor fuente de motivación.

TABLE OF CONTENTS

Declaration III

Note to the Reader V

Resumen VII

1. Contexto de la investigación y motivaciónVII

2. ObjetivosVIII

3. MetodologíaX

4. ConclusiónXV

Resum XXI

1. Context de la investigació i motivacióXXI

2 ObjectiusXXII

3 MetodologiaXXIV

4. ConclusióXXIX

AbstractXXXV

AcknowledgementsXXXVII

Table of contents XLI

List of Figures XLIII

Chapter 1. Introduction 1

1.1 Research Context And Motivation 1

1.2 Research Objectives 2

1.3 Thesis Structure 4

1.4 Thesis Framework 5

Chapter 2. Background 7

2.1 Brief overview of welding resistance process 7

2.1.1.	Resistance welding process	7
2.1.2.	Welding Parameters	12
2.1.3.	Quality Issues	18
2.2	Industrial Condition Monitoring	23
<i>Chapter 3. Detection Of Poor Electrode Milling By Means Of Unsupervised Classification</i>		<i>27</i>
3.1	Scientific article I	29
<i>Chapter 4. Real-Time Monitoring Of Electrode Alignment</i>		<i>45</i>
4.1	Scientific conference article I.....	47
4.2	Scientific conference article II.....	57
4.3	Scientific article II.	75
<i>Chapter 5. Virtual Sensor For The Detection Of Wear In The Secondary Circuit Of The Welding Gun.....</i>		<i>91</i>
5.1	Scientific conference article III.....	93
5.2	Scientific article III	103
<i>Chapter 6. Conclusion and Future Works</i>		<i>125</i>
6.1	Conclusion.....	125
6.2	Future Works.....	129
<i>Reference</i>		<i>133</i>

LIST OF FIGURES

Figure 1. Schematic overview of the resistance welding process....	8
Figure 2. Schematic summary of the resistances involved in the welding process.....	9
Figure 3. Schematic representation of the AC power circuit of resistance spot welding	10
Figure 4. Schematic representation of the MFDC power circuit of resistance spot welding	11
Figure 5. Comparison of Electrode Wear. (a) Electrode without wear. (b) Worn Electrode with Partial Contamination"	15
Figure 6. Types of electrode misalignment. Axial Misalignment-Angular Misalignment.....	17
Table 1. Matrix of Issues and their root causes	21
Figure 7. Manufacturing cost based on the type of maintenance performed	24
Figure 8. Evolution of scientific articles containing the term "Condition Monitoring" by decades.....	25

Chapter 1. INTRODUCTION

The introductory chapter presents the context in which this Ph.D. study is framed together with the unresolved challenges of the resistance spot welding.

1.1 RESEARCH CONTEXT AND MOTIVATION

The optimization of production processes has become one of the fundamental pillars of modern industry. The constant search for cost reduction, both in economic and energy terms, as well as the improvement of the final product quality, has led to a constant evolution and improvement of production processes in various industrial sectors. In this context, the analysis and optimization of production processes is key, through the identification of critical factors and the design of solutions to improve the efficiency and effectiveness of such processes. In this sense, resistance welding, one of the most widely used joining processes in industry, is an area of great interest for process optimization and research.

Furthermore, the growing digitization of production processes in industry is serving as a breeding ground for process optimization and research. The large amount of data generated in production processes, thanks to the use of sensors and control systems, allows for greater visibility and control of processes, as well as real-time data collection that can be analyzed later. In this context, resistance welding is an area of research that greatly benefits from digitization, as it allows for better process monitoring and greater data analysis capacity. In this sense, this Ph.D. study focuses on the application of advanced data analysis techniques to improve the efficiency and quality of resistance welding processes in industry.

Generally, research in the field of resistance welding has been focused on laboratory tests to find optimal parameterizations, advanced methods of predicting quality problems, correlation between parameters and quality problems, among other aspects. However, the main obstacle of these studies is that they can hardly be implemented in a high production

factory due to the lack of capacity for data extraction and analysis, and the high variability in the process, in contrast to laboratory studies.

In this context, this Ph.D. study seeks to address an existing problem in the industry, which is the maintenance of equipment used in resistance welding. Specifically, it is based on the premise that if equipment is generating a correct weld with an established parameterization, and the process does not change, the quality should not change. However, equipment used in resistance welding, such as welding tongs, have a useful life, wear out, and suffer breakdowns. Therefore, this Ph.D. study focuses on detecting the end of the useful life of equipment and wear before they can cause quality problems, thus contributing to the improvement of efficiency and quality in industry production.

Finally, it should be noted that this Ph.D. study has been developed in an industrial environment, using data acquired from real production lines. All algorithms and mathematical models have been developed and validated using real industry data, which guarantees the applicability of the results obtained in a real production environment.

1.2 RESEARCH OBJECTIVES

Based on the research context and motivation presented in the in the previous section, the main objective is to improve the efficiency and quality of resistance welding processes in the industry through the application of advanced data analysis techniques. Specifically, the aim is to detect the end of useful life and wear of welding equipment before they cause quality problems, contributing to the improvement of efficiency and quality in industrial production.

The main research objective can be further subdivided into specific goals or milestones, which are expected to be achieved throughout the course of the Ph.D. study. These specific goals (S.O), also known as "sub-objectives," are essential to achieving the overall research objective and

serve as a roadmap to guide the research process. The specific goals of this Ph.D. study are as follows:

- S.O1.** To analyze and gain a deeper understanding of the parameters that affect welding quality and how these are related to common mechanical problems in welding guns, specifically. This will allow us to delve deeper into and comprehend the behavior of production lines based on the experience of operators.
- S.O2.** To identify those variables that are most influenced by electrode wear so that through the analysis and monitoring of these variables, we can determine the wear state of the electrodes. The ultimate goal is to establish a method for detecting variations in welding electrode wear through data analysis.
- S.O3.** The development of a pattern system to detect electrode misalignment in welding tongs using simulation models will allow us to determine how misalignment affects the physical variables that are modified by it, such as the generated magnetic field. This will be validated through simulation.
- S.O4.** Building on the findings from S.O3, the objective is to develop a method and a device capable of measuring the state of misalignment in production welding lines. This will enable the implementation of the results obtained in S.O3.
- S.O5.** By analyzing the behavior of the welding gun and the power circuit of the welding gun, to determine the existence of energy loss points and, therefore, wear and tear in the welding gun. Ultimately, the goal is to develop a method to prevent line stoppages and quality problems caused by welding gun wear.

1.3 THESIS STRUCTURE

The doctoral thesis is structured into six well-differentiated chapters, which illustrate the progression of the research carried out. The main content of the thesis is contained in chapters 3, 4 and 5, in three peer-reviewed scientific articles and three peer-reviewed conference articles are presented, which effectively meet the objectives set out in Section 1.2.

Chapter 1 provides an overview of the context and unresolved challenges related to the research topic that is addressed in the Ph.D. study.

Chapter 2 provides the theoretical background of the resistance welding process along with a review of relevant literature. The chapter begins with a summary of the welding process and the existing problems in the process. It then proceeds to review literature that illustrates the importance of each of the welding parameters.

Chapter 3 presents a paper on a novel unsupervised classification method for detecting poor electrode milling in resistance spot welding. The chapter provides a detailed explanation of the methodology and results of the study, which demonstrate the effectiveness of the unsupervised classification approach in detecting electrode wear.

Chapter 4 focuses on a new advancement in the detection method for electrode misalignment in resistance spot welding (RSW). The chapter features three papers: the first proposes a new method for detecting misalignment through the analysis of the magnetic field generated by short-circuited electrodes; the second delves deeper into the optimization of the method and examines the robustness of the magnetic field in welding electrodes through simulations; and the last presents an implementable solution for the detection of misalignments in real industrial production lines.

Chapter 5 describes a new method developed for the detection of wear in the secondary circuit of resistance welding guns. The chapter includes two papers: the first shows the first approximation to the detection of wear through the analysis of duty cycle of the power circuit of the welding

control, while the second paper goes further by adding the variables of the secondary resistances by means of a virtual sensor, allowing early detection of wear that occurs in welding guns.

Chapter 6 summarizes the conclusions derived from the research carried out in the Ph.D. study. It also introduces possible lines of future research that can be explored based on the findings obtained during this study.

1.4 THESIS FRAMEWORK

The present doctoral research summarizes the work carried out by the author during the period of 2018-2023 as a member of the Digital Systems and Communications Design (DSDC) Group within the Electronic Engineering Department of the University of Valencia.

Specifically, this doctoral study has been conducted under a specific collaboration agreement between the Foundation for Development and Innovation (FDI) and the University of Valencia, aimed at the development of a doctoral program within the Industry 4.0 framework.

FDI is a non-profit organization that was created in collaboration with Ford Spain and the Generalitat Valenciana in 1998. Its main objective is to promote the economic growth of the Valencian Community by improving the quality of products and systems, promoting the protection of the environment, and supporting scientific, technical, social, and cultural development. FDI also plays an important role in promoting knowledge transfer through various training programs and initiatives

Within this collaboration framework, research lines have been developed at the Ford Almussafes factory, which has served as a large-scale testing ground to achieve the objectives set out in the collaboration agreement. Specifically, this industrial thesis has been developed mainly in the body shops at Ford Almussafes, equipped with approximately more than 1000 welding guns, which has allowed the author to develop each of the proposed objectives in a framework of real application, making it easily transferable to other

factories. This collaboration with the Ford Almussafes and the FDI has provided access to state-of-the-art technologies and resources, enabling the author to conduct cutting-edge research and development in the field of Industry 4.0.

Chapter 2. BACKGROUND

This chapter shows the theoretical background of the resistance welding process along with a review of the bibliography that serves as basis of this Ph.D. study. First, a summary of the welding process is presented together with the existing problems in the process. Subsequently, a review of the literature is made, in which the importance of each of the welding parameters is shown.

2.1 BRIEF OVERVIEW OF WELDING RESISTANCE PROCESS

2.1.1. RESISTANCE WELDING PROCESS

The resistance welding process is considered one of the most important metal joining processes in the manufacturing industry due to its high efficiency and suitability [1]. Specifically, in the automobile manufacturing industry, this process can represent around 90% of the joints made in a body, reaching 7000-12000 welding joints in a single body, depending on the model [2]. One of the main advantages of using the resistance welding process is its ability to produce high quality welds with a high degree of repeatability and consistency. This is due to the fact that the process is highly controlled, with the current, voltage, and time parameters being precisely regulated to ensure optimal welding conditions. Additionally, the process is relatively fast, with the welding time typically being in the range of milliseconds, depending on the thickness and type of metal being welded. Another advantage of resistance welding is its ability to produce welds with minimal distortion or warping of the metal sheets being joined. This is because the heat generated by the resistance welding process is localized to the area of the weld, minimizing the amount of heat that is transferred to the surrounding metal. This results in less thermal stress on the metal and less distortion or warping of the final welded joint.

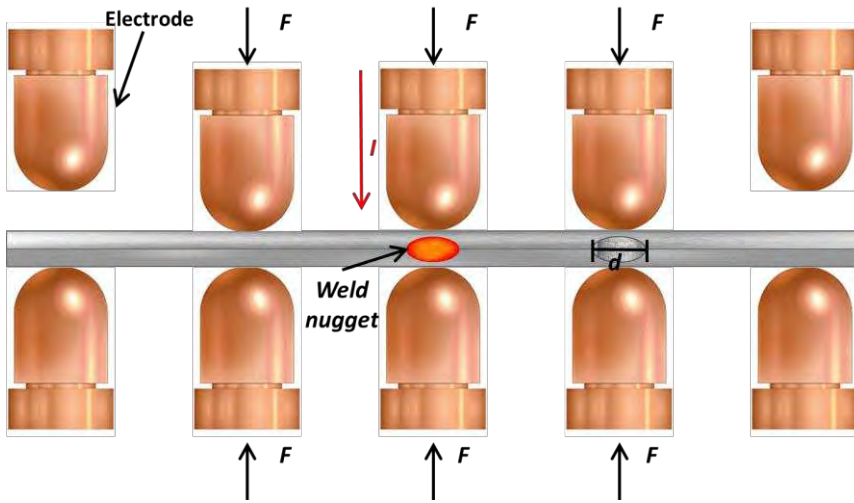


Figure 1. Schematic overview of the resistance welding process.

To carry out the union of two metals through the resistance spot welding process, the two sheets of metal to be joined are compressed by the electrodes of the welding gun, causing good electrical contact between both metals. Once this electrical contact is reached, current flows through them, heating them until they begin to melt just at the point where contact between the metal sheets occurs. Molten metal from the two metal sheets is joined into a single weld nugget. At this point, when the proper weld joint consistency is reached, the current is removed and the weld nugget solidifies, forming a solid metal connection. Therefore, the term "resistance welding" comes from the fact that it is the electrical property of the resistance of the metal sheet being welded that causes heat to be generated when a current flows through it [3] (**Figure 1**). Welding current therefore depends on the resistances that form the power circuit. Typically, these resistances can be summarized in seven resistances: the own resistance of each one of the electrodes (R_1 , R_7), electrode-sheet contact resistances (R_2 , R_6), the own resistance of the metal sheets (R_3 , R_5) and finally contact resistance between sheets (R_4), as shown in **Figure 2** [4].

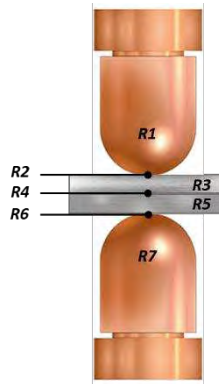


Figure 2. Schematic summary of the resistances involved in the welding process.

The main consequence of the passage of current through these resistances is the generation of heat Q which also depends, in addition to the resistance R_T and the current I_w , on the period T in which the current is applied [5]. The heat generated is determined by means of the joule heat equation:

$$Q = \int_0^T I_w^2(t) R_T(t) dt ; R_T = \sum_{i=1}^7 R_i \quad (1)$$

From equation 1 it can be deduced that the spatial distribution of heat depends on the value of each of the resistances. The objective of this process must be that most of the heat is generated in the contact between the metal sheets, or what is the same, that the contact resistance between the sheets is much greater than the sum of the other resistances involved in the generated heat. Therefore, a deviation in the other resistances of the system will cause a different distribution of the generated heat and, therefore, an undesired quality of the welding joint.

In the same way, the quality of welding will depend on how the current is applied to the welding point. Mainly, welding machines can be divided into two groups based on the power supply circuit, alternating current welding guns and medium frequency welding guns. First, the AC power supply uses two Silicon Controlled Rectifiers (SCRs) connected in

parallel, allowing current to flow during the positive half cycle through one of the rectifiers and during the negative half cycle through one of the rectifiers to the other rectifier. The primary current is started with a gate pulse for each of the rectifiers. The primary current begins upon receiving the pulse until the end of each half cycle is reached. In short, it is the firing angle α that determines the effective value of the primary current. Therefore, along with the transformer setting, the firing angle is used to control the effective welding current [6].

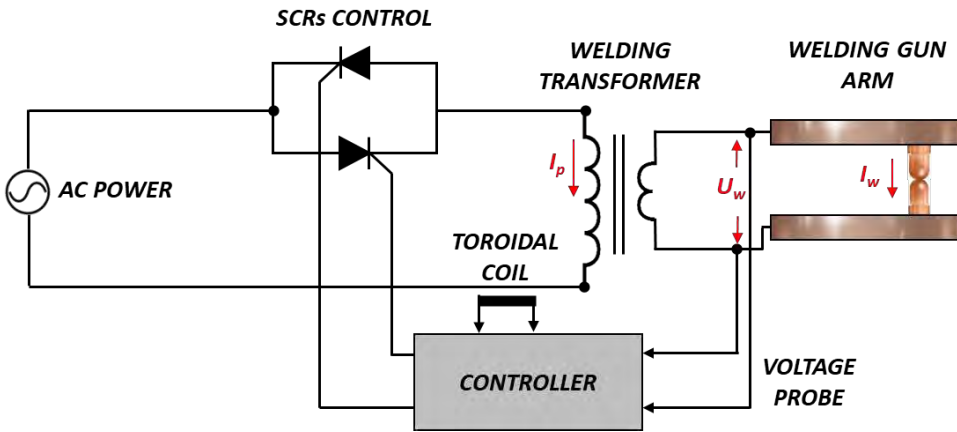


Figure 3. Schematic representation of the AC power circuit of resistance spot welding

As shown in **Figure 3**, the primary current is determined by the weld control. The firing angle of the SCRs is set by the welding control based on the current and voltage values measured during the welding process. This type of power supply has two main disadvantages: First, due to the control of the SCRs, during certain periods of time the current applied to the weld is zero, which causes the weld nugget to cool down during these periods of time, therefore, a longer welding time is necessary to achieve adequate results [7]. Secondly, the output can only be changed twice during each frequency period, so when working at mains frequency, it makes it difficult to control the current applied during welding.

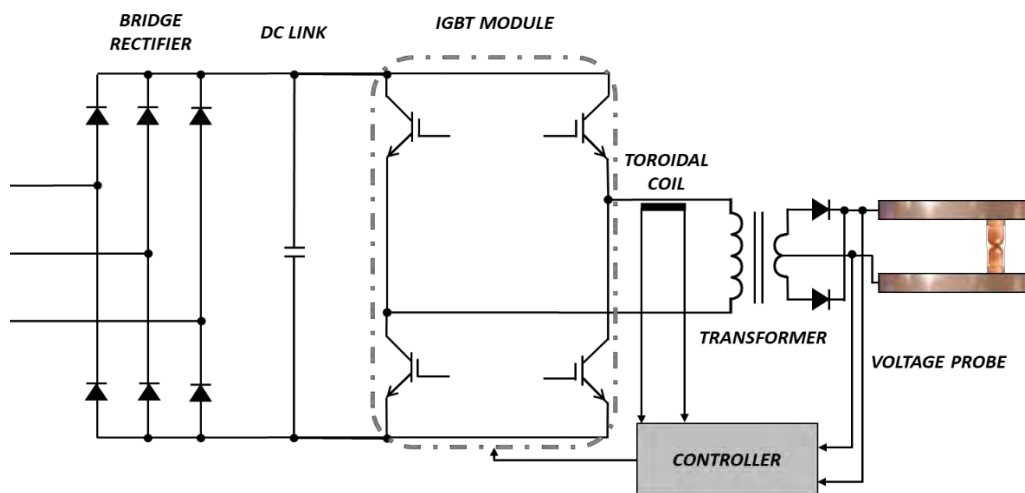


Figure 4. Schematic representation of the MFDC power circuit of resistance spot welding

Due to the disadvantages of the single-phase AC power supply, three-phase medium-frequency DC power sources, known as MFDC welding machines, are increasingly used in the automotive industry.

In **Figure 4**, the power circuit for a resistance welding machine of the MFDC type can be observed. Unlike the circuit in **Figure 3**, in MFDC machines, the management of the power provided to the welding point is done by controlling the triggering of a bridge of IGBTs. The MFDC welding power source offers several advantages over traditional welding power sources. One of the main benefits is its ability to control the amount of power delivered to the welding point with high precision. This is achieved through the use of IGBTs (Insulated Gate Bipolar Transistor) in the power circuit. The IGBTs act as a switch, allowing for precise control of the power delivered to the welding point by controlling the frequency and duration of their firing.

Another advantage of MFDC power sources is their ability to handle a wide range of welding materials and thicknesses. They are particularly well-suited for welding aluminium and other non-ferrous metals, as well as for thin sheet metal and dissimilar materials. This is due to their ability to

produce a stable arc with little spatter, and to maintain a consistent weld bead shape.

MFDC power sources also have a high level of energy efficiency, as they use a direct current power source and do not require the use of a transformer. This means that less energy is lost during the welding process, resulting in lower operating costs. Additionally, MFDC power sources have a smaller footprint and are lighter in weight compared to traditional welding power sources, making them more portable and easier to move around on a job site.

In summary, MFDC welding power sources offer improved precision and control, greater versatility, and increased energy efficiency compared to traditional welding power sources. They are an excellent choice for a wide range of welding applications.

2.1.2. WELDING PARAMETERS

The parameters that affect the quality of resistance welding are numerous and include factors such as welding pressure, electrode condition, misalignment, and the way in which current is applied. These parameters play a crucial role in determining the quality of the weld and should be carefully considered when performing resistance welding. In this section, a detailed examination of these parameters will be presented in order to provide a comprehensive understanding of how they impact the welding process. Additionally, the ways in which these parameters can be adjusted and controlled to achieve optimal welding results will also be discussed. It is important to note that the proper control and adjustment of these parameters is essential for achieving consistent, high-quality welds in resistance welding.

I. WELD FORCE

The welding force applied to the welding point during the welding process is a crucial parameter that greatly affects the quality of the weld.

The pressure applied is responsible for maintaining the proper alignment of the workpieces being welded, as well as ensuring that the electrodes are in proper contact with the workpieces. The pressure applied should be consistent and within the recommended range for the particular welding process being used. If the pressure is too low, the weld may be weak and porous, while if the pressure is too high, the electrodes may become distorted, or the workpieces may be damaged.

Maintaining consistent pressure during the welding process is crucial for ensuring the quality of the weld. However, in production lines, the fatigue of the welding gun may cause it to be unable to maintain the desired pressure throughout the manufacturing process. In servo-pilot guns, this can be caused by misalignment between the control signal from the servomotor and the pressure applied. In pneumatic guns, this is due to air pressure losses in the pneumatic circuit. For minor cases, recalibrating the control signals of the guns can restore the desired pressure, but in more severe cases, it may be necessary to replace the element of the gun that is causing the pressure losses.

The welding force plays a crucial role in the quality of the weld as it is correlated with the welding resistance and therefore with the heat generated during the process. As seen in equation 2, the welding force (F_w) is related to the contact area (A) of the electrodes and the weld pressure (P_w), similarly, equation 3 relates the value of the resistance (R) to the resistivity (ρ), the area (A), and the length (L). Therefore, from these two equations, equation 4 can be obtained where it can be observed how the force and resistance are inversely proportional. Therefore, an excess of force causes a very low resistance and therefore a lower heat and consequently inconsistent welds are generated. On the other hand, too low a force causes an excessive amount of heat, resulting in projections and burrs.

$$F_w = P_w A \quad (2)$$

$$R = \frac{\rho L}{A} \quad (3)$$

$$F_w = P_w \frac{\rho L}{R} \quad (4)$$

Different authors have focused their research on studying the importance of force in resistance welding. Wohner et al [9] discussed in their research the reduced process stability in press-hardened steels with an aluminium-silicon coating due to a smaller welding range. They proposed the use of an analytical methodology to optimize welding parameters and extend the welding range. Sun et al [10], on the other hand, investigated the influence of variable electrode force on the weld quality and weldability using a design of experiment approach with the help of servo gun. They found that the weld quality and weldability can be increased significantly by using the optimum parameter of variable electrode force. Finally, Tang et al [11] studied the intentional force increase during the resistance spot welding process, focusing on the effects of varying forging force and exploring the mechanism of the forging effects through the analysis of dynamic electrical resistance. This study aimed to achieve a better understanding of forging force application and its benefits on weld quality.

II. *ELECTRODE WEAR*

The wear of electrodes in resistance welding refers to the gradual deterioration of the electrodes due to friction and heat generated during the welding process. This can manifest itself in a reduction of electrode diameter, a loss of conductivity, or a decrease in the ability to transfer heat to the welding point. The wear of electrodes is a common phenomenon in resistance welding and can have a significant impact on the quality and efficiency of the welding process.

In addition to the mechanical properties of the electrode, the wear of electrodes can be affected by various factors such as the coating of the

metals being welded, the milling process, and the sealant used between the metal sheets. The use of a coating on the metal can alter the mechanical properties of the copper electrode when alloyed with the coating. Improper milling can result in inconsistent electrode diameter. The use of sealant can also increase dirt on the electrodes, thereby modifying their resistance. These factors must be carefully considered in order to ensure optimal electrode wear and performance during the resistance welding process. In Figure 5, two distinct states of electrode wear are shown as examples. Firstly, Figure 5a depicts an electrode without wear, that is, with its geometry and mechanical properties intact. On the other hand, Figure 5b shows an electrode that has undergone wear, with partial dirt on its active face.

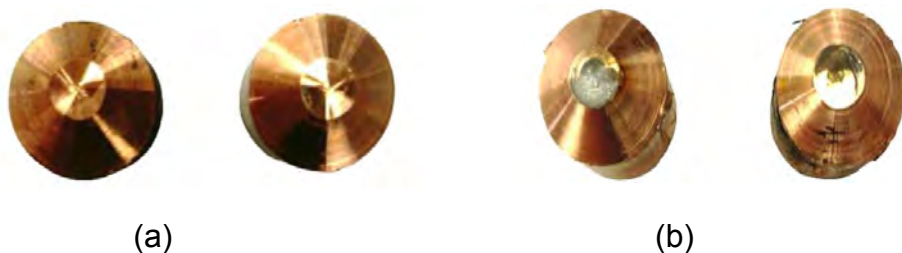


Figure 5. Comparison of Electrode Wear. (a) Electrode without wear. (b) Worn Electrode with Partial Contamination"

The resistance equation, equation 3, states that the resistance of a conductor is directly proportional to its resistivity and length, and inversely proportional to its cross section. Applying this equation to resistance welding electrodes, it can be inferred that any change in the mechanical properties of the copper electrode, such as its hardness or resistivity, will result in a change in its resistance. In the same way, a variation in the diameter of the active face of the electrodes or an irregularity in its surface will affect the contact area with the metal and therefore the welding resistance.

There is a multitude of studies on the parameter of electrode wear due to its crucial role in welding quality. Zhang et al [12] has conducted research on the effect of welding current on electrode wear in resistance

spot welding, showing that as the welding current increases, the electrode wear also increases. Chen et al [13] has studied the wear characteristics of copper-coated electrodes in resistance spot welding, finding that the wear rate of the electrode decreases as the electrode force increases. Zhang et al [14] has investigated the characteristics of electrode wear in welding hot galvanization dual-phase steel, which has high strength and good corrosion resistance but leads to serious and uncertain electrode wear when welded. The study found that more alloy products and electrode deformation were produced when welding this type of steel, leading to a higher electrode wear rate. Panza et al [15] has proposed a novel approach to indirectly monitor electrode degradation during welding by analysing the electrode displacement signal and the electrode tip shape. The study found that the electrode speed during the final hold stage is the most explanatory feature describing electrode displacement, and that a regression analysis and a neural network can be used to infer the relationship between electrode speed and contact area, representative of tool wear.

III. ELECTRODE ALIGNMENT

The electrode misalignment is a critical factor in the quality of the resistance spot welding process. This term refers to the deviation of the electrode axis from its ideal position in the welding process. This deviation can lead to various problems that affect the quality of the final welding, such as changes in resistance and force, among others.

The origin of electrode misalignment can be attributed to various factors, such as the flexibility of the welding machine gun or poor fit-up. Additionally, it can also be due to the natural wear and tear of the electrodes over time. It is important to note that electrode misalignment can occur in various degrees, ranging from minor deviations to major ones, which can affect the quality of the welding process.



Figure 6. Types of electrode misalignment. Axial Misalignment-Angular Misalignment

This reduction in contact surface area leads to an increase in heat generation due to the Joule's law, causing metal projections during welding. The change in resistance is a direct result of the change in surface area of contact. As the surface area decreases, so does the resistance, causing an increase in heat generation and the potential for metal projections. In addition, electrode misalignment also affects the distribution of force during the welding process. When the electrodes are misaligned, the pressure distribution becomes asymmetrical, which results in a distorted nugget shape and a higher tendency for metal expulsion.

Several authors have conducted research on electrode misalignment in RSW, each focusing on different aspects of the issue. Nielsen et al [16] studied the effect of electrode misalignment on the quality of dissimilar metal welding and found that small deviations in the electrode axis can result in significant changes in the final welding quality. On the other hand, Charde et al [17] studied the relationship between electrode misalignment and electrode degradation and found that misalignment can lead to electrode degradation and reduce the electrode's lifespan in general.

Charde et al [18] conducted a study to analyse electrode alignment and resulting "bulging" effects in carbon steel and stainless-steel welding. The study was carried out using a spot welding machine with an AC waveform, and the results showed that the common welding regions were well noticed on the carbon steel side, but not on the stainless-steel side. Additionally, the electrode "bulging" effect on both sides of the electrodes

was not parallel and had some negative impacts on the internal structure. Li et al [19] presented a non-contact system for measuring electrode misalignment using industrial CCD cameras. The results of the study showed that the system could quickly and accurately measure electrode misalignment during the welding process and provide critical input for equipment adjustment and maintenance.

Finally, Xing et al [20] investigated the degradation of electrodes while welding galvanized steel and found that the electrodes experienced more severe degradation compared to previous studies with aligned electrodes. The results also showed that initial electrode pitting occurred after 50 welds and that the recrystallized grains of the worn electrodes turned under the asymmetrical pressure distribution caused by the misalignment.

In conclusion, electrode misalignment is a critical issue in resistance spot welding that affects the quality of the weld in a number of ways. The reduction in surface area of contact, change in resistance, and asymmetrical pressure distribution all contribute to the problem and must be carefully managed to ensure high-quality welding. The studies conducted by the five authors provide valuable insight into the various aspects of electrode misalignment and highlight the importance of ongoing research in this area. By understanding the relationship between electrode misalignment, resistance, and the distribution of force, engineers and technicians can take steps to minimize the effects of misalignment and ensure high-quality welding.

2.1.3. QUALITY ISSUES

The quality of the weld point is crucial in many industrial applications, especially in those where the joined elements are subjected to high loads and fatigue, as is the case in the manufacture of automobiles, airplanes, metallic structures, among others. If the quality of the weld point is insufficient, this can cause a decrease in the mechanical resistance and

durability of the joint, which in turn can affect the safety and functionality of the final product.

Ensuring weld quality can be expensive for companies. If a quality problem is found in a finished product, it often needs to be repaired or replaced, which can be costly and time consuming. Therefore, it is essential for companies to invest in welding quality control from the beginning.

- Undersized Weld: This issue occurs when the diameter of the weld button or nugget does not meet the specifications required.
- Stuck Weld: A stuck weld happens when the workpieces are held together by localized fusion, but no weld button forms.
- Excessive Indentation: This issue occurs when the depression left by the electrode on the workpiece exceeds the manufacturer's specifications.
- Expulsion or Burn-Through: Expulsion occurs when molten metal is forcefully ejected from the weld, while burn-through happens when material is expelled, creating a hole through the weld.
- Cracks and Holes: This issue happens due to discontinuities in the weld nugget and surrounding areas resulting from metallurgical changes from welding.
- Mislocated/Edge Welds: A mislocated weld is one that is incorrectly positioned compared to the current workpiece design, while edge welds are those that touch or extend beyond the edge of the workpiece.
- Inconsistent Weld Quality: This issue occurs when the quality of the weld varies, with some welds not meeting the applicable quality standards.

Considering all the quality issues described earlier, there are numerous parameters or factors that could be the root cause of them. In the **Table 1** a summary of the possible causes for each issue is presented. The table displays each cause with its corresponding issue in a matrix form, providing a clear overview of the relationships between the different factors and quality issues. This comprehensive approach can help to identify the most critical factors and prioritize our efforts to address them. It is essential to carefully analyse each of these factors to identify the underlying problem and implement effective solutions that ensure a high-quality of the weld nugget.

To reduce this quality issues, companies typically focus on two main areas: process monitoring to reduce quality issues during manufacturing, and product monitoring to detect quality issues early. Process monitoring involves the identification and control of welding process parameter that affect weld quality. Product monitoring involves non-destructive testing to detect possible quality problems in the finished product.

Due to the importance of weld quality, extensive research has been carried out to study the factors that influence weld quality and to develop methods of early detection of quality problems. Many authors have studied the influence of welding parameters, such as current intensity, welding time, sheet thickness and electrode geometry, on the quality of the weld. Other authors have investigated how to measure the quality of the weld by analyzing characteristics such as dynamic resistance or displacement of the electrode.

In recent years, researchers have focused on predicting or early detection of quality issues with the increasing digitalization of the industry. The use of machine learning and deep learning techniques has been essential for the development of quality control frameworks based on dynamic resistance signals, infrared camera data, and welding process data. The work of Zhao et al [21] and Zhou et al [22] has been centered on developing mathematical models and machine learning pipelines, respectively, to investigate the relationship among dynamic resistance signals, welding quality, and welding parameters, for resistance spot welding. They utilized various feature engineering strategies and regression techniques to predict welding quality based on laboratory or experimental data and real production data. On the other hand, Dai et al [23] proposed a quality evaluation framework based on dynamic resistance signals and deep learning models. They developed a one-dimensional convolutional neural network with channel attention mechanism to accurately predict welding quality by integrating welding process stability with deep learning models. Lastly, Stavropoulos [24] introduced an online quality assessment approach that utilized machine learning techniques on data captured from an infrared camera mounted on an RSW-robotized system. They found that the maximum IR intensity and the temporal features of the IR cooldown profile offered the greatest class separability and marked the corresponding classifiers as the most successful ones.

In short, one of the most important challenges faced by any production process, and specifically that of metal manufacturing, is to guarantee the quality of the final product. Therefore, it is essential to implement processes and systems that are capable of detecting quality defects early and reliably.

2.2 INDUSTRIAL CONDITION MONITORING

In the past, the maintenance strategy adopted by many industries was reactive or corrective maintenance, which involved repairing equipment or machinery after a breakdown occurred. However, this approach was not only costly but also led to prolonged periods of equipment downtime, which had a significant impact on production schedules and ultimately, the company's bottom line. The introduction of more sophisticated maintenance strategies such as predictive maintenance, preventive maintenance, and condition monitoring has been a game-changer for many industries. In particular, condition monitoring has gained significant popularity in recent times, primarily due to the increased digitization of industrial processes. The primary objective of condition monitoring is to detect and diagnose any changes in the condition of a machine or process, so that maintenance actions can be taken before a breakdown occurs. Condition monitoring techniques can help to minimize downtime, extend the lifespan of equipment, and reduce maintenance costs [25,26].

The use of condition monitoring has become more prevalent in recent years due to the increasing adoption of digital technologies in the manufacturing industry. With the advent of Industry 4.0 and the Industrial Internet of Things (IIoT), sensors and other monitoring devices have become more widely available, enabling manufacturers to collect and analyze data from their machines and processes in real-time. This data can be used to gain insights into the condition of equipment, identify potential issues before they become critical, and optimize maintenance schedules [27-29].

One of the advantages of condition monitoring is that it can be implemented without the need for additional sensors or equipment in some cases. Manufacturers can use existing data sources, such as equipment performance metrics, to monitor the condition of their machines. This can help to focus maintenance actions on specific areas of concern, reducing

the risk of machine failures and downtime. Furthermore, by monitoring the process, it is possible to indirectly monitor the quality of the product, ensuring that it meets the required specifications.

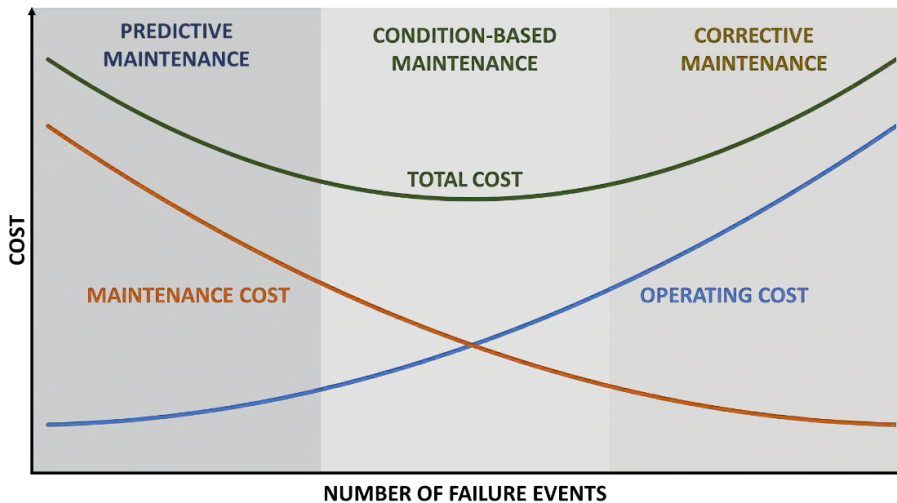


Figure 7. *Manufacturing cost based on the type of maintenance performed*

Condition monitoring differs from traditional predictive maintenance techniques in that it focuses on monitoring the condition of a machine or process, rather than predicting when a failure will occur. Predictive maintenance is based on the idea that machines will exhibit certain behaviors or symptoms before they fail, such as increased vibration or unusual noises. By monitoring these symptoms, it is possible to predict when a failure is likely to occur and take action before it happens. However, condition monitoring is a more proactive approach, as it seeks to detect changes in the condition of a machine or process before any symptoms are evident.

There are several benefits to using condition monitoring over traditional predictive maintenance techniques. First, condition monitoring can detect changes in machine condition earlier, allowing maintenance actions to be taken before a failure occurs. This can help to minimize downtime and extend the lifespan of equipment. Second, by monitoring the

condition of a machine or process, it is possible to optimize maintenance schedules, ensuring that maintenance is performed at the most appropriate time. This can help to reduce maintenance costs and minimize the impact of maintenance activities on production schedules. Finally, by monitoring the process, it is possible to indirectly monitor the quality of the product, ensuring that it meets the required specifications.

The method of Condition Monitoring has been under investigation for several decades, however, since this method bases its operation on the monitoring and analysis of the data acquired using sensors during the production process, it has been greatly influenced by the progress in data analysis and processing methods. **Figure 8** shows the evolution of the mention of the term "Condition Monitoring" in scientific articles by decades since 1970. The growing importance of condition monitoring in the industry is undeniable and the need to continue researching in this direction.

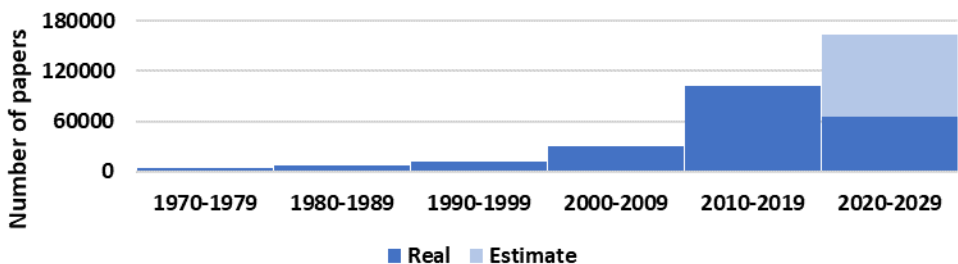


Figure 8. Evolution of scientific articles containing the term "Condition Monitoring" by decades

As a result, in recent years, there have been numerous research studies aimed at improving the effectiveness and efficiency of condition monitoring methods. These studies have explored various aspects of condition monitoring, such as sensor placement [30,31], data processing [32-34], fault detection algorithms [35,36], and machine learning techniques [37,38]. The research has also focused on developing new condition monitoring technologies and integrating them with other advanced technologies such as the internet of things (IoT) and big data analytics.

Overall, the advancements in condition monitoring research have led to the development of more accurate and reliable methods for detecting and diagnosing faults in machines and equipment. These developments have significant implications for industries such as manufacturing, transportation, and energy, where the early detection of machine faults can help avoid costly downtime and increase productivity.

Chapter 3. DETECTION OF POOR ELECTRODE MILLING BY MEANS OF UNSUPERVISED CLASSIFICATION

This chapter presents a paper on a novel unsupervised classification method for detecting poor electrode milling in resistance spot welding. Poor electrode milling can cause significant quality issues by altering the geometry of the electrode's active face, affecting power delivery to the weld point and distribution of force. The proposed method offers a solution to this problem by enabling early detection of electrode wear, facilitating timely corrective actions and improving quality control. This chapter details the methodology and results of the study, demonstrating the effectiveness of the unsupervised classification approach in detecting electrode wear

Resistance welding gun electrodes are critical components in welding operations, and their quality is essential to guarantee the success of the process. One of the significant problems associated with welding gun electrodes is their wear due to constant use, leading to changes in the electrode geometry. As a result, the uniformity of the force and current distribution is affected, leading to a decrease in the quality of the welds produced. Therefore, it is essential to maintain the electrode geometry through proper milling to avoid these problems.

The significance of ensuring proper milling cannot be overstated, as it has a direct impact on the electrode geometry, and consequently, the quality of the welds. A constant electrode geometry guarantees uniform force and current distribution, leading to high-quality welds. However, improper milling can result in uneven electrode surfaces,

leading to uneven force and current distribution, resulting in poor quality welds. Therefore, to maintain a constant electrode geometry, it is crucial to guarantee proper milling.

To detect the quality of milling in resistance welding gun electrodes, an unsupervised detection method was developed. The method involves collecting tension and current data from the electrodes after milling. The collected data is then subjected to feature extraction to reduce the number of input variables, the final feature extraction variables are then used as inputs for the K-means algorithm. The output of the K-means algorithm is classified into three groups: 'ok,' 'alarm,' and 'pre-alarm.'

The 'ok' group indicates that the electrode's milling quality is within the acceptable range, and no further action is required. The 'pre-alarm' group indicates that the electrode's milling quality is below the acceptable range, and maintenance is required soon. Finally, the 'alarm' group indicates that the electrode's milling quality is deteriorating, and maintenance is required in the near future.

3.1 SCIENTIFIC ARTICLE I

Title: An Unsupervised Condition Monitoring System for Electrode Milling Problems in the Resistance Welding Process.

Authors: Daniel Ibáñez, Eduardo García, Julio Martos and Jesús Soret.

Published in: Sensors 2022, 22(12), 4311; Special Issue: Machine Health Monitoring and Fault Diagnosis Technique <https://doi.org/10.3390/s22124311>

Impact factor: 3.847 (2021). Quartile (category: "Instruments & Instrumentation"): Q2 (2021)

Citations: 1 (accessed on March 2022).




Description: Sensors is a leading, peer-reviewed, open access journal that publishes scientific research on the science and technology of sensors. It is published semi-monthly online by MDPI, and is affiliated with several societies, including the Polish Society of Applied Electromagnetics, the Japan Society of Photogrammetry and Remote Sensing, the Spanish Society of Biomedical Engineering, and the International Society for the Measurement of Physical Behaviour. The journal is indexed in several databases, including Scopus, SCIE (Web of Science), PubMed, MEDLINE, PMC, Embase, Ei Compendex, Inspec, Astrophysics Data System, and others.

The special issue of Sensors titled "Machine Health Monitoring and Fault Diagnosis Techniques" focuses on the use of intelligent fault diagnosis methodologies for machine health monitoring and fault diagnosis in industrial plants. It highlights state-of-the-art techniques for fault feature extraction, intelligent machine monitoring, and algorithm development, including early fault detection features, few-shot sample machine learning algorithms,

data augmentation techniques for deep learning, data fusion methods for domain adaptation, feature representation with self-supervision, and interpretable deep learning algorithms. The aim of this special issue is to further investigate these issues and advance the field of machine health monitoring and fault diagnosis.

Article

An Unsupervised Condition Monitoring System for Electrode Milling Problems in the Resistance Welding Process

Daniel Ibáñez ^{1,*} , Eduardo García ², Jesús Soret ¹  and Julio Martos ¹ 

¹ Department of Electronic Engineering, Universidad de Valencia, Campus de Burjassot, 46100 Burjassot, Spain; jesus.soret@uv.es (J.S.); julio.martos@uv.es (J.M.)

² Ford Spain, Poligono Industrial Ford S/N, 46440 Almussafes, Spain; egarci75@ford.com

* Correspondence: daniel.ibanez@uv.es; Tel.: +34-961-791-543

Abstract: Resistance spot welding is one of the most widely used metal joining processes in the manufacturing industry, used for structural body manufacturing, railway vehicle construction, electronics manufacturing, battery manufacturing, etc. Due to its wide use, the quality of welded joints is of great importance to the manufacturing industry, as it is critical for ensuring the integrity of finished products, such as car bodies, that withstand high levels of stress. The quality of the welding is influenced both by the programming of the welding and by the good condition of the mechanical part that carries out the welding. These mechanical factors, such as electrode geometry and wear, degrade over time. As the welding points are made, the geometry and properties of the electrodes change, so they undergo a milling process to remove impurities and return them to their initial geometry. Sometimes the milling is deficient, and the electrode continues to wear, causing welding problems such as loose spots and metal spatter. This article presents a method for condition monitoring of the milling process and weld wear based on existing data in real production lines. The use of unsupervised clustering methods is proposed to perform a check by which, using current and resistance data, the electrode wear is grouped. Specifically, a method using multidimensional k-means for the condition monitoring of electrode wear is established. This research gives a real and applicable solution for reducing the quality problems caused by milling defects and electrode wear in the production lines of high-production manufacturing industries, presenting a system for sending alarms based on the behavior of welding variables.

Keywords: resistance spot welding; electrode wear; condition monitoring; milling machine; unsupervised clustering



Citation: Ibáñez, D.; García, E.; Soret, J.; Martos, J. An Unsupervised Condition Monitoring System for Electrode Milling Problems in the Resistance Welding Process. *Sensors* **2022**, *22*, 4311. <https://doi.org/10.3390/s22124311>

Academic Editors: Shilong Sun, Changqing Shen and Dong Wang

Received: 13 May 2022

Accepted: 5 June 2022

Published: 7 June 2022

Publisher's Note: MDPI stays neutral with regard to jurisdictional claims in published maps and institutional affiliations.



Copyright: © 2022 by the authors. Licensee MDPI, Basel, Switzerland. This article is an open access article distributed under the terms and conditions of the Creative Commons Attribution (CC BY) license (<https://creativecommons.org/licenses/by/4.0/>).

1. Introduction

Resistance spot welding is one of the most important joining processes in the metal-lurgy industry due to its efficiency and suitability for automation [1]. Specifically in the automotive industry, modern auto-body assembly needs 7000 to 12,000 spots of welding, and, thus, resistance welding plays a crucial role, representing approximately 90% of the welded joints carried out for body assembly [2].

The welding process can be summarized very simply; the sheet of metal to be welded is placed between water-cooled electrodes and then heat is obtained by passing a large electric current through them for a short period of time [3].

Although this process can be summarized in a very simple way, in reality, there are many factors that affect the achievement of the desired quality. Many programmable parameters affect weld quality. These parameters are given by Joule's law and are the welding time, the current and the resistance, which is related to the pressure achieved by the electrodes [4]. These parameters must be configured to achieve the desired quality and stability over time. In addition, several factors play an important role in the quality of the weld, such as voltage fluctuation, the misalignment of electrodes or loss of electrode

pressure. The shared characteristic of these factors is that they do not change during the lifetime of the welding electrodes and can be better controlled by a better welding controller or machine maintenance [5].

However, another parameter is inherent to the number of welds performed throughout the life of the electrodes: wear. The wear of the electrodes increases as the number of welds increases, modifying both the electrical and thermomechanical properties between the electrodes and the sheets. There are special cases in which this wear is even more pronounced, in particular, in those cases in which the sheets are coated with zinc or when sealer is used between the sheets to be welded. These special cases tend to stick to the copper electrodes, thus, causing a further increase in wear [6].

The heating of the metal can be described according to Joule's law, represented in Equation (1), where Q is the heat generated during welding by passing a current (I) along the metal–metal and metal–electrode resistance (R) over a period of time [7]:

$$Q = I^2 R t \quad (1)$$

In Figure 1, it can be seen schematically, as in resistance spot welding, that three different types of process resistance determine the resistance represented by Joule's law: contact resistors R_3 , R_4 and R_5 between sheet metal resistors R_1 and R_2 . Contact resistance refers to the resistance generated at the interface between the electrode and the metal sheet (R_3 and R_5) and the resistance between the metal sheets (R_4). The resistance of the sheets is determined by the resistivity and the thickness of the metal. Normally, these resistances are higher than the contact resistance between the electrodes, which causes the fusion to begin at the union of the two metals [8].

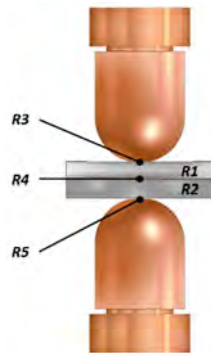


Figure 1. Resistances involved in a resistance spot weld.

From Figure 1, it can also be concluded that good contact between the electrodes and the metal is essential so that the electrode–sheet contact resistance is lower than the metal–metal resistance in such a way that the fusion begins between the metal-to-metal contacts. This bad contact between the electrodes and the metal can be due to different circumstances: misalignment of the electrodes, bad programming of the position of the welding point, dirt on the metals, deformation and wear of the electrodes, etc.

To avoid and correct the wear of the electrodes, a series of milling operations are carried out throughout the electrodes' useful life. Sometimes, these mills fail to reshape the electrode, leaving dirt in the capsule or leaving the electrode with a different shape to the desired one. This causes the contact resistance to vary, and, in addition, an increase in welding quality problems, such as small, deformed or even non-existent nuggets. Due to the increase in resistance and, therefore, the increase in heat, metal ejections can occur during welding, causing a quality and safety problem in the production line [9].

2. Electrode Wear and Milling

Electrode wear is one of the most important issues to research in the resistance welding process. Specifically, studies have focused on determining the factors that influence the appearance of electrode wear. First, Tanaka et al. [10] found that electrode wear could be reduced by increasing the nickel content of the metal foils. In this same line, Rashid et al. [11] demonstrated how a good choice of lubricant coated on the metal sheets could increase the useful life of the electrodes. Similarly, different authors have described the relationship between the different welded materials and the useful life of the electrodes [12–16].

In the same way, the decrease in welding quality caused by the wear of the electrodes has been widely investigated. The reduction in quality is determined by the increase in the diameter of the contact face of the tips [17]. This is because the increase in the diameter of the tip of the electrode, which results in a reduction of the heat generation of the welding joint, causes a decrease in the electrode and is the main reason for the decrease in the size of the nugget [18].

The deposition of the metal coating on the copper electrodes generates a change in the properties of the electrode and, therefore, the wear of the tips [19]. In addition to the reduction of the size of the nugget, the wear of the electrode is of great importance in the presence of weld ejections and other quality defects and can be the cause of 60% of quality problems [20].

Finally, due to the great importance of this defect, different authors have proposed methods for estimating wear or evaluating it. Gauthier et al. [21] and Raelison et al. [22] demonstrated a method for the numerical modeling of electrode wear which is useful for theoretical estimation but can hardly be applied to real cases where different factors interfere, such as mechanical problems or changes in the production process. Peng et al. [23] proposed the use of images for the analysis of the degradation of the electrodes; the main disadvantage for the application of this system in large production factories is the cost associated with the acquisition of the equipment.

On the other hand, Zhang et al. [24] proposed the use of electrode displacement to determine electrode wear; the discussed method provides a convincing solution but can only be carried out in those welding guns that have an integrated measurement system for electrode displacement, something that is usually lacking in pneumatic welding guns.

Finally, Zhou et al. [25] presented a method based on the analysis of dynamic resistance during welding to determine wear. The main disadvantage of this study is that it assumed that the dynamic resistance trend depends only on the wear of the electrodes when, actually, this variation can depend on different factors, such as the final quality of the welding point, as stated by Zhao et al. [26], or the temperature and pressure, as stated by Whang et al. [27], among many other factors.

All these proposed methods were based on the premise that, after performing the milling, the electrodes return to their original geometric state. On multiple occasions, due to mechanical problems of both the welding gun and the milling machine, such as blade wear or issues with milling, as shown in Figure 2, the restoration of the geometry does not occur.

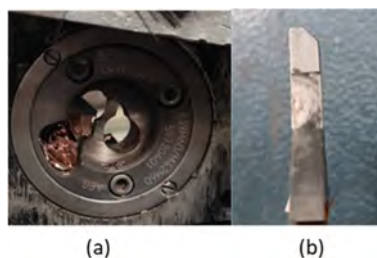


Figure 2. Typical defects of milling machines. (a) Milling machine covered by the chips from the electrodes. (b) Dull blade.

Therefore, the objective of this research is not to propose a system that only determines the wear of the electrode, but one which determines the milling problems that may occur during the production process; that is, the main objective of this research is to avoid the quality problems caused by the wear of the electrodes.

3. Materials and Methods

For the creation of the milling problem detection system, it was essential to be able to relate a real variable to an existing defect; this variable had to be acquired and treated to then proceed to the analysis and the elaboration of a data analysis system for evaluation.

Specifically, due to its existing relationship, the use of the measurement of the electrode resistance is proposed for subsequent preprocessing with normalization and feature extraction to later carry out an unsupervised classification method. This allows the setting of detection thresholds based on the behavior of the resistance data.

3.1. Electrode Resistance Measurement Method

Electrode wear is one of the essential external factors that determines the stability of weld joints in the resistance welding process.

To avoid these quality problems, after a certain number of welding points, a shaping of the tips is carried out by means of a milling machine. This process can be automatic or manual depending on the type of production line. Sometimes, due to a malfunction of the milling machine, such as an issue with the cutter, a force problem in the welding gun, poor positioning of the milling machine, etc., the electrodes are not well shaped. This is a problem since, until the next milling or replacement of electrodes, they will continue to function with inadequate wear, which can cause serious quality problems.

Figure 3 shows the real differences between electrodes after adequate milling and those after defective milling. The electrodes in Figure 3a correspond to 16 mm type F electrodes, according to DIN EN ISO 5821, before being milled for the first time. Figure 3b shows some electrodes that, after executing a certain number of welding points, were milled and returned to their original geometry. Finally, comparing Figure 3b,c, a clear example of poor milling can be seen. In Figure 3c, the active face of the electrodes has been partially cleaned, showing the dirt that generates quality problems.

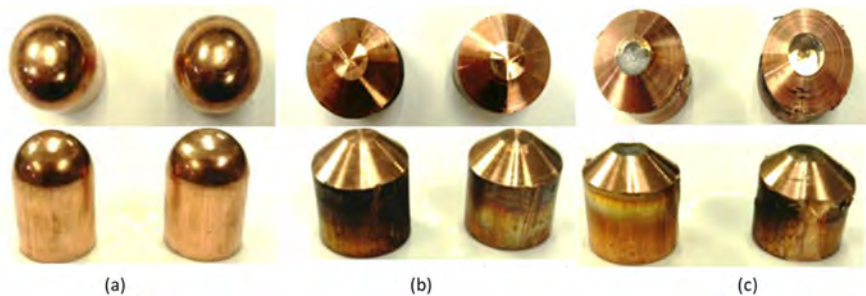


Figure 3. Evolution of the state of the electrodes. (a) Type F electrode before milling. (b) Type F electrode after good milling. (c) F-type electrode after poor milling.

Due to this uncertainty regarding the good milling of the electrodes, a method was established to measure the resistance after each milling is performed, acquiring the voltage and the average current measured between the short-cut electrodes, as shown in Figure 4.

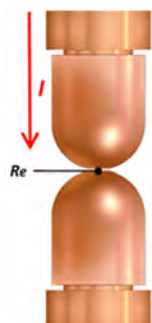


Figure 4. Schema—electrode resistance contact (R_e) measurement.

This check is carried out at a constant primary voltage so that when there is a change in the contact resistance of the electrodes (R_e) due to the wear of the electrodes, the voltage measured at the electrodes and the current vary according to Ohm's law.

3.2. Data Acquisition

For this article, 650 welding guns located in a real production line were analyzed, as well as a total of 100 millings carried out for each of the electrodes. The welding controls used for the study were BOS6000 with medium-frequency transformers. Regarding the welding guns, the analysis was carried out with no differences between pneumatic guns and servo guns. Similarly, two different welding electrodes were used for the study, 6 mm and 8 mm tip face electrodes, but, at the time of analysis, this difference was considered insignificant for the detection of electrode wear.

In relation to the type of milling machine and electrode, milling machines with an average speed greater than 290 min^{-1} and 25 Nm of torque were used to reset the geometry of the electrode, capable of restoring the geometry of the electrodes according to DIN EN ISO 5821 F1-16-20 [28].

For data acquisition, a pipeline system was implemented between the welding controller and the database through the ELK stack [29]. In this way, a protocol was established to send the welding data to the database every time a welding point occurred, which allowed real-time data analysis, both for machine failure detection and, in this case, for the performance of predictive analysis of weld quality.

For our case, the data acquisition protocol was established, as shown in Figure 5. In the first place, once the maximum number of the welding joints that an electrode could make was reached, keeping the welding quality constant, the electrodes were sent for milling. When the milling was finished, the electrodes were short-circuited by passing a current at constant voltage (PHA method). Finally, the data were stored in the database for further analysis.

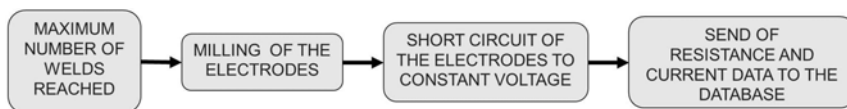


Figure 5. Data acquisition protocol.

3.3. Preprocessing and Feature Extraction

Once the necessary programming was carried out in the welding lines, all the data of the 650 welding guns were stored in the database.

In Figure 6, the data for two different welding guns are shown; it can be seen that the average value of the resistance for each of the cases was different. The difference observed was due to the characteristics of each of the guns, which depended on where the terminals

of the voltage probe were located; they affected not only the resistance of the electrodes but also the resistance of the welding arm. The data were always analyzed as normalized data to eliminate this difference from the analysis. Therefore, the z-score normalization, shown in Equation (2), was used. This normalization based on the mean and the standard deviation allowed the reduction of variations if high current and resistance data series were added to the analysis [30].

$$x' = \frac{x - \bar{x}}{\sigma} \quad (2)$$

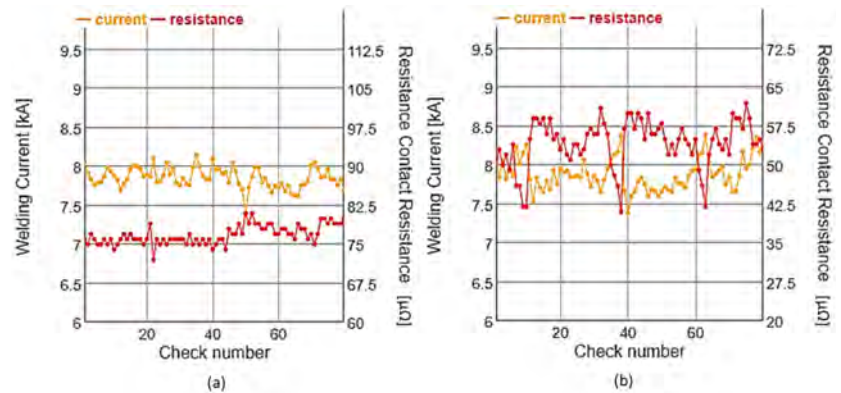


Figure 6. Example of current and resistance data acquired for a weld control. (a) Example of the data acquired for a welding gun with correct milling; (b) Example of the data acquired for a welding gun with poor milling.

Similarly, in this preprocessing stage, the data were subjected to data cleaning. First, the existing zeros in the time series were removed since those values were meaningless. This is because, when problems appeared when carrying out the check or in the voltage and current measurement probes, a zero was stored in the database. After eliminating the zeros, the atypical data of the time series were calculated, and the outliers were eliminated, for which the expressed formula in Equation (3) was used.

$$\begin{aligned} Max &= Q_3 + 1.5IQR \\ Min &= Q_1 - 1.5IQR \end{aligned} \quad (3)$$

Once this signal was filtered, the feature extraction process was carried out. Feature extraction in machine learning is a process of extracting significant attributes of the data. Feature extraction allows the height of dimensions of a series of data to be reduced to a smaller number of dimensions through unique mapping techniques [31].

For this study, the time series of both resistance and current were reduced to five statistical variables, which allowed the reduction of the dimensions by eighty times for each signal. The calculated variables were:

- The coefficient of variation (CV): the ratio of the standard deviation to the mean;
- Quartile Q_1 ;
- Quartile Q_3 ;
- Inter-decile range (IDR): the difference between D9 and D1;
- Median.

As there were two summary signals, in total we had 10 statistical variables as an input dataset for each welding control. The input dataset for the k-mean algorithm was a 650×10 array of values. Finally, before proceeding to k-means, the input dataset was standardized to obtain a more precise result in the next section.

3.4. K-Means Clustering

In this research, the use of unsupervised clustering using k-means was proposed, Algorithm 1. In general, for this method, the optimal number of clusters for the existing amount of data to be processed is selected first. This parameter represents the number of desired groupings.

Algorithm 1: K-means Clustering.

Input:
 $X = \{x_1, x_2, \dots, x_n\}$ (input data)

 k (number of clusters)
Output:
 $C = \{c_1, c_2, \dots, c_k\}$ (set of cluster centroids)
Initialization:
for each $c_i \in C$ **do**:

 $c_i \leftarrow x_j \in X$ (random selection)

while: Convergence or max iteration reached

for each $x_i \in X$ **do**:

 $\text{minDist} \leftarrow \min_{j \in \{1 \dots k\}} \text{Distance}(x_i, c_j)$;

 (based on Euclidian distance $\frac{1}{n} \sum (\min_j d^2(x_i, c_j))$ for $i = 1$ to n)

 UpdateCluster(c_i)

Based on the dataset, the k-means groups them in the programmed number of clusters k , assigning them to the closest centroid. Finally, the algorithm returns both the cluster and the respective centroid. Starting from an initial, non-optimized grouping, the algorithm relocates each point to the nearest new center. It then updates the centers of each cluster based on the mean of the points, repeating this relocation and updating the process until the convergence criteria are satisfied; this process is summarized in the flowchart of Figure 7 [32–34].

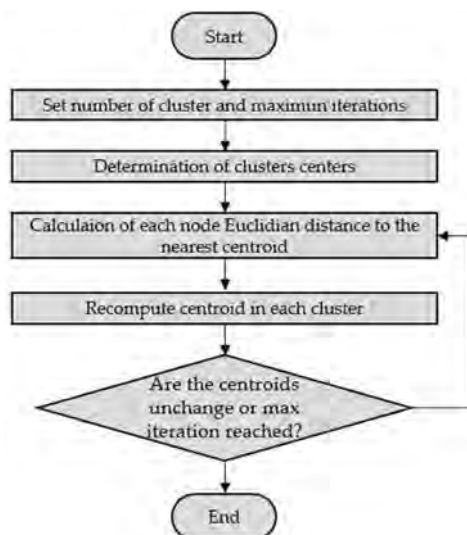


Figure 7. K-means flowchart.

One of the main advantages of using k-means and unsupervised learning is that it is not necessary to have labeled data. In this study, the population of equipment analyzed was large and varied, which is why it was difficult and inaccurate to label each series of data with the current state of the machine. In this way, it was not necessary to know the characteristics of each of the possible faults that may occur in the milling or in the

electrodes, but rather the k-means algorithm, based on the behaviors, assigned each series of data to each cluster.

The purpose of this analysis was to detect any variation in the milling process through its influence on the k-means clustering algorithm. In this case, three different data behavior clusters were expected, and we aimed to establish three machine status criteria: alarm, pre-alarm and good status.

As previously mentioned, the ten statistical variables calculated for the simplification of the model were used as an input dataset for the k-means clustering algorithm. There are different techniques to determine the optimal number of clusters, such as silhouette width, AIC [35] and BIC [36] within the sum of the square (WSS) [37] and NbClust [38]. In this investigation, given that the performance of the AIC and BIC techniques decreases as the dimensionality of the data increases [39] and that the NbClust technique has higher precision than the WSS technique, the optimal number of clusters was identified by the NbClust technique. Specifically, as can be seen in Figure 7, the NbClust function for the input dataset discussed above gave the optimal cluster number for the k-means of the three clusters.

In Figure 8a, the result of the average silhouette technique for choosing the optimal number of clusters is shown; it can be seen that the results for two and three clusters were very close, although the test showed that two was the optimal number of clusters. The same is observable in Figure 8c; although the values of two and three were similar, this technique stated that the optimal choice was two clusters. On the other hand, using the elbow method, as shown in Figure 8b, it was observed that the optimal number of clusters was between three and four clusters. Finally, in Figure 8d, corresponding to the results of the NbClust method, it can be seen that the number of optimal clusters was between two and four, obtaining the highest result for three clusters. Therefore, based on these four analyses and taking into account the greater reliability of the NbClust method, it was established that the optimal number of clusters in this study for the input dataset was three.

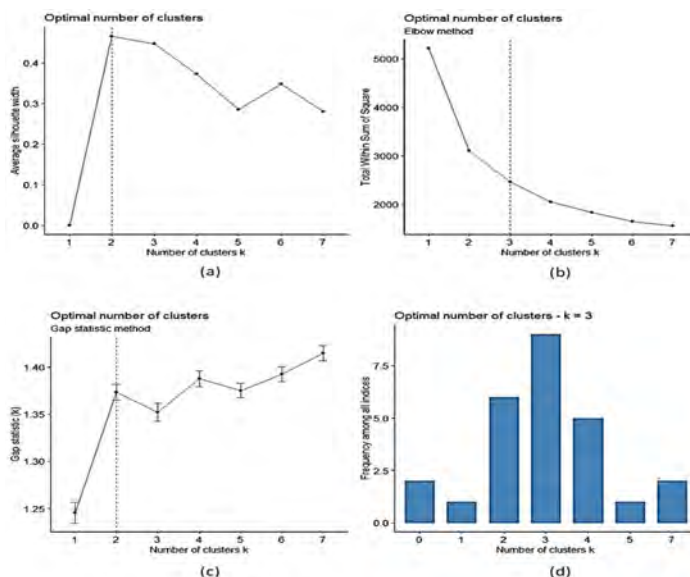


Figure 8. Determination of the optimal number of clusters, (a) average silhouette, (b) WSS and elbow technique, (c) gap statistic method, (d) NbClust.

4. Evaluation and Results

Throughout the previous section, the methodology used, the signals that were analyzed and their dimensional conversion into statistical variables were shown, ending with the method used for clustering and the optimal number of clusters for the proposed dataset.

This section shows the results obtained after using k-means for the grouping of the input dataset. First, the statistical data of each cluster generated were analyzed to determine the behavior corresponding to each cluster.

Table 1 shows the average distance between the points per cluster pair and the distance between the centers of each of the clusters. Several conclusions can be drawn from these values; the distance between centroids was greater between cluster 2 and cluster 3, so cluster 1 could be considered as the central cluster of data deviation, establishing itself as the pre-alarm cluster. Similarly, it was observed that the distance between cluster 1 and cluster 2 was greater than the distance between cluster 2 and cluster 3. This suggests that, due to the dispersion of the data, cluster 2 could be the cluster of points in alarm state.

Table 1. Matrix of separation values between all pairs of clusters and distance between centroids.

Cluster	1		2		3	
	Separation	Centroids	Separation	Centroids	Separation	Centroids
1	0.00	0.00	0.98	5.66	0.48	3.11
2	0.98	5.66	0.00	0.00	3.70	8.10
3	0.481	3.11	3.70	8.10	0.00	0.00

Table 2 shows the centroids obtained by k-means for each of the input variables; these centroids are the ones that were used to assign the membership of the checks to each cluster and, therefore, their alarm status.

Table 2. Cluster centroids for each dimension.

Cluster	C CV	C Q ₁	R CV	R Q ₁	C Q ₃	R Q ₃	IDR R	C Q ₂	R Q ₂	IDR C	DIM 1	DIM 2
1	0.71	0.64	0.48	0.65	−0.66	−0.62	0.83	−0.16	0.25	0.82	−1.58	−0.18
2	2.23	2.19	2.11	2.39	−2.39	−2.15	1.96	2.42	−2.61	1.83	1.86	0.67
3	−0.60	−0.55	−0.45	−0.57	0.58	0.54	−0.65	−0.11	0.07	−0.63	6.69	−2.26

To simplify the cluster plotting process for analysis, these centroids were dimensionally reduced from being ten dimensions, one for each input variable, to two dimensions. These two dimensions were obtained by means of PCA [40]. In Table 2, this reduction in dimensions can be observed with the centroids for dimension 1 (DIM 1) and dimension 2 (DIM 2).

To continue with the analysis of the results, the graphs in Figure 9 were analyzed. In this figure, the clusters are represented after their dimensional reduction to two unique dimensions, DIM 1 and DIM2, in order to plot a simpler graph. In the figure, four graphs are represented; two of them show the density distribution for each dimensional reduction. With the help of these two graphs, it can be concluded that, in cluster 3, there were data of those guns with a more stable milling and, therefore, they were correct. This can be confirmed since, observing the distributions of cluster 3 in both dimensions, it can be seen that there was a lower dispersion and a greater normality compared to the other clusters.

In the same way, following the same reasoning as for cluster 3, it was established that cluster 1 represents the millings that begin to be deficient, while cluster 2 groups the deficient millings that start to create quality problems in the welding points due to excessive wear of the electrodes.

Finally, Figure 10 shows the current graphs corresponding to each of the clusters. In Figure 10, three current curves grouped in cluster 3 are shown, which correspond to correct

operation; if compared with Figure 10a it can be observed that the curves of both graphs have a low dispersion and a stable behavior.

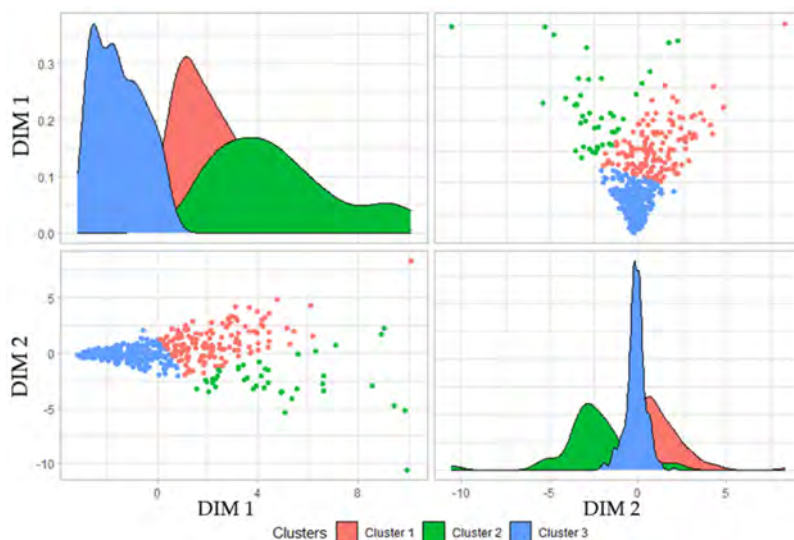


Figure 9. Result with dimensional reduction of the clustering for the input dataset.

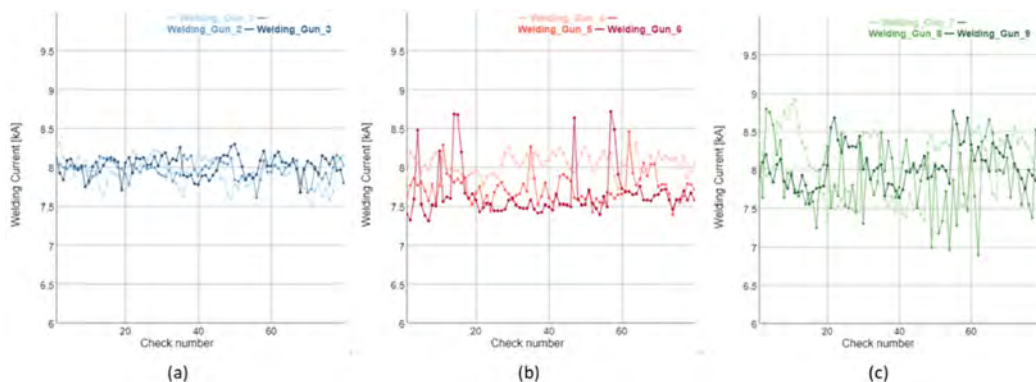


Figure 10. Examples of current measured depending on the cluster for different welding guns. (a) Cluster 3, determined as correct operation, (b) Cluster 1, determined as pre-alarm, (c) cluster 2, determined as alarm.

Figure 10b,c shows the current curves for clusters 1 and 2, respectively. From their analysis, it can be concluded that, as the data are assigned from pre-alarm cluster 1 to alarm cluster 2, the curves begin to show greater variance instability, which is an unequivocal sign that the electrodes presented a problem in milling and, therefore, increased wear, which will inevitably turn into quality problems at the weld point.

5. Application of the System for Real-Time Detection

This research was not only focused on finding a method that allows the detection of milling problems. The high production rate of manufacturing factories makes it essential that production defects are evaluated in real time. This allows the reduction of costs caused by having to repair products manufactured with poor quality since early detection can reduce the number of poor-quality products manufactured.

The clustering method for the detection of milling problems and electrode wear groups the behavior of the data series in three differentiated clusters: correct operation, pre-alarm and alarm. These three clusters, therefore, allow an algorithm to evaluate and label the status of each of the welding guns in a factory. The real-time detection system is designed to analyze each welding gun in particular and send the operators in charge of that welding line the alarm so that the defect and its possible consequences can be repaired.

As mentioned in the previous sections, a communication structure is necessary between the welding equipment and the database so that the data from all the welding equipment is accessible from the data analysis software. The system for detecting milling problems and electrode wear first collects resistance and current data from each of the welding equipment, labeling those controls that do not have enough data due to communication problems. Next, the extracted data are normalized, as described in the previous sections, and the dimensional reduction of input variables is carried out.

Once the reduction of the time series to the ten input variables has been carried out, the cluster each one of the analyzed pieces of welding equipment belongs to is determined. The assignment of each cluster is carried out by calculating the distance between each point with respect to the centroids of each of the clusters.

The assignment of each of the clusters determined after measuring the distance to each of them allows each piece of the welding equipment to be labeled according to its status in such a way that the welding equipment that is assigned to cluster 3 presents correct operation, and those in cluster 2 are in alarm and, therefore, require corrective action to be carried out.

Finally, once it has been determined that the welding guns have a behavior typical of electrodes with high wear, the alarm dispatch system is carried out to the production lines. In this case, a publish/subscribe protocol based on AMQP is established [41]. This protocol allows the sending of messages in specific queues. In this case, queues managed by RabbitMQ are used, which allows the sending of alarms through Webex to those in charge of repairing the conflicting equipment. The system is like the one proposed by García and Montes [42] for the acquisition of data from PLC in real time in factories, but, in this case, it is not based on data stored in a PLC but rather the welding equipment itself stores the data through Logstash, making it accessible from the data collector. In short, as described in Figure 11, the proposed system collects data directly from the real production lines and, after data processing, can label defects and send alarms for the repair and correction of quality problems produced.



Figure 11. Real-time data collection schema.

6. Conclusions

This research presents a novel method for the detection of milling problems and electrode wear using unsupervised clustering methods. Throughout this article, the relationship between the serial time data of resistance and the variation of the mechanical properties of the electrodes was described.

Despite working with time series, feature extraction was carried out to reduce dimensionality, which allowed the reduction of the number of input inputs of the clustering algorithm. This also allowed the input data to be scaled so that they were not influenced by the resistance differences existing in each welding gun.

The main advances obtained from this research were the following:

- A method for detecting the relationship between welding variables and milling state;
- An alarm system, where pre-alarm status and correct operation are established according to the output of the clustering algorithm;
- A system for the collection of data in a welding line that allows the realization of data analysis in real time, both for this investigation and for future investigations.

Despite the advances described, the system is still not capable of differentiating between types of fault. Different mechanical factors influence milling problems, such as worn blades, transformer secondary circuit problems, etc. The objective of future work in this investigation should go from the cataloging of faults as alarm, pre-alarm and correct status to a fault labeling system based on behavior pattern. In the same way, throughout this investigation, unsupervised learning methods were used due to the characteristics of the sample, but, in future works, we expect to continue in the line of experimentation with other analysis methods that could improve the detection system.

Author Contributions: Conceptualization, D.I., E.G. and J.S.; Formal analysis, D.I.; Investigation, D.I., E.G., J.S. and J.M.; Methodology, J.S. and J.M.; Project administration, E.G. and J.M.; Supervision, E.G. and J.S.; Validation, D.I. and J.M.; Visualization, D.I. and J.M.; Writing—original draft, D.I.; Writing—review & editing, E.G., J.S. and J.M. All authors have read and agreed to the published version of the manuscript.

Funding: This research received no external funding.

Institutional Review Board Statement: Not applicable.

Informed Consent Statement: Not applicable.

Data Availability Statement: Not applicable.

Acknowledgments: The authors thank Ford España S.A., and, in particular, the Almussafes Factory, for their support in the investigation. Likewise, the authors express their greatest gratitude to the “Fundación para el desarrollo y la innovación” (FDI), together with the Generalitat Valenciana, for supporting this research.

Conflicts of Interest: The authors declare no conflict of interest.

References

1. Hou, Z.; Kim, I.-S.; Wang, Y.; Li, C.; Chen, C. Finite element analysis for the mechanical features of resistance spot welding process. *J. Mater. Process. Technol.* **2007**, *185*, 160–165. [\[CrossRef\]](#)
2. Huh, H.; Kang, W. Electrothermal analysis of electric resistance spot welding processes by a 3-D finite element method. *J. Mater. Process. Technol.* **1997**, *63*, 672–677. [\[CrossRef\]](#)
3. Özyürek, D. An effect of weld current and weld atmosphere on the resistance spot weld ability of 304L austenitic stainless steel. *Mater. Des.* **2008**, *29*, 597–603. [\[CrossRef\]](#)
4. Aravinthan, A.; Nachimani, C. Analysis of Spot Weld Growth on Mild and Stainless Steel. *Weld. J.* **2011**, *90*, 143–147.
5. Tang, H.; Hou, W.; Hu, S.J.; Zhang, H.Y.; Feng, Z.; Kimchi, M. Influence of welding machine mechanical characteristics on the resistance spot welding process and weld quality. *Weld. J.* **2003**, *82*, 116–S–124–S.
6. Zhang, J.; Zhang, P.X.; Xu, X.J. A Model for Predicting the Wear Degree of Electrode Tip. *Appl. Mech. Mater.* **2014**, *574*, 292–297. [\[CrossRef\]](#)
7. Jeffus, L. *Welding Principles and Applications*, 4th ed.; Thomson Learning: Philadelphia, PA, USA, 1999; pp. 678–681.

8. Del Vecchio, E.J. (Ed.) *Resistance Welding Manual*; Resistance Welder Manufacturers' Association: Philadelphia, PA, USA, 1956; Volume 1.
9. Zhang, X.; Chen, G.; Zhang, Y. Characteristics of electrode wear in resistance spot welding dual-phase steels. *Mater. Des.* **2008**, *29*, 279–283. [\[CrossRef\]](#)
10. Tanaka, Y.; Sakaguchi, M.; Shirasawa, H. Electrode life in resistance spot welding of zinc plated steel sheets. *Int. J. Mater. Prod. Technol.* **1987**, *2*, 64–74.
11. Rashid, M.; Fukumoto, S.; Medley, J.B.; Villafuerte, J.; Zhou, Y. Influence of lubricants on electrode life in resistance spot welding of aluminum alloys. *Weld. J.* **2007**, *86*, 62-s.
12. Kondo, M.; Konishi, T.; Nomura, K.; Kokawa, H. Degradation mechanism of electrode tip during alternate resistance spot welding of zinc-coated galvanized and uncoated steel sheets. *Weld. Int.* **2013**, *27*, 770–778. [\[CrossRef\]](#)
13. Gould, J.E.; Kimchi, M.; Campbell, D.H. *Weldability and Electrode Wear Characteristics of Hot-Dip Galvanized Steel with and without a Ferrophos Containing Primer*; Report No. 880370; SAE: Detroit, MI, USA, 1988.
14. Saito, T.; Takahashi, Y.; Nishi, T. Electrode Tip Life in Resistance Spot Welding of Zinc and Zinc Alloy Coated Sheet Steels. *Nippon. Steel Tech. Rep.* **1988**, *37*, 24–30.
15. Athi, N.; Cullen, J.; Al-Jader, M.; Wylie, S.; Al-Shamma'A, A.; Shaw, A.; Hyde, M. Experimental and Theoretical Investigations to the Effects of Zinc Coatings and Splash on Electrode Cap Wear. *Measurement* **2009**, *42*, 944–953. [\[CrossRef\]](#)
16. De, A.; Dorn, L.; Gupta, O. Analysis and Optimisation of Electrode Life for Conventional and Compound Tip Electrodes During Resistance Spot Welding of Electrogalvanised Steels. *Sci. Technol. Weld. Join.* **2000**, *5*, 49–57. [\[CrossRef\]](#)
17. Fukumoto, S.; Lum, I.; Biro, E.; Boomer, D.R.; Zhou, Y. Effects of electrode degradation on electrode life in resistance spot welding of aluminum alloy 5182. *Weld. J.* **2003**, *82*, 307–312.
18. Wang, B.; Hua, L.; Wang, X.; Song, Y.; Liu, Y. Effects of electrode tip morphology on resistance spot welding quality of dp590 dual-phase steel. *Int. J. Adv. Manuf. Technol.* **2015**, *83*, 1917–1926. [\[CrossRef\]](#)
19. Chan, K.R. *Weldability and Degradation Study of Coated Electrodes for Resistance Spot Welding*. Master's Thesis, University of Waterloo, Waterloo, ON, Canada, 2005.
20. Xia, Y.-J.; Su, Z.-W.; Li, Y.-B.; Zhou, L.; Shen, Y. Online quantitative evaluation of expulsion in resistance spot welding. *J. Manuf. Process.* **2019**, *46*, 34–43. [\[CrossRef\]](#)
21. Gauthier, E.; Carron, D.; Rogeon, P.; Pilvin, P.; Pouvreau, C.; Lety, T.; Primaux, F. Numerical Modeling of Electrode Degradation During Resistance Spot Welding Using CuCrZr Electrodes. *J. Mater. Eng. Perform.* **2014**, *23*, 1593–1599. [\[CrossRef\]](#)
22. Raoelison, R.; Fuentes, A.; Pouvreau, C.; Rogeon, P.; Carré, P.; Dechalotte, F. Modeling and numerical simulation of the resistance spot welding of zinc coated steel sheets using rounded tip electrode: Analysis of required conditions. *Appl. Math. Model.* **2014**, *38*, 2505–2521. [\[CrossRef\]](#)
23. Peng, J.; Fukumoto, S.; Brown, L.; Zhou, N. Image analysis of electrode degradation in resistance spot welding of aluminium. *Sci. Technol. Weld. Join.* **2004**, *9*, 331–336. [\[CrossRef\]](#)
24. Zhang, Y.S.; Wang, H.; Chen, G.L.; Zhang, X.Q. Monitoring and intelligent control of electrode wear based on a measured electrode displacement curve in resistance spot welding. *Meas. Sci. Technol.* **2007**, *18*, 867–876. [\[CrossRef\]](#)
25. Zhou, L.; Li, T.; Zheng, W.; Zhang, Z.; Lei, Z.; Wu, L.; Zhu, S.; Wang, W. Online monitoring of resistance spot welding electrode wear state based on dynamic resistance. *J. Intell. Manuf.* **2020**, *33*, 91–101. [\[CrossRef\]](#)
26. Zhao, D.; Bezgans, Y.; Wang, Y.; Du, W.; Vdonin, N. Research on the correlation between dynamic resistance and quality estimation of resistance spot welding. *Measurement* **2021**, *168*, 108299. [\[CrossRef\]](#)
27. Wang, S.C.; Wei, P.-S. Modeling Dynamic Electrical Resistance During Resistance Spot Welding. *J. Heat Transf.* **2000**, *123*, 576–585. [\[CrossRef\]](#)
28. *DIN EN ISO 5821:2010-04*; Resistance Welding—Spot Welding Electrode Caps (ISO 5821:2009). German Version EN ISO 5821:2009; ISO: Geneva, Switzerland, 2009.
29. Michael, M.; Davvid, S. The Rise of Elastic Stack. 2016. Available online: https://www.researchgate.net/publication/309732494_The_Rise_of_Elastic_Stack?channel=doi&linkId=5820655c08ae40da2cb4e19a&showFulltext=true (accessed on 20 April 2022).
30. Mohamad, I.B.; Usman, D. Standardization and Its Effects on K-Means Clustering Algorithm. *Res. J. Appl. Sci. Eng. Technol.* **2013**, *6*, 3299–3303. [\[CrossRef\]](#)
31. Lakshmanan, M.; Karnan, H.; Natarajan, S. *Smart Diagnosis of Cardiac Arrhythmias Using Optimal Feature Rank Score Algorithm for Solar Based Energy Storage ECG Acquisition System*; Academic Press: Cambridge, MA, USA, 2020. [\[CrossRef\]](#)
32. MacQueen, J. Some methods for classification and analysis of multivariate observations. In Proceedings of the Fifth Berkeley Symposium on Mathematical Statistics and Probability, Berkeley, CA, USA, 21 June–18 July 1965 and 27 December 1965–7 January 1966; Statistical Laboratory of the University of California: Berkeley, CA, USA, 1967.
33. Steinley, D. K-means clustering: A half-century synthesis. *Br. J. Math. Stat. Psychol.* **2006**, *59 Pt 1*, 1–34. [\[CrossRef\]](#) [\[PubMed\]](#)
34. Swana, E.; Doorsamy, W. An Unsupervised Learning Approach to Condition Assessment on a Wound-Rotor Induction Generator. *Energies* **2021**, *14*, 602. [\[CrossRef\]](#)
35. Akaike, H. Factor analysis and AIC. *Psychometrika* **1987**, *52*, 371–386. [\[CrossRef\]](#)
36. Burnham, K.P.; Anderson, D.R. Multimodel inference: Understanding AIC and BIC in model selection. *Sociol. Methods Res.* **2004**, *33*, 261–304. [\[CrossRef\]](#)

37. Amruthnath, N.; Gupta, T. Fault Class Prediction in Unsupervised Learning using Model-Based Clustering Approach. In Proceedings of the 2018 International Conference on Information and Computer Technologies (ICICT), Libertad City, Ecuador, 10–12 January 2018; pp. 5–12.
38. Malika, C.; Ghazzali, N.; Boiteau, V.; Niknafs, A. NbClust: An R Package for Determining the Relevant Number of Clusters in a Data Set. *J. Stat. Softw.* **2014**, *61*, 1–36.
39. Broman, K.W.; Speed, T.P. A model selection approach for the identification of quantitative trait loci in experimental crosses. *J. R. Stat. Soc. Ser. B (Stat. Methodol.)* **2002**, *64*, 641–656. [[CrossRef](#)]
40. Salem, N.; Hussein, S. Data dimensional reduction and principal components analysis. *Procedia Comput. Sci.* **2019**, *163*, 292–299. [[CrossRef](#)]
41. AMQP: Advanced Message Queuing Protocol, Version 0.8. AMQP Working Group Protocol Specification. 2006. Available online: <https://www.rabbitmq.com/resources/specs/amqp0-8.pdf> (accessed on 20 April 2022).
42. Garcia, E.; Montes, N. Mini-term, a novel paradigm for fault detection. *IFAC-PapersOnLine* **2019**, *52*, 165–170. [[CrossRef](#)]

Chapter 4. REAL-TIME MONITORING OF ELECTRODE ALIGNMENT

This chapter presents a new advancement of the detection method for electrode misalignment in resistance spot welding (RSW). Electrode misalignment is a common mechanical problem that causes quality issues such as undersized welds and non-rounded joints. The first paper presents a first proposal of a new method for detecting misalignment through the analysis of the magnetic field generated by short-circuited electrodes. Second paper delves deeper into the optimization of the method and examines the robustness of the magnetic field in welding electrodes through simulations. Finally, the last paper presents an implementable solution for the detection of misalignments in real industrial production lines.

During this research, three scientific articles were developed to address the issue of electrode misalignment in resistance spot welding (RSW). The first article provides a starting point for the investigation by discussing the significance of electrode misalignment as a mechanical factor in RSW and the problems it causes, including increased cost due to manual repairs. The article proposes a novel solution to detecting misalignment through measurement of the magnetic field generated by the electrodes. The method is validated through simulation and tested in an automotive production line.

The second article furthers the study of the proposed method by analyzing the robustness of the magnetic field analysis in different typical welding gun scenarios. The goal is to determine if other mechanical problems in the welding gun could cause false positives in misalignment detection and to what extent they can be detected.

The third article presents a practical solution for the detection of electrode misalignment in an industrial setting. The method for monitoring electrode alignment is developed based on previous research, which showed the relationship between misalignment and the magnetic field generated by short-circuited electrodes. A device is created to measure the magnetic field, and a system is implemented for real-time detection of misalignments. This system sets behaviour thresholds based on experimentation and allows for condition monitoring after each welding cycle.

Overall, the three articles contribute to the advancement of understanding and addressing the issue of electrode misalignment in RSW. Through this research, a novel approach to detecting misalignment has been proposed, tested, and proven to be a valuable solution for the industry.

4.1 SCIENTIFIC CONFERENCE ARTICLE I

Title: Real-time Electrode Misalignment Detection Device for RSW Basing on Magnetic Fields.

Authors: Daniel Ibáñez, Eduardo García, Julio Martos and Jesús Soret.

Published in: Proceedings of the 17th International Conference on Informatics in Control, Automation and Robotics (ICINCO 2020), Paris, France. 2020. p. 7-9.

Description: ICINCO (International Conference on Informatics in Control, Automation and Robotics) is an annual international conference organized by the Institute for Systems and Technologies of Information, Control and Communication (INSTICC), a non-profit scientific organization aimed at promoting research and education in the areas of systems and information technologies and control. The main goal of ICINCO is to bring together researchers, engineers, and academics from all over the world to present and discuss the latest advances in the fields of informatics, control, automation, and robotics. Each article presented at the conference goes through a peer review process to ensure its quality and originality. Since its establishment in 2004, ICINCO has become a significant platform for the presentation and discussion of the latest advances in these fields, attracting participants from all over the world.

Real-Time electrode misalignment detection device for RSW basing on magnetic fields

D.Ibáñez¹^a, E. García²^b, J.Martos¹^c and J. Soret¹^d

¹ Dept. of Electrical and Electronic Engineering, University of Valencia, Burjassot, Valencia, Spain

² Ford Valencia, 46440, Valencia, Spain

{Daniel.ibanez, Jesus.Soret,Julio.Martos}@uv.es, egarci72@ford.com

Keywords: Resistance spot welding, detection, Hall Effect sensors, electrodes, misalignment, magnetic field, simulation.

Abstract: Electrodes misalignments are considered one of the most important mechanical factors involved in RSW (Resistance Spot Welding). Misalignment causes quality problems as undersized weld, expulsions or nonrounded-weld. Man-power needed in the automotive production lines is increased so as to repair the lack of quality, which means an increase in the cost of production. Consequently, an implantable solution for the automotive industry should be developed in order to detect misalignment when this happens. This research gives an answer by measuring the electrode misalignment by means of the generated magnetic field for the electrodes. The proposed method is validated by Multiphysics simulation measurement. Finally, this method is put into practice by creating a device tested in an automotive production line at the assembly and body plant in Ford Valencia. Together with the device, a communication system is implemented to carry out predictive management. This research initiates a novel line of research for the early and online detection of misalignment problems in welding guns.

1. INTRODUCTION

The resistance spot welding process bases its operation on a current flow from the tip of the upper electrode between the metals to be welded to the tip of the lower electrode. When the current circulates through the metals, and due to Joule's law, the heat generated melts the metals forming a weld joint between the metal sheets through the fusion and the result is a strong weld between sheets without additional substances. Therefore, the growth of the weld (welding nugget) depends on the density of welding current, the welding time, the force exerted by the electrodes on the sheets and the area of the electrode tip (Aravinthan et al.,2011)

This dependence is different depending on the parameter, since the time and the current make the welding, while the pressure and the area of the electrode tip have a direct relationship with the final quality of the welding.

Misalignment of the electrodes causes a variation in the contact area between the electrode tips. The alignment of electrodes can be classified into three types depending on their orientation. The electrodes can be perfectly aligned, axially misaligned or angularly misaligned, as shown in Figure 1(Zhang et al.,2005).

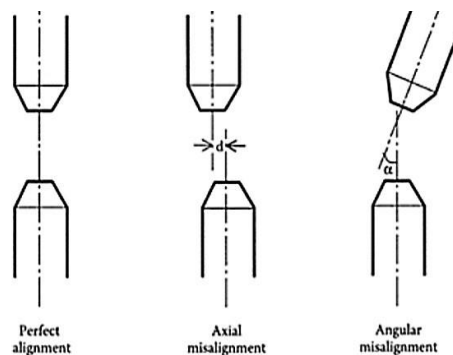






Figure 1. Types of electrode misalignment RSW.

^a <https://orcid.org/0000-0002-3917-9875>

^b <https://orcid.org/0000-0002-4210-9835>

^c <https://orcid.org/0000-0002-8455-6369>

^d <https://orcid.org/0000-0001-8695-6334>

Different studies have shown the alignment of the electrode plays an important role in the geometry of the welding point, Figure 2, in addition the misalignment of the electrode causes expulsion, which leads to poor welding zones Tang et al.,2003), (Charde,2012).



Figure 2. Poor-quality spot causes by misalignment.

Some authors have proposed different methods for detecting misalignment using image processing methods, by which they are able to determine the direction and angle of misalignment with good results (Li et al.2019). The main problem presented by this method is the cost of implementation for a high production line with many welding guns. Therefore, there is not a viable method for detecting misalignment in this type of production lines.

Due to the reasons mentioned above, there is a need to investigate a simple and economical method for the detection of misalignment, since what is sought is that it can be used in the high-production automotive industry.

The theoretical basis of this method is laid on the variation of the current density at the tip of the electrode. Specifically, what is intended with this method is to identify the change in current density as the misalignment appears.

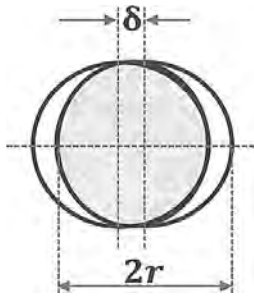


Figure 3. Geometric model for calculating contact area due to axial misalignment.

When the electrodes are misaligned, as shown in

Figure 3, the contact area (C_a) of the electrode tips varies according to the equation 1.

$$C_a = 2r^2 \sin^{-1} \left(\sqrt{1 - \left(\frac{\delta}{2r} \right)^2} \right) - \delta \sqrt{r^2 - \left(\frac{\delta}{2} \right)^2}$$

where C_a is the contact area of the electrodes, r is the radius of the electrode and δ is the amount of misalignment.

It can be seen from the equation that the reduction of the contact area is strongly correlated with the axial misalignment.

From the Ampère's Integral Law can be obtained the relationship between the magnetic field (B) and the current density. This law relates the magnetic field intensity to its source, the current density.

$$\oint_C \vec{B} \cdot d\vec{l} = \mu_0 \int_S \vec{J} \cdot d\vec{S} + \mu_0 \epsilon_0 \int_S \vec{E} \cdot d\vec{S}$$

Where the magnetic field is described by the variable B , the current density by J and the electric field by E .

Following the equation 2, it can be affirmed that if the current flows through the electrodes, and therefore there is a current density, a rotational magnetic field around the electrodes appear and the rotor of the magnetic field points in the same direction that the current density, this behaviour is represented in Figure 4.

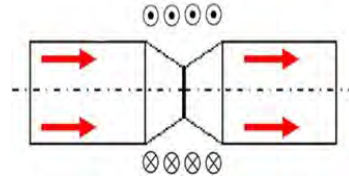


Figure 4. Generated Magnetic Field.

As a result, basing in this equation, it can be affirmed that when electrodes are misaligned, the contact area of the electrodes decreases, which produces a raising on the current density and consequently a magnetic field higher than which is generated with a correct electrode alignment.

2. MISALIGNMENT DETECTION METHOD.

As shown in the previous section, a possible relationship between the magnetic field generated by the short-circuited electrodes and their misalignment can be deduced mathematically. The

proposed method for the detection of the misalignment is based on the measurement of the magnetic field in the contact plane of the electrodes.

The measurements should be carried out in such a way that a value is obtained for determining the direction of the misalignment of the electrodes.

For this, it is postulate that if the contact plane is divided into the Cartesian axes and measurements are made at different distances from the centre of the ideal contact surface of the electrodes, could be detected the misalignment of the electrodes and its direction.

This means that if the magnetic field can be measured in both Cartesian axes, both in positive and in negative, it will be possible to determine the difference of the magnetic field generated by the misaligned electrodes in comparison with the one generated by the perfectly aligned electrodes.

As it is a novel hypothesis, due to the fact that other researchers haven't published anything related to the relationship between the magnetic field and the misalignment, it is fundamental to demonstrate it. Firstly, performing a validation by means of simulation of the physical phenomenon, to verify that, in fact, the mathematical assumption is fulfilled.

For the validation of this method, software of simulation of the physical phenomenon based on magnetic field theory is used.

Once the hypothesis has been validated for the proposed method, a device would be developed for taking measurements in an industrial environment, capable of determining the differences between simulation and real experimentation to finally design an automatic system for detecting problems of alignment of welding electrodes in real time.

3. MATERIALS AND METHODS

For the analysis of the behaviour of the magnetic field depending on the state of the misalignment, a physical phenomenon simulation software is drawn on. The simulations are carried out for the symmetry of an F- type electrode (ISO 5821,2007) with the following data:

- Current flowing through the electrode: 8 kA.
- Diameter of the electrode tip: 6mm.
- Electrode body diameter: 20 mm.
- Cone height: 5mm.

These simulations are performed simulating a current flowing between the electrodes shorted. To obtain the relationship between misalignment and generated magnetic field.

During this validation, three tests will be performed. In the first one, the magnetic field

generated for an electrode in which $\delta = 0$ mm, i.e., a perfectly aligned electrodes, is simulated. In the second, the value of δ is increased up to 1mm and the magnetic field is simulated, comparing the values of both cases. Finally, the value δ is increased again up to 2mm and the simulation is carried out, comparing all the obtained values.

For each of the cases, two simulations are carried out. In the first simulation, the values of the magnetic field are collected depending on the distance on the x- axis to the centre of the electrode. These values are simulated for both the contact plane of the electrodes, $z = 0$ mm, as for planes situated $z = 10$ mm and $z = -10$ mm.

In the second simulation, the data is acquired in this case as a function of the displacement in the z- axis. In this simulation, two data curves are obtained: the variation of the magnetic field on the z-axis when $x = 20$ mm and the variation of the magnetic field on the Z-axis when $x = -20$ mm.

4. MAGNETIC FIELD SIMULATION

This section shows the results of the different simulations carried out as described in the previous section.

4.1 $\delta=0$ mm

As mentioned, simulations are carried out for three different scenarios. In this first case, two electrodes perfectly aligned are simulated, $\delta=0$ mm and $S= 50.26$ mm². This first case points what is the ideal value of the magnetic field generated by the electrodes. The following cases should therefore be compared with this to determine if there is certainly a relationship between the misalignment and the generated magnetic field.

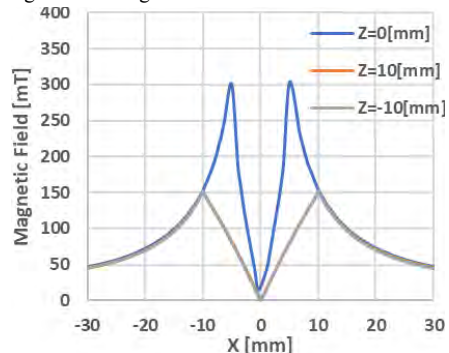


Figure 5. Magnetic Field Generated for aligned electrodes. X-axis displacement

From this simulation, the data represented in Figure 5 and Figure 6 are obtained. As it can be seen, both in the data of Figure 5, which shows the evolution of the magnetic field on the x axis, and the one of Figure 6, which shows the evolution of the magnetic field in the y-axis, there is a symmetry in the generated magnetic field.

Hence, this means that when measuring at the same distances from the centre of the generated magnetic field, the same value is obtained. This point is very important because what is sought in this study is to be able to determine the misalignment but also the direction of it.

In addition, this data also shows how the Ampere law is fulfilled. By analysing the three curves of Figure 7, it can be observed how those taken on the planes $z = -10\text{mm}$ and $z = 10\text{mm}$, present a lower magnetic field value. This is because at this height, the surface through which the intensity flows are $S = 314.15\text{mm}^2$. This makes the current density lower and therefore the magnetic field is lower too

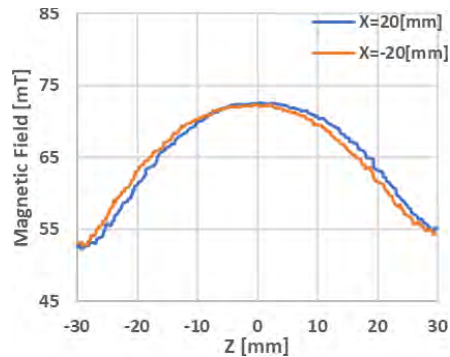


Figure 6 Magnetic Field Generated for aligned electrodes. z-Axis displacement

4.2 $\delta=1\text{mm}$

In this second case, electrodes with a displacement of the upper electrode of 1mm are simulated, that is, $\delta = 1\text{mm}$. Using equation 1 it can be calculated that the contact surface for this case will be $S = S \cdot \text{Cr} = 50.26 \cdot 0.7623 = 38.31 \text{ mm}^2$.

Therefore, according to the hypothesis, the magnetic field generated by the electrodes must be higher since the current density increases.

Figure 7 shows how, as expected, the simulated magnetic field is greater than the magnetic field of Figure 5. The maximum value of the generated magnetic field is 340 mT, which represents an increase in the magnetic field by approximately 111% compared to the field generated by the

perfectly aligned electrodes.

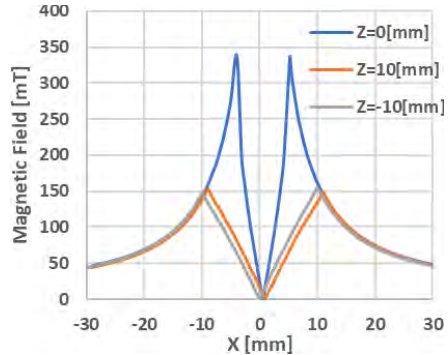


Figure 7. Magnetic Field Generated for electrodes with $\delta=1\text{mm}$. X-axis displacement.

To make the comparison between the different cases, the data is analysed at 20mm from the centre of the magnetic field for the perfectly aligned electrodes. This centre is shown in the graphs as the zero of the coordinate axes. This analysis is done in a more graphical way observing the Figure 6 and 8 that represents the displacement in the Z-axis, since the data represented in it are those corresponding to the distances 20mm and -20mm.

If the data of $x = 20\text{mm}$ and $x = -20\text{mm}$ are taken at the time when $z = 0\text{mm}$, it can be observed that for the aligned electrodes this takes a similar value of 72 mT approximately.

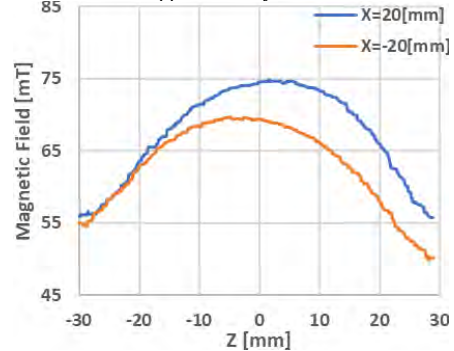


Figure 8. Magnetic Field Generated for electrodes with $\delta=1\text{mm}$. z-Axis displacement

On the other hand, with the data collected for this second case, it is observed that for $x = 20\text{mm}$ the value of the magnetic field is equal to 74.5 mT, while for $x = -20\text{mm}$ the magnetic field is equal to 69.5mT. This means that while in the first case the difference between $x = 20\text{mm}$ and $x = -20\text{mm}$ is 0

mT, in the second case this difference increases significantly up to 5 mT.

It is also important to point out that because of the fact that one of the electrodes has moved but the other has been fixed, the centre of the magnetic field has been shifted 0.5 mm. This also rise the difference between the values in the x positive and negative x.

4.3 $\delta=3\text{mm}$.

In this last case the misalignment of the electrodes increases δ up to 3 mm. This supposes a misalignment of 50% of the maxim misalignment. This last simulation helps to determine in a more reliable way if it is possible to differentiate different states of misalignment.

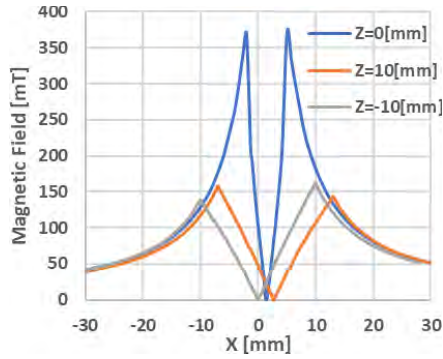


Figure 9 Magnetic Field Generated for electrodes with $\delta=2\text{mm}$. X-axis displacement.

In this case, using equation 1 again, the actual contact surface of the electrodes can be calculated. Since δ has increased to 2mm, the ratio between the ideal surface and this new surface decreases to 0.5309. Therefore, the current surface is 26.68 mm^2 .

As in the previous case, it can be seen in Figure 9 that the maximum magnetic field generated is higher than the other two cases, taking a value of 376 mT.

This represents an increase of 123% and 111% respectively.

Following in this case the previous analysis about the measurement differences between $x = 20\text{mm}$ and $x = -20$ can be seen, as in the previous result, that there is no symmetry. For $x = 20\text{mm}$ a value of 81 mT is recorded, while for $x = -20\text{mm}$ a value of 65mT is recorded.

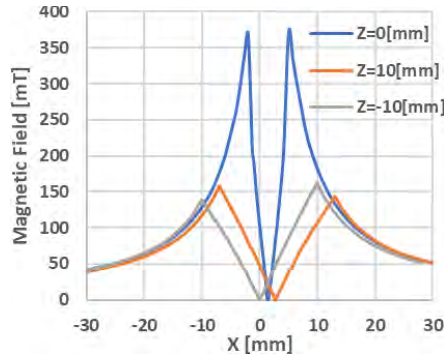


Figure 10. Magnetic Field Generated for electrodes with $\delta=2\text{mm}$. X-axis displacement.

Therefore, in this third case it can be seen how the difference between both measures increases again while the misalignment increases too, going from a difference of 0 mT for the misaligned electrodes to a difference of 16 mT

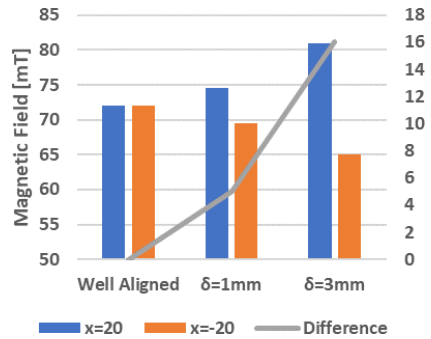


Figure 11. Summary of simulation result.

Finally, Figure 11 summarizes the most relevant values of this validation by simulation. Then, the results show that there is a strong relationship between the generated magnetic field and the alignment of the electrodes. So, the hypothesis has been validated.

5. SIMPLE DEVELOPMENT OF A DEVICE FOR THE DETECTION

Once the hypothesis has been validated, it is necessary to study how this new method can be applied to the high production industry of the automobile.

As it has been explained, it is necessary to make measurements of the magnetic field in the contact plane of the electrodes. Therefore, it is necessary to perform four measurements of the magnetic field, two for each of the axes x-y. For this, it is necessary to located sensors capable of performing these measurements at $x = 20\text{mm}$, $x = -20\text{mm}$, $y = 20\text{mm}$ and $y = -20\text{mm}$.

In this case, two PCB are manufactured, one in which four low-cost hall effect sensors are located, which will be where the measurement is made. In this first PCB it is designed with a circular hole in the middle, so that the four hall effect sensors are distributed to perform measurements on the two cartesian axes.

In the second PCB the microcontroller used to control the signals collected by the sensors is located. To isolate the two PCBs, a 3D printed PCA encapsulation is performed. This design is made to optimize costs and increase the robustness of the design.

This device is designed so that the electrodes can be closed and positioned in the middle of the four sensors. Once located in that position, a current is passed between the short-circuited electrodes and the sensors measure the generated magnetic field.

Figure 12 shows the location on the real welding line of the PCB on which the Hall Effect sensors are mounted.



Figure 12. Actual PCB location for magnetic field measurement.

This measured magnetic field data is sent to the second PCB where the microprocessor that manages these signals is located. There the voltage values measured by the sensors are converted to magnetic field units.



Figure 13. Actual PCB location for collection of the data.

Figure 13 shows the situation of the PCB, in which the microprocessor is located, in the actual welding line.

The signal management is carried out following the flow chart of Figure 15. Once the microcontroller is initialized, a first measurement of the magnetic field is made to determine the offset of the sensors, thus eliminating the possible differences between the measurements.

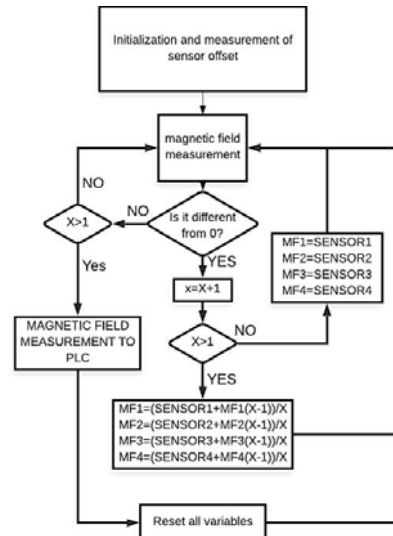


Figure 14. Operating flow chart

Once this action is carried out, the four sensors begin to record the magnetic field value, if the measured magnetic field is zero, the microcontroller



Figure 15. Measurement process flow

does not perform any calculation. Once the electrodes are short-circuited and generate a magnetic field, the microcontroller begins to register the values by calculating at all times the average value of the magnetic field measured in that period of time, so that the possible peaks that could appear are reduced by Use the average.

When the electrodes stop conducting current, the sensors re-measure the absence of magnetic field and at that time, the microcontroller sends the values to the PLC.

After communication with the PLC, the variables are reset to 0 and the measurement is restarted waiting again for the magnetic field generated by the electrodes in short circuit.

6. REAL-TIME CONTROL APPLICATION

Once a device capable of detecting the magnetic field has been developed, and therefore, the problems of alignment of the electrodes in the welding clamps, it is necessary to develop a final system capable of carrying out preventive maintenance on the actual welding line.

In such a way that patterns of misalignment behaviour and work limits are established based on history and experimentation. To do this, once the process described in Figure 14 is finished, when the data is already in the PLC, this data is stored in a database and sent to a web server. This whole process can be summarized in Figure 15.

In this case, in order to reduce the number of variables on which to perform the analysis, the four variables of each of the sensors are reduced by only two.

These two variables are calculated by subtraction between the sensors placed antiparallel, therefore, the two final variables will represent the displacement of the centre of the magnetic field on the X and Y axes, eliminating the absolute value of

each of the four sensors.

Starting from the established values of the simulation first and after the values stored in the history, the alarm and pre-alarm levels for each of the Cartesian axes can be established. As shown in figure 16.

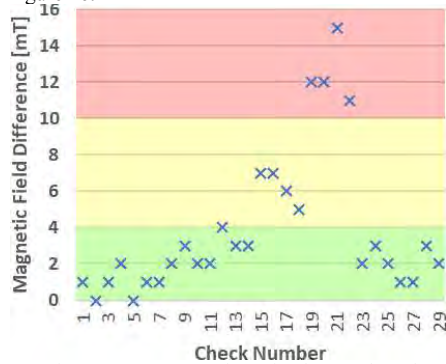


Figure 16. Example of alarms based on simulation.

Currently, this whole real-time medicine process is installed in a welding line. This application allows to obtain the data of each check in the attempt in which it is performed.

This last part of the investigation is still in an exact process of validation, since it is convenient to test all the cases and the real behaviour of a welding clamp, beyond the simulation results.

7. CONCLUSION

This article tries to give a solution to this important problem of misalignment in the electrodes of the welding guns. This problem directly affects the

costs of production of automobile manufacturing, so it is mandatory to find a solution that can be implantable, i.e., a solution that does not involve a high cost of implementation. This

article responds positively, presenting a method for detecting the misalignment by magnetic fields.

For the method validation, mathematical calculations and simulations are used, in which it is observed how, unequivocally, there is a strong relationship between both factors.

Finally, a device for measuring the magnetic field is proposed, this device is composed of four hall effect sensors managed by a microcontroller. For the validation of the sensor, tests in a line of production of the automobile in Valencia Body and Assembly plant are carried out.

Although the data collection is not yet extensive enough, a historical data collection is begun to monitor the behaviour of the magnetic field generated by real misaligned electrodes.

In future investigations, the data obtained in the actual welding line should be analysed. Based on these results, a possible update of the method and the designed device should be performed.

In addition, an exhaustive study of the influence of the existing noises on the production lines and their influence on the measures taken must be made.

ACKNOWLEDGEMENT

The authors wish to thank Ford España S.A, in particular, the Almussafes factory for their support in the present research.

REFERENCES

Aravinthan, A. and Nachimani, C. 2011. Analysis of Spot Weld Growth on Mild and Stainless Steel. *Welding Journal* August 2011: 143-147.

Claude Cohen-Tannoudji; Bernard Diu et Frank Lalœ 1977. *Mécanique quantique*, vol. I et II. Paris: Collection Enseignement des sciences (Hermann).

Richard Feynman 1974. *Feynman lectures on physics* Volume 2. Addison Wesley Longman.

ISO 5821 [2007] Resistance Spot Welding Electrode Caps. Tang, He (Herman) & Hou, W. & Hu, S.J. &

Zhang, H.Y. & Feng, Z. & Kimchi, Menachem. 2003. Influence of welding machine mechanical characteristics on the resistance spot welding process and weld quality. *Welding journal*. 82. 116/S-124/S.

Charde, Nachi Mani. 2012. Effects of electrode deformation on carbon steel Weld. *International Journal of Advance Innovation, Thoughts and Ideas*. 1. 8.

Li, Yanqing & Tang, Guokun & Ma, Yongsheng & Shuangyu, Liu & Ren, Tao. (2019). An electrode misalignment inspection system for resistance spot welding based on image processing technology.

Measurement Science and Technology. 30. 10.1088/1361- 6501/ab1245.

Zhang, H. & Senkara, J. 2005. *Resistance welding: Fundamentals and applications*.

Walker, Jearl; Halliday, David; Resnick, Robert 2014. *Fundamentals of physics* (10th ed.). Hoboken, NJ: Wiley. p. 749.

4.2 SCIENTIFIC CONFERENCE ARTICLE II

Title: Influence of Mechanical Failures of the Welding Gun on the Magnetic Field Generated in the Measurement of Misalignment.

Authors: Daniel Ibáñez, Eduardo García, Julio Martos and Jesús Soret.

Published in: Informatics in Control, Automation and Robotics: 17th International Conference, ICINCO 2020 Lieusaint-Paris, France, July 7–9, 2020, Revised Selected Papers (pp. 32-46). Springer International Publishing.

Description: Lecture Notes in Electrical Engineering (LNEE) is a book series published by Springer that covers various topics related to electrical engineering. The series aims to publish high-quality, peer-reviewed books that provide comprehensive coverage of current research in electrical engineering. Volume 793 contains the "Informatics in Control, Automation and Robotics: 17th International Conference, ICINCO 2020 Lieusaint - Paris, France, July 7–9, 2020, Revised Selected Papers". This book includes selected papers from the 17th International Conference on Informatics in Control, Automation and Robotics (ICINCO 2020).



Influence of Mechanical Failures of the Welding Gun on the Magnetic Field Generated in the Measurement of Misalignment

D. Ibañez¹ , E. García² , J. Soret¹ , and J. Martos¹ 

¹ Department of Electrical and Electronic Engineering, University of Valencia, Burjassot, Valencia, Spain

{Daniel.Ibanez, Jesus.Soret, Julio.Martos}@uv.es

² Ford Valencia, Valencia, Spain

egarci75@ford.com

Abstract. The present work presents an advance in the method for the detection of electrode misalignment. In previous research, a new method for detecting misalignment of the electrodes was shown, in which, it was stated that by means of the analysis of the magnetic field generated by the short-circuited electrodes, it was possible to determine if the electrodes were well aligned [1]. This paper seeks to continue with the optimization of the method, delving into the behavior of the magnetic field in the welding electrodes. Throughout this paper simulations of the different typical cases of welding guns that could influence the measurement of the magnetic field are carried out. In short, this work analyzes the theoretical robustness of the method. Welding guns often present other mechanical problems apart from misalignment of the electrodes, therefore, it is essential to study if these problems would cause false positives in detection and to what extent these mechanical problems could or could not be detected using the same method. This paper serves to validate the method definitively and give a positive response to what has been carried out in previous publications.

Keywords: Resistance spot welding · Electrode misalignment · Current density · Multiphysics simulation · Magnetic field

1 Introduction

In production processes adapted to the new era of industry, such as vehicle production processes, a high product quality is required. New advanced technologies are increasingly necessary for maintenance for both preventive and predictive maintenance [2, 3].

Due to this, a profound improvement of the automobile production process is increasingly essential, optimizing the way of carrying out the maintenance of production lines. Resistance spot welding (RSW) is the most common process for joining thin metal in automotive body structures [4, 5], currently it is estimated that around 2500–5000 weld joints are used during the manufacturing process of a car body, so it is essential to avoid any type of quality defect caused by equipment malfunction [6].

Currently, the monitoring and diagnosis methods of the tool's conditions can be classified into two methods: offline and online. The method carried out offline, usually requires a direct measurement of the tool or the equipment to measure during the process and, therefore, production must be stopped frequently to carry out the necessary measurements to determine the state of the tool or the quality of the production measurement [7].

Normally, offline methods provide a better result in the motorization of defects since the measurement is taken directly on the tool or the manufactured part. The main problem with this method is that it is sometimes not applicable in an automated manufacturing system since the costs in the stoppages due to the processes to take the measurements can increase the downtime of the machines and, consequently, they are increased by production cycle times.

On the other hand, online detection methods, which can also be referred to as indirect methods, provide better responses in automated production processes. Usually these methods do not work through a direct measurement, as in online methods, but usually require external signals and a subsequent processing of the signals to determine the status of the tools or the quality of the production. This allows detection to be carried out on-site and line downtime is reduced.

In this paper, the axial misalignment of the electrode is considered one of the main causes of quality defects in resistance welding. The misalignment of the electrodes usually causes a variation in both the shape and the contact area of the electrodes. This misalignment greatly influences the final geometry of the weld joint. In the same way, the variation of the contact surface modifies the way in which the welding energy is supplied to the joint so that sometimes projections and loose welds can be caused. Ultimately, misalignment can cause most of the defects present in resistance welding [8, 9].

The main goal is to develop an improved diagnosis system that works robustly in real time. To this end, research continues on the detection of misalignment of the electrodes by means of magnetic fields [1].

$$C_a = 2r^2 \sin^{-1} \left(\sqrt{1 - \left(\frac{\delta}{2r} \right)^2} \right) - \delta \sqrt{r^2 - \left(\frac{\delta}{2} \right)^2} \quad (1)$$

In the previous research, the relationship between the misalignment of the electrodes and the value of the magnetic field was unequivocally demonstrated. This method bases its operation on the variation of the contact surface when misalignment (δ) occurs (1), this variation causes a change in the current density that exists in the short-circuited electrodes, Fig. 1.

Based on Faraday's law, it is stated that if there is a variation in the current density, there must also be a variation in the generated magnetic field [10–12] Fig. 2, so that a misalignment of the electrodes causes an increase in the generated magnetic field.

This research seeks to go further in the robustness of the method, since other mechanical defects of the welding guns could cause changes in the current density parameters. This study aims to rule out future problems in the possible applications of this method in real welding lines, avoiding false positives due to other defects.

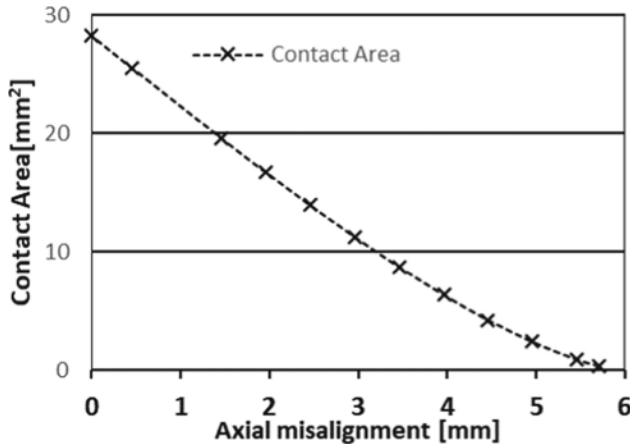


Fig. 1. Relationship between axial misalignment and contact area.

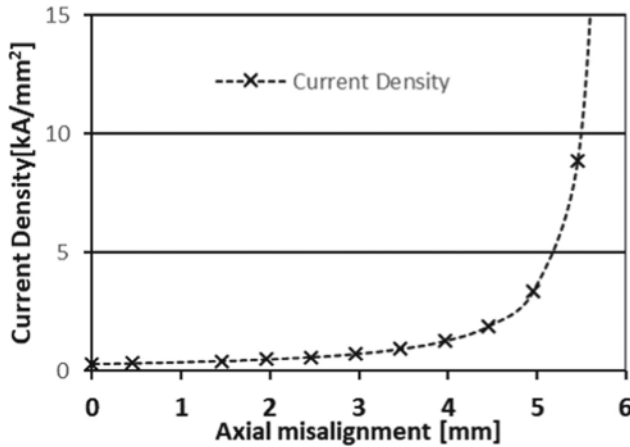


Fig. 2. Variation of current density with respect to axial misalignment.

2 Materials and Methods

For the analysis of the behaviour of the magnetic field depending on the state of the misalignment, a physical phenomenon simulation software is drawn on. The simulations are carried out for the symmetry of a water-cooled electrode caps of the F16 type according to DIN ISO 5821 were used for the welding tests, with a working surface of 6 mm. In this paper COMSOL Multiphysics software [13, 14] has been used to model the RSW alignment. A transient electromagnetic model has been developed to model the RSW alignment behaviour with the following data:

- Current flowing through the electrode: 8 kA.
- Diameter of the electrode tip: 6 mm.
- Electrode body diameter: 20 mm.
- Cone height: 5 mm.

These simulations are performed simulating a current flowing between the electrodes shorted. To obtain the relationship between misalignment and generated magnetic field, four different simulation cases are carried out. In the first one, only the upper electrode is misaligned at different distances, in order to verify how this misalignment influences the generated magnetic field without considering variations in the electrode geometry.

In the second case, the misaligned electrodes are simulated in the same way and the generated magnetic field is measured, but, in this case, the variation of the diameter of the electrode tip is added to the simulation. This simulation allows to observe the behaviour that could be expected in a real line due to one of the typical electrode defects such as mushrooming or milling problems.

For the third case, another typical defect that can be found in a real welding line is also simulated, in this case the electrodes with different cone height are simulated. This defect can be caused both by poor milling and by an error in the type of electrode used.

Finally, in order to optimize a possible device by applying the proposed method, it is simulated what would happen if the measurements of the magnetic field were not taken in the plane of contact of the electrode tips. This simulation is necessary since sometimes, due to an equalizing problem in pneumatic guns or a poor TCP adjustment in electric guns, the electrode contact plane varies in position, therefore, this could generate erroneous measurements.

In all these simulations only, the axial misalignment is analysed, since the angular misalignment is not present when only the electrodes without metal plates between them are studied. Angular misalignment transforms into axial misalignment when pressure is applied between the shorted electrodes, as the bending of the welding arms absorbs the angular misalignment.

3 Results and Discussion

For the study, the theoretical magnetic field generated for the different defects that can be found in the electrodes of a real welding gun is simulated. In this way, while studying whether misalignment detection is possible through the measurement of the magnetic field, the robustness of the detection can also be checked, preventing and avoiding in this way the false positives that could have in a real application of the method.

3.1 Simulation 1: Magnetic Field Generated by Electrodes with Constant Geometry

In this first part of the study, different simulations are performed for seven different cases depending on the direction and magnitude of the displacement of the upper electrode with respect to the lower one, that is, depending on the direction and magnitude of the misalignment.

In this case, the contact plane of the electrodes is only considered for the simulation data collection, that is, the z coordinate is discarded, using only the X and Y axis of the plane. The centre of the plane is taken as the centre of the contact surface for perfectly aligned electrodes.

For each of the seven simulations, four measurements of the magnetic field at different distances from the centre of the electrode contact plane are made. On the one hand, measurements are taken at $X = 20$ mm and $X = -20$ mm, maintaining $Y = 0$ mm. On the other hand, the values for $Y = 20$ mm and $Y = -20$ mm are acquired, maintaining the $X = 0$ mm (Table 1).

Table 1. Simulation 1: Summary.

N° simulation	$X\delta$ [mm]	$Y\delta$ [mm]
1	0	0
2	1.5	0
3	3	0
4	0	1.5
5	0	3
6	1.5	3
7	1.5	1.5

These four measurements for each of the seven simulations are performed in order to observe the variation of the symmetry of the magnetic field in the contact plane.

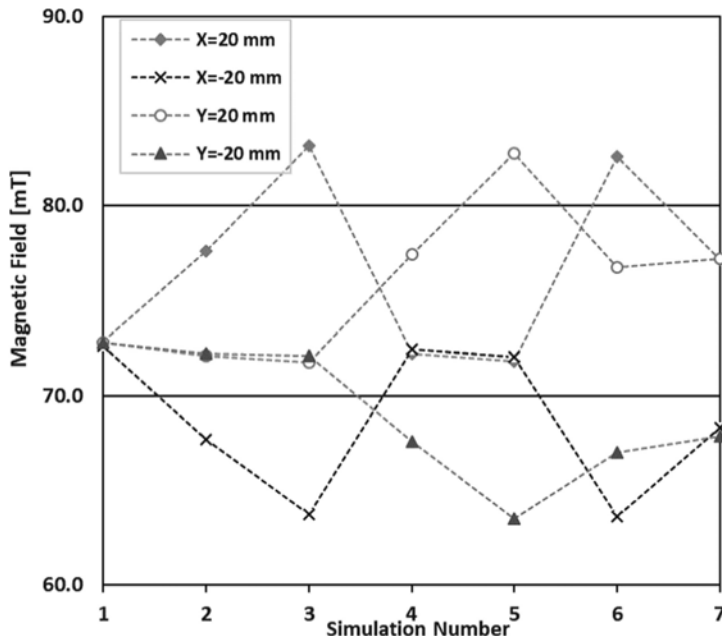


Fig. 3. Results of the magnetic field simulation for different misalignment taken at different distances from the centre of the contact plane.

The results of this first simulation are shown in Fig. 3. In this is shown what happens with the magnetic field depending on the direction of the misalignment. First, the first simulation shows when a current flow through the short-circuited electrodes and these are correctly aligned, the measurements taken at all four distances are similar, so it can be said that the generated magnetic field is symmetrical.

Similarly, if the data obtained for the other simulations are analysed, from 2 to 7, it can be observed that depending on the direction of the misalignment, the values of the magnetic field recorded at the different distances change. This change is increasing when the direction of misalignment coincides with the direction in which the measurement is taken. Likewise, the value is lower when the direction of the misalignment is opposite to the direction in which the measurement is taken.

If the difference of the measurements on each side of every single axis is calculated, that is, the difference between the measurements made for $X = 20$ mm and $X = -20$ mm and the difference between the measurements at $Y = 20$ mm and $Y = -20$ mm, the behaviour of the magnetic field can be observed for each of the proposed cases, Fig. 4.

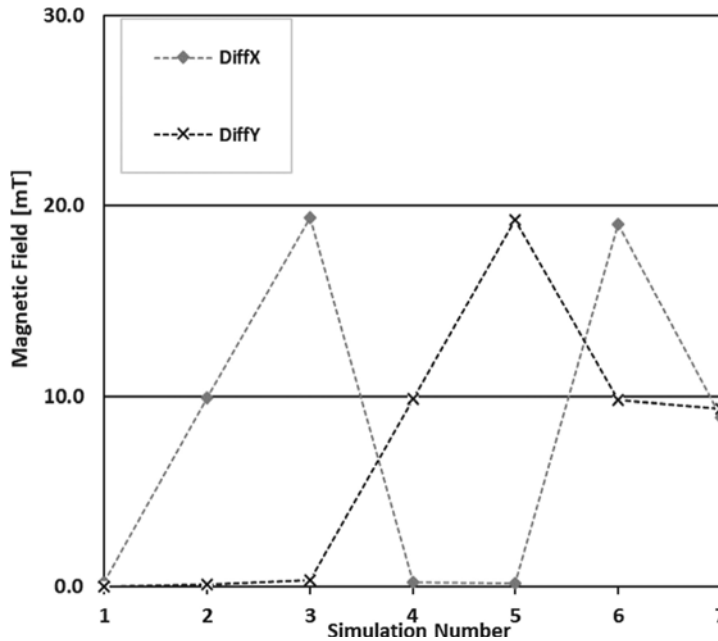


Fig. 4. Value of the magnetic field difference for X measurements and Y measurements. Simulation 1.

After analysing this simulation, it can be stated that there is a relationship between misalignment and the generated magnetic field. In this first simulation, it is only hoped to find a relationship between the magnetic field and the desalination measuring only in the contact plane and assuming that the electrode geometry is constant. After analysing this simulation, it can be stated that there is a relationship between misalignment and the generated magnetic field. In this first simulation it is only possible to find a relationship

between the magnetic field and the misalignment of the electrodes by measuring only in the contact plane and assuming that the geometry of the electrodes is constant.

However, it should be considered that in a welding line different mechanical problem arise that could influence the measurement of the generated field.

Therefore, more simulations are carried out to study the reliability of the method against different problems that may arise in the electrodes. Specifically, throughout this section is analysed the magnetic field generated by adding the mechanical problems presented below:

- Variation of the diameter of the active face of the electrode due to improper milling.
- Variation of electrode cone height due to improper milling.
- Malfunction of the equalizing system in pneumatic guns or bad configuration of the Tool Centre Point (TCP) for electric guns operated by robot

3.2 Simulation 2: Variation of the Diameter of the Active Face of the Electrode

Occasionally, due to a failure in milling pressure or a poor condition of the milling cutter blades, the surface of the active face of the electrodes varies, increasing or decreasing in size [15].

What is intended with this section is to see what influence this defect has with the generated magnetic field, so that it can be determined if in case of using this method for misalignment detection, false positives or negatives could occur.

In this case, six different simulations are carried out, as detailed in Table 2.

Table 2. Simulation 2. Summary.

N° simulation	Xδ [mm]	Yδ [mm]	Ø [mm]
1	0	0	6.6
2	0	0	6
3	0	0	5.4
4	3	0	6.6
5	3	0	6
6	3	0	5.4

By means of these six cases, it is tried to verify what happens when the diameter of the active face is different from the expected, in this case a variation of 10%, for the cases in which the electrodes are aligned or misaligned 3 mm in the X direction.

As mentioned in previous sections, the magnetic field generated depends on the current density. This current density depends on the contact surface of the electrodes. Therefore, an increase in the magnetic field is expected for those points where the diameter of the active face is lower.

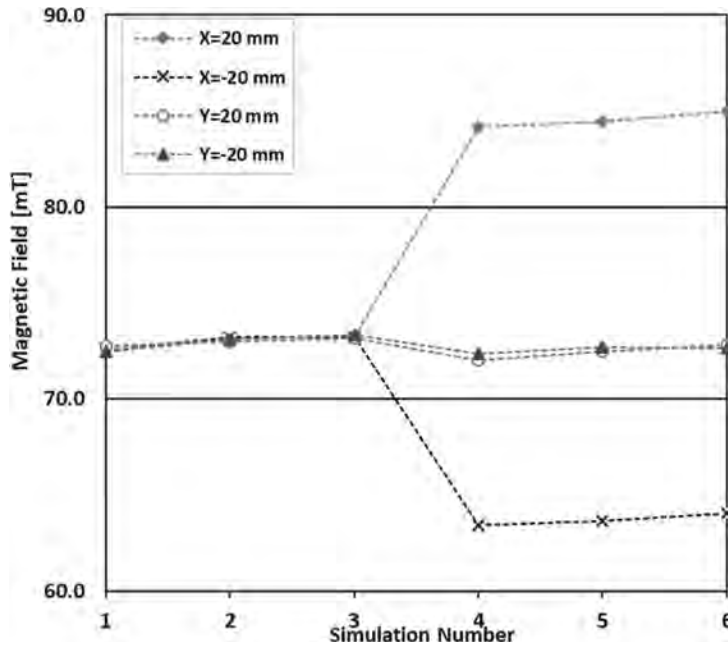


Fig. 5. Results of the magnetic field simulation for different electrode face diameter taken at different distances from the centre of the contact plane.

If the data in Fig. 5 is analysed, it can be seen how the variation of the electrode diameter implies a variation of the magnetic field generated for both aligned and misaligned electrodes. Obviously, this is due to the variation of the active face of the electrode that directly influences the current density. However, this variation in the magnetic field due to the change in the electrode diameter is insignificant with respect to the variation generated by misalignment.

Comparing the data shown in Fig. 6, it can be seen more clearly how the difference between the measurements for each axis is substantial depending on whether the electrode is aligned or not. If we analyse the last three points of the graph, 4, 5 and 6, it can be seen how this value not varies for each of these simulations. Therefore, it could be expected that in a possible real implementation, this defect will not have a significant influence on the detection of misalignment. So, in any case, this defect may hide a problem of electrode misalignment.

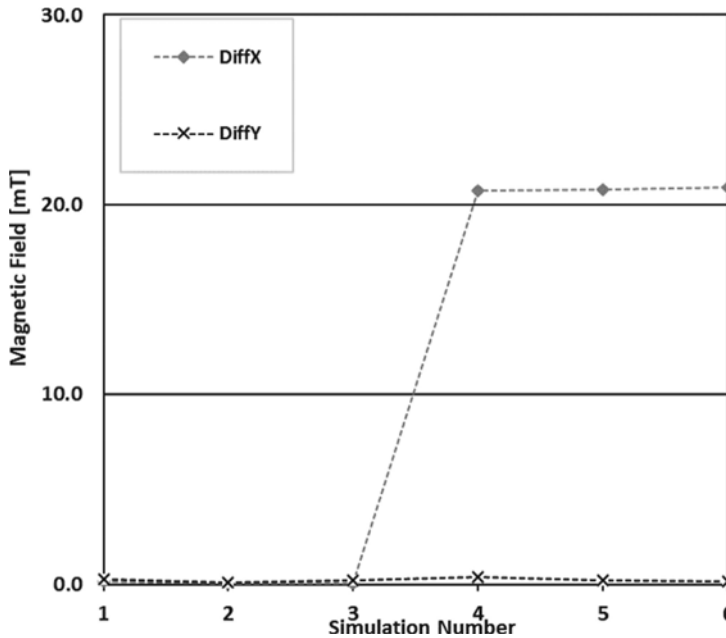


Fig. 6. Value of the magnetic field difference for X measurements and Y measurements. Simulation 2.

3.3 Simulation 3: Variation of Electrode Cone Height

As in the previous case, due to mechanical problems of the welding gun, milling can cause differences in electrode geometry. In this case, the variation of the magnetic field is analysed according to the variation of the height of the welding cone [15].

As in the previous case, due to mechanical problems of the welding gun, milling can cause differences in electrode geometry. In this case, the variation of the magnetic field is analysed according to the variation of the height of the welding cone.

In this case, six simulations are performed in the same way, as shown in Table 3.

Table 3. Simulation 3: Summary.

N° simulation	Xδ [mm]	Yδ [mm]	h [mm]
1	0	0	4.5
2	0	0	5
3	0	0	5.5
4	3	0	4.5
5	3	0	5
6	3	0	5.5

At this time, it should be noted that the magnetic field at each point of the simulated space is determined by all other points in the space. In the previous cases, this has been omitted since apart from the electrode contact plane the other geometry remained constant.

On the other hand, at this point, the variation in the height of the cone causes a variation in the area through which the current circulates and therefore a variation in the current density.

Therefore, the values obtained in this simulation will depend so much on the magnetic field caused in the plane of contact of the electrodes according to the existing misalignment as much as by the variation of the height of the cone. Since at a higher height there is a higher current density along the electrode, it is expected to find in this simulation an increase in the magnetic field as the cone height increases.

The values in Fig. 7 show how, as previously assumed, as the height of the cone decreases, the values of the magnetic field are lower. If the values of cases 4, 5 and 6 are analysed, for misaligned electrodes, this can be seen more clearly.

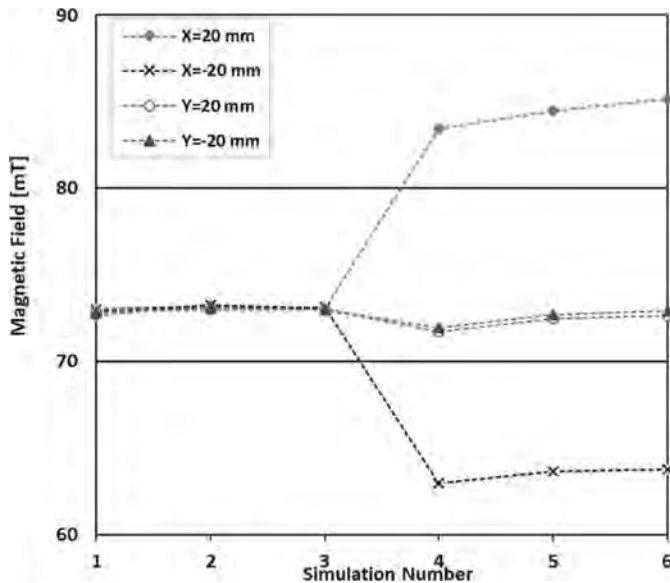


Fig. 7. Results of the magnetic field simulation for different cone height taken at different distances from the centre of the contact plane.

Similarly, in Fig. 8 it can be seen what happens with respect to the symmetry of the axes. Analysing the cases for misaligned electrodes, it can be determined that if the difference between both sides of each axis is made, the difference of the magnetic field values for each cone height could be considered negligible.

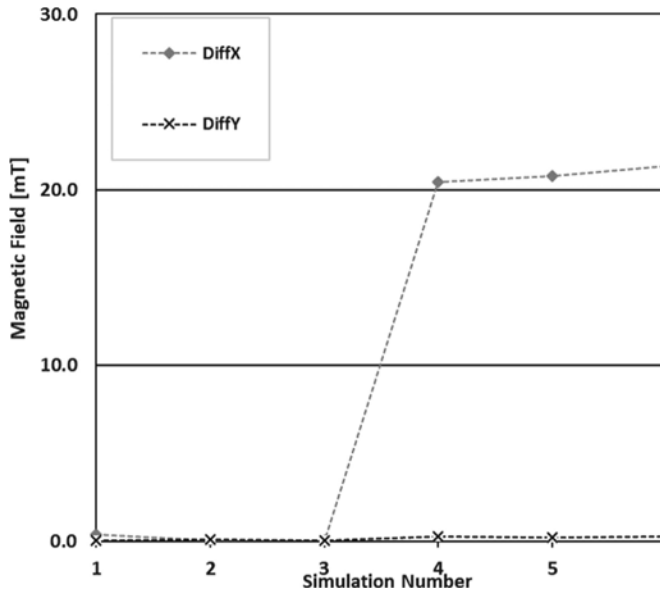


Fig. 8. Value of the magnetic field difference for X measurements and Y measurements. Simulation 3.

However, although the magnetic field increases as the height of the cone increases, this increase does not represent a significant increase to hide the increase in the magnetic field caused by misalignment.

Therefore, unless very extreme cases of cone height variation are reached, this defect should not cause any future problems in the detection of misalignment.

3.4 Simulation 4: Inadequate Welding Gun Equalization - Bad Configuration of TCP

The equalizing system compensates for welding conditions in which the closing weld tips are offset from the plane of the workpiece. As one of the electrodes touch the workpiece, a force is created that slides the gun to a position that centres the gun electrodes about the workpiece.

Sometimes, due to a bad adjustment of the equalizing system, a displacement of the contact surface occurs, this is due to a bad adjustment of the pneumatic equalizing valves for pneumatic guns or a bad adjustment of the TCP (Tool Centre Point) for servo-gun.

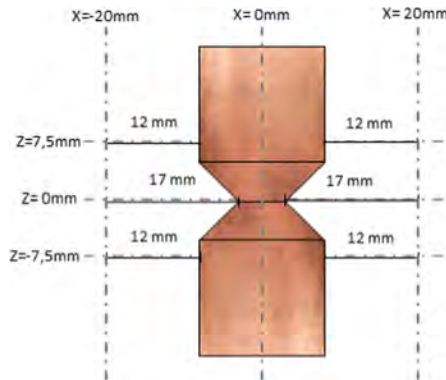
Finally, in this case, it is studied how the displacement of the contact plane of the electrodes can influence the measurements or, in other words, how the problems of equalizing guns, both pneumatic and electric, influence the measurements.

In this analysis, the reference plane is modified for taking measurements, that is, instead of taking the data at $Z = 0$ mm, the magnetic field data is also taken for the $Z = \pm 7.5$ mm planes. In this way the bad adjustment of the contact area of the electrode tip can be simulated. In this simulation only the data for $X = \pm 20$ mm is collected following the Table 4.

Table 4. Simulation 4. Summary.

N° simulation	$Z_{\text{electrode}}$ [mm]	$Y\delta$ [mm]
1	0	0
2	7.5	0
3	-7.5	0
4	0	1.5
5	7.5	1.5
6	-7.5	1.5
7	0	3
8	7.5	3
9	-7.5	3

In this case, it is necessary to make some initial considerations before proceeding to the analysis of the results. The measured magnetic field depends on both the current density and the distance at which the data is taken, giving the maximum magnetic field value at the edge of the electrodes, therefore it is necessary to consider not only the distance to the reference centre but the distance to the edge of the electrodes.

**Fig. 9.** Distances to the edge of the electrode for the different values of z .

In the ideal case, electrodes aligned and measured on the plane $Z = 0$ mm, the distance between the data collection in x and the edge of the electrode will be 17 mm, however, in $Z = \pm 7.5$ mm, this distance will be 12 mm as shown in Fig. 9.

In Fig. 10, the behaviour of the magnetic field can be seen in each of the three proposed z planes for a misalignment equal to 3 mm. In the curve for $Z = 0$ mm, the generated magnetic field is displaced to the left, being greater the measurement in $X = 20$ mm than in $X = -20$ mm. This is the same for the curve for $Z = 7.5$ mm since the upper electrode is misaligned 3 mm in the positive direction of the x axis. In contrast,

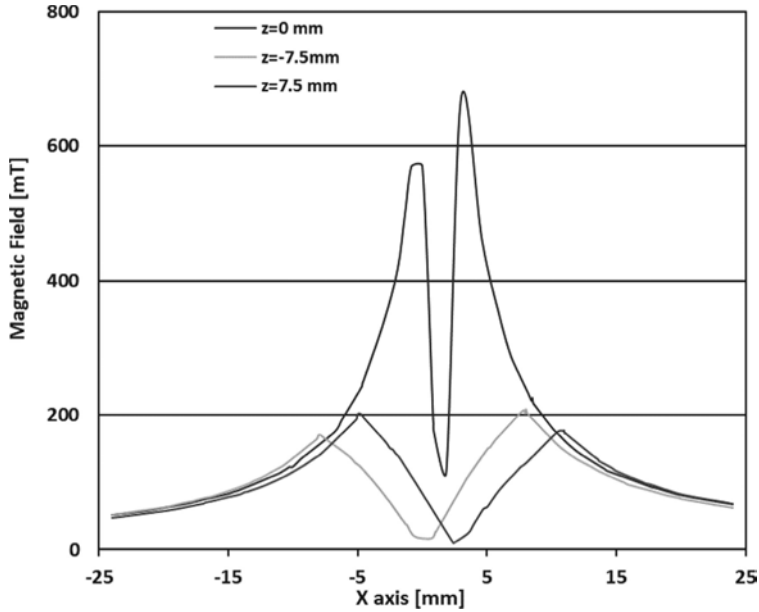


Fig. 10. Magnetic field measurement for different planes in z along the x axis for a 3 mm misaligned electrodes.

the magnetic field value for the curve of $Z = -7.5$ mm the values are inverse to those taken for the curve $Z = 7.5$ mm.

The simulation results for misalignments of 0, 1, 5 and 3 are shown in Fig. 11. For misalignment equal to 0, simulations 1, 2 and 3, the value of the magnetic field is higher when the data is not taken on the contact plane of the electrodes. This also happens in the various cases of misalignment. As the misalignment increases the magnetic field values increase, maintaining as previously discussed the inverse relationship between the values taken at $Z = -7.5$ mm and $Z = 7.5$ mm.

These results show how the analysed defect influences the magnetic field values. It can be affirmed that although this defect alters the values of the measured magnetic field, it is possible to discriminate between different degrees of misalignment despite taking measurements in different planes of z . It is true that in some cases the values taken would not really represent the degree of misalignment but in no case would it give rise to false positives.

After the four simulated cases, it can be affirmed that there is a real relationship between the misalignment in the welding electrodes and the magnetic field that they generate when a current flow between them short-circuited. In addition, the simulations of cases 3.2, 3.3 and 3.4 show how the different defects that can occur in the electrodes or the welding gun would not have an important influence on the measurement and therefore give reliability to the method.

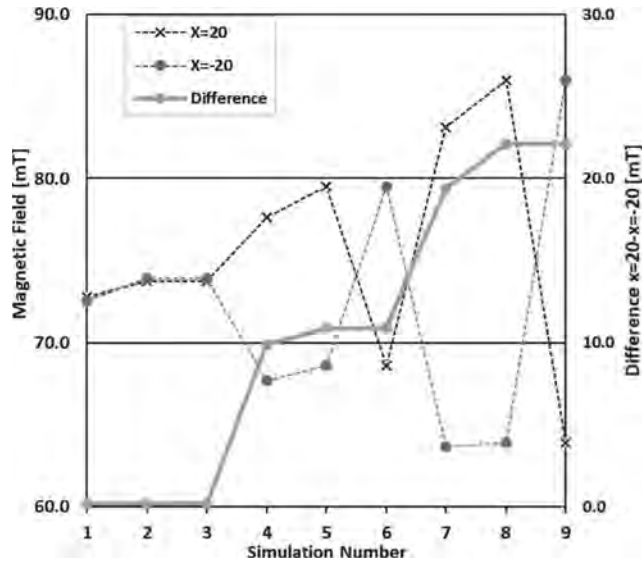


Fig. 11. Results of the magnetic field simulation for different position of the contact plane. Simulation 4.

4 Conclusion

This paper seeks to continue with the proposed method for detecting misalignment in welding lines. In previous research, an initial response to this method was given, but it was necessary to carry out a more exhaustive analysis of the behaviour of the magnetic field for each of the different faults that may participate in welding [1].

This paper develops one of the future work points raised in the previous research. During the investigation, an exhaustive analysis is carried out of those defects that could generate false measurements of misalignment.

For the method validation, mathematical calculations and simulations are used, in which it is observed how, unequivocally, there is a strong relationship between both factors.

The following conclusions can be drawn from all cases and simulations performed:

- There is a real relationship between the misalignment of the electrodes and the current density in them. Therefore, there is a relationship between misalignment and the generated magnetic field.
- When there are milling problems that influence the area of the electrode tip or the height of the cone, this also causes a variation of the magnetic field. This variation is insignificant with respect to the stranding of the magnetic field by misalignment. Therefore, the proposed method is robust in relation to this defect.
- A bad equalizing adjustment or a bad TCP configuration causes a displacement of the contact plane of the electrode tip. This displacement generates a variation in the measurement of the magnetic field. In this case the variation is high but not enough to generate false positives in the measurements.

- It is possible to detect the misalignment of the electrodes by measuring the generated magnetic field.

In future research, the similarity of the results obtained from the simulations carried out and the data obtained in the production line should be verified.

Acknowledgement. The authors wish to thank Ford España S.A, in particular, the Almussafes factory for their support in the present research.

Also, the authors wish to extend this thanks to the Foundation for Development and Innovation of the Valencian Community (FDI).

References

1. Ibáñez, D., García, E., Martos, J., Soret, J.: Real-time electrode misalignment detection device for RSW basing on magnetic fields. In: Proceedings of the 17th International Conference on Informatics in Control, Automation and Robotics. ICINCO, vol. 1, pp. 142–149 (2020). <https://doi.org/10.5220/0009820801420149>. ISBN 978-989-758-442-8
2. Kang, H.S., et al.: Smart manufacturing: past research, present findings, and future directions. *Int. J. Precis. Eng. Manuf. Green Technol.* **3**(1), 111–128 (2016). <https://doi.org/10.1007/s40684-016-0015-5>
3. Benhabib, B.: *Manufacturing: Design, Production, Automation, and Integration*, chap. 12. CRC Press, Boca Raton (2003). ISBN: 9780824742737
4. Jou, M.: Real time monitoring weld quality of resistance spot welding for the fabrication of sheet metal assemblies. *J. Mater. Process. Technol.* **132**(1–3), 102–113 (2003)
5. Lee, H.T., Wang, M., Maev, R., Maeva, E.: A study on using scanning acoustic microscopy and neural network techniques to evaluate the quality of resistance spot welding. *Int. J. Adv. Manuf. Technol.* **22**(9–10), 727–732 (2003)
6. Goodarzi, M., Marashi, S.P.H., Pouranvari, M.: Dependence of overload performance on weld attributes for resistance spot welded galvanized low carbon steel. *J. Mater. Process. Technol.* **209**(9), 4379–4384 (2009)
7. Ertunc, H.M., Leoparo, K.A., Ocak, H.: Tool wear condition monitoring in drilling operations using Hidden Markov models (HMMs). *Int. J. Mach. Tools Manuf.* **41**(9), 1364–1384 (2001)
8. Li, Y., Tang, G., Ma, Y., Shuangyu, L., Ren, T.: An electrode misalignment inspection system for resistance spot welding based on image processing technology. *Measur. Sci. Technol.* **30** (2019). <https://doi.org/10.1088/1361-6501/ab1245>
9. Zhang, H., Senkara, J.: *Resistance welding: fundamentals and applications* (2005)
10. Walker, J., Halliday, D., Resnick, R.: *Fundamentals of Physics*, 10th edn, p. 749. Wiley, Hoboken (2014)
11. Cohen-Tannoudji, C., Diu, B., Laloë, F.: *Mécanique quantique*, vol. I and II. Collection Enseignement des sciences (Hermann), Paris (1977)
12. Feynman, R.: *Feynman Lectures on Physics*, vol. 2. Addison Wesley Longman (1974)
13. Comsol MultiPhysics 4.2. <http://www.comsol.com>
14. COMSOL Multiphysics 3.5a: User's Guide 3.5a
15. Kusano, H.: Electrode dressing makes a better spot weld. *Weld. J.* **90**, 28–32 (2011)

4.3 SCIENTIFIC ARTICLE II.

Title: Real-Time Condition Monitoring System for Electrode Alignment in Resistance Welding Electrodes.

Authors: Daniel Ibáñez, Eduardo García, Julio Martos and Jesús Soret.

Published in: Sensors 2022 , 22, 8412, Special Issue: Sensors and Sensing Systems for Condition Monitoring
<https://doi.org/10.3390/s22218412>

Impact factor: 3.847 (2021). Quartile (category: "Instruments & Instrumentation"): Q2 (2021)



Citations: 1 (accessed on March 2022).

Description: Sensors journal is a peer-reviewed open access scientific publication that is published by MDPI (Multidisciplinary Digital Publishing Institute). The journal focuses on research and development of sensors and sensor systems, as well as their applications in different fields such as biomedicine, engineering, chemistry, physics, and computer science, among others. The journal has a broad readership that includes researchers, engineers, scientists, and other professionals interested in sensor technology.

The special issue "Sensors and Sensing Systems for Condition Monitoring" is focused on condition monitoring and measurement systems used in this field. The aim of this special issue is to bring together innovative and original works in areas such as sensors, detection materials, measurement techniques, electronics for hazardous environments, signal processing, data mining, artificial intelligence, and other related topics.

Article

Real-Time Condition Monitoring System for Electrode Alignment in Resistance Welding Electrodes

Daniel Ibáñez ^{1,*} , Eduardo García ², Jesús Soret ¹  and Julio Martos ¹¹ Department of Electronic Engineering, Campus de Burjassot, Universidad de Valencia, CP 46100 Valencia, Spain² Ford Spain, Poligono Industrial Ford S/N, Almussafes, CP 46440 Valencia, Spain

* Correspondence: daniel.ibanez@uv.es; Tel.: +34-961-791-543

Abstract: Electrode misalignment, produced by mechanical fatigue or bad adjustments of the welding gun, leads to an increase in expulsions, deformations and quality problems of the welding joints. Different studies have focused on evaluations of the influence of a misalignment of the electrodes and the final quality of the weld nugget. However, few studies have focused on determining a misalignment of the electrodes to avoid problems caused by this defect, especially in industrial environments. In this paper, a method for performing the condition monitoring of electrode alignment degradation was developed following previous research, which has shown the relationship between the misalignment of short-circuited electrodes and the magnetic field generated by them. This method was carried out by means of a device capable of measuring the magnetic field. Finally, an integral system for the detection of misalignments in real production lines is presented. This system set behavior thresholds based on the experimentation, allowing the condition monitoring of the alignment after each welding cycle.

Keywords: resistance spot welding; magnetic field; condition monitoring; welding quality



Citation: Ibáñez, D.; García, E.; Soret, J.; Martos, J. Real-Time Condition Monitoring System for Electrode Alignment in Resistance Welding Electrodes. *Sensors* **2022**, *22*, 8412. <https://doi.org/10.3390/s22218412>

Academic Editors: Ada Fort and Tommaso Addabbo

Received: 10 October 2022

Accepted: 31 October 2022

Published: 1 November 2022

Publisher's Note: MDPI stays neutral with regard to jurisdictional claims in published maps and institutional affiliations.



Copyright: © 2022 by the authors. Licensee MDPI, Basel, Switzerland. This article is an open access article distributed under the terms and conditions of the Creative Commons Attribution (CC BY) license (<https://creativecommons.org/licenses/by/4.0/>).

1. Introduction

The welding process is one of the most used metal joining methods in the manufacturing industry. Specifically, in the automobile manufacturing process, it represents more than 90% of all the welded joints of the bodywork [1–3]. The resistance welding process bases its operation on Joule's law, which states that when a current flows through the metal to be melted with a certain resistance, heat is generated that melts the metal, causing the welded joint [4–6].

Figure 1 shows the standard layout of a resistance welding spot, in which two copper electrodes apply pressure and a current flows through the metal sheets to be welded. In the manufacture of a car body, the metals to be welded are usually steel, with a resistance greater than the resistance of the copper electrodes. As a result, heat is primarily generated in the metals to be welded. In addition, as can be seen in Figure 1, the contact resistance between the sheets, R_4 , is even greater than the resistance of the sheets themselves, R_3 – R_5 . This allows a nugget to begin to be formed between the metal sheets. The electrical circuit can be summarized in seven resistances from the flow of the current from one electrode to another: the resistance of the electrodes (R_1 and R_7); the contact resistance of the electrode and the metal sheet (R_2 and R_6); the self-resistance of the metal (R_3 and R_5); and the contact resistance of the metal sheets [7–9].

Bearing in mind these seven resistances, it can be affirmed that each one of these resistances has a fundamental role in the generation of heat and its distribution during the welding process. In short, each one of these resistances has a crucial role in the weld quality.

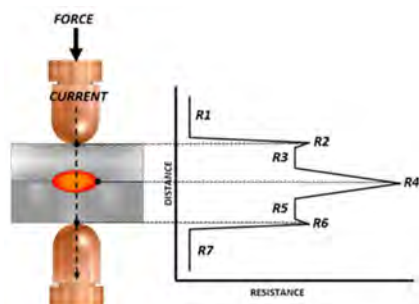


Figure 1. Layout of the resistance welding process.

Consequently, different authors have investigated how to guarantee or evaluate the quality of a weld based on these resistances, mainly in those resistances that are more critical and variable such as the contact resistance between the electrode and the sheet (R2 and R6) and the resistance caused by contact between the sheets (R4). Regarding contact resistance, Chen et al. [10] showed a coating designed as a barrier to prevent the electrodes from alloying with the Zn coating and causing degradation by pitting or erosion, reducing the variations in the contact resistance. Other studies have shown the importance of keeping the geometry of the electrodes constant to reduce variations in the diameter of the active face of the electrodes, either due to excess dirt or mushrooming [11–16]. In the same way, the contact resistance between metals (R4) has a great importance in the different research that has been carried out; i.e., different authors have focused their studies on the influence that the gap between sheets has on the final quality of the welding point [17–19].

In this study, we focused on the detection of problems in the contact resistance of electrodes, specifically those related to the alignment of the electrodes.

Electrode Misalignment

Eventually, due to mechanical fatigue, electrodes lose their working axis, presenting angular (α) or axial (δ) displacements with respect to their reference axis. This defect, shown in Figure 2, is known as misalignment. An electrode misalignment provokes unfavorable characteristics during the welding process as well as in the quality of the welded joints. Misalignments, whether axial or angular, can cause irregularly shaped welds as well as a reduced weld size and projections due to an asymmetric distribution of the force and a change in the contact surface [20–28].

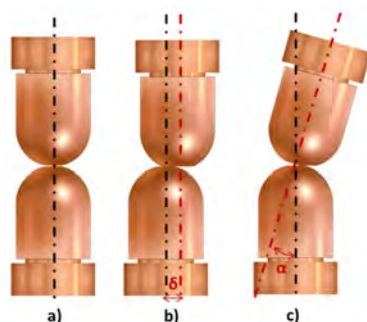


Figure 2. Electrode alignment status. (a) Aligned electrode. (b) Axial misalignment. (c) Angular misalignment.

This research focused on the detection of an axial misalignment, as shown in Figure 2b, because it is more common in production lines but it could be extrapolated to any type of

misalignment. As mentioned previously, a modification of the contact surface is caused by a misalignment and it is expressed by the equation of the contact surface (C_a) (Equation (1)), from which it can be deduced that the greater the misalignment, the smaller the contact surface between both electrodes.

$$C_a = 2r^2 \sin^{-1} \left(\sqrt{1 - \left(\frac{\delta}{2r} \right)^2} \right) - \delta \sqrt{r^2 - \left(\frac{\delta}{2} \right)^2} \quad (1)$$

where r represents the radius of the tip of the electrodes and δ is the misalignment between the electrodes.

Hence, the alignment of welding electrodes has a major impact on the quality of the spot welding joint. As a result, it is fundamental to analyze the alignment condition for each welding gun.

2. Research Objectives

The aim of this research was not only to find a relationship between misalignments and a measurable physical variable, but also to find a complete system for measuring and detecting the alignment state in real-time that was applicable to high-production factories by means of resistance welding.

Several authors have proposed methods for the detection of electrode misalignments in the resistance welding process. Li et al. [29] discovered a method for detection by means of an image analysis. The results obtained by this method suggested that it was possible to determine if the electrodes were properly aligned. The main disadvantage of the use of images resides in the cost of the implantation of the cameras and their integration into productive lines. In addition, due to the environment in which the cameras are located, continuous maintenance is needed to prevent the lenses from getting dirty or the measurements from being miscalibrated. For these reasons, the implementation of this method in a high-production factory is not feasible. On the other hand, Xing et al. [30] presented in their research different methods to determine the state of alignment of the electrodes. One was based on the analysis of images of the carbon footprint of the electrodes, presenting the same disadvantages as the previous method; a second method studied the displacement of the electrodes and the applied force. The main drawback of this last method was that not only was the misalignment of the electrodes analyzed, but also the general conditions of the state of the electrodes, making difficult to determine if the change in conditions was due to a misalignment or other mechanical defects. Finally, Lee et al. [31] proposed a method for the detection of an angular misalignment by means of machine learning. Specifically, the proposed method used the signals of dynamic resistance, voltage and current to extract the critical features for training a neural network. Despite the good results of this research, the high processing and computing capacity required for each welding gun makes its installation complex in a high-production industry, necessitating training for each welding gun.

Therefore, the objective of this research was to find a method for the detection of misalignments. This method had to be robust, implantable and focused on the alignment of the electrodes.

In previous investigations, an initial method for the detection of misalignments by measuring magnetic fields was proposed. First, the theoretical influence between the state of the alignment of the electrodes and the magnetic field generated by them was investigated [32]. By reducing the electrodes to a wire with a constant current density, it could be stated that the behavior of the generated magnetic field followed Ampere's law [33,34], where the magnitude of the magnetic field fundamentally depends on the distance toward the origin of the magnetic field; in this case, the center of the contact surface of the electrodes. When a misalignment appeared, the center of the magnetic field moved in the same direction as the misalignment. This provoked an asymmetry in the generated magnetic field compared with the perfectly aligned electrodes, Figure 3.

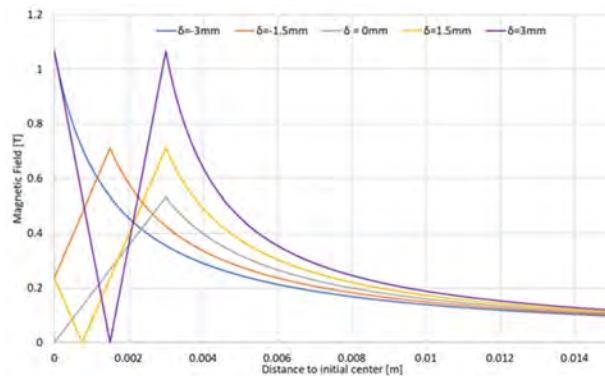


Figure 3. Magnetic field generated as a function of the state of alignment of the electrodes.

If the center of the coordinates is considered to be the center of the aligned electrodes, Ampere's law can be summarized according to Equation (2):

$$B(R) = \begin{cases} \frac{\mu_0 I}{2\pi(r - \frac{\delta}{2})^2} R, & R < r - \frac{\delta}{2} \\ \frac{\mu_0 I}{2\pi R}, & R > r - \frac{\delta}{2} \end{cases} \quad (2)$$

where r is the radius of the active face of the electrodes, usually 6 mm; R is the distance to the center of the generated magnetic field and δ is the magnitude of the misalignment in the direction of R .

To confirm the robustness and the influence of other mechanical defects, the behavior of the magnetic field generated for each of the different possible mechanical defects was studied [35], verifying that the influence of a misalignment was greater than any other mechanical defect studied.

In conclusion, what was sought in this last phase of the investigation was to apply the previous investigations in a real industry, presenting a system capable of being integrated into high-production lines of the automobile industry in an effective and efficient way.

3. Material and Methods

Electrode Misalignment Detection Device

To measure misalignments, a device capable of measuring the magnetic field was developed. In addition, according to the objectives of this research, the device was also capable of being integrated within the idiosyncrasy of a factory, being easily installable and allowing interactions with the other components involved in production (e.g., PLC and databases).

The magnetic field measurements were carried out by means of four hall effect sensors, specifically SS49E [36] manufactured by the Honeywell Corporation. These were used in the device due to their range of measurements as well as their linearity and bipolarity. The measurements were made by the four hall effect sensors, which were located antiparallel in such a way that the values were collected in the four Cartesian axes, as shown on the PCB in Figure 4.

To obtain the magnetic field value, the following protocol was followed. The electrodes were milled after a certain number of welding points in order to keep their geometry constant. Once the electrodes were milled, they were short-circuited in the middle of the circumference of the PCB. When the electrodes were in position, a current then flowed between them, generating a magnetic field that was measured by the four hall effect sensors. These four sensors measured the magnetic field and converted that value into a voltage, according to Figure 5. The objective of the measurement of the magnetic field was not to quantify it, but to determine the variations in the acquired values; therefore, the use of the

unit of the magnetic field in mT or in mV was indifferent. For this reason, and throughout this paper, the value in volts of the magnetic field was taken as the unit of measurement of the magnetic field.



Figure 4. Hall effect sensor PCB.

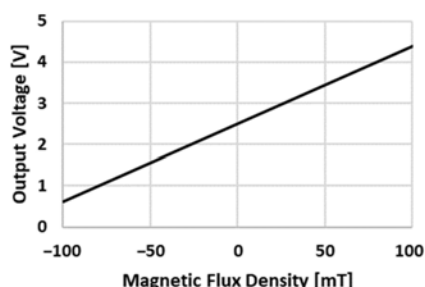


Figure 5. SS49E transfer characteristics.

The magnetic field values were acquired by a microcontroller based on the ESP32 that received the information, calculated the magnetic field difference in each axis and then sent the values to the PLC. Figure 6 shows the communication protocol between the device and the database. The data were acquired by the device and sent to the gateway through the LoRaWAN communication protocol, which in turn sent the data to the PLC. Finally, the PLC acted as a gateway between the LoRa gateway and the database in which the data were stored to be analyzed.

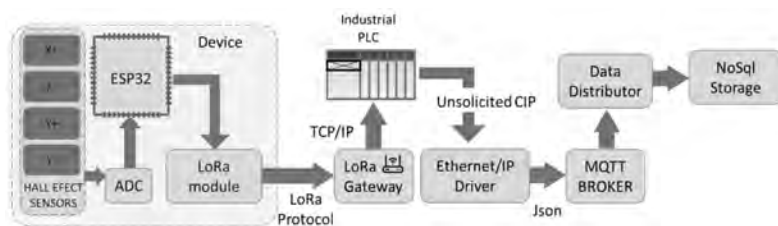


Figure 6. Scheme for sending the data collected during the check.

4. Experiment and Results

For the method and device performance validation, the device was installed in a real production station so that it could be validated under real operating conditions. The data collected during the misalignment check were stored and analyzed in the database. Initially, a calibration of the data was carried out on the basis that the initial data corresponded with the correct operation of the welding gun. Filtering and outlier elimination methods were applied to these data.

As mentioned above, the magnitude of the magnetic field depended on the direction in which the misalignment occurred. Thus, to determinate the state of the misalignment, the magnetic field values collected on the x -axis and y -axis were independently analyzed.

To check for a correct operation, an ARO 3G gun with 16 mm type-F electrodes was used, according to DIN EN ISO 5821 [37]. This experiment was carried out inside a production welding gun to approximate the study to a completely real case, as can be seen in Figure 7.

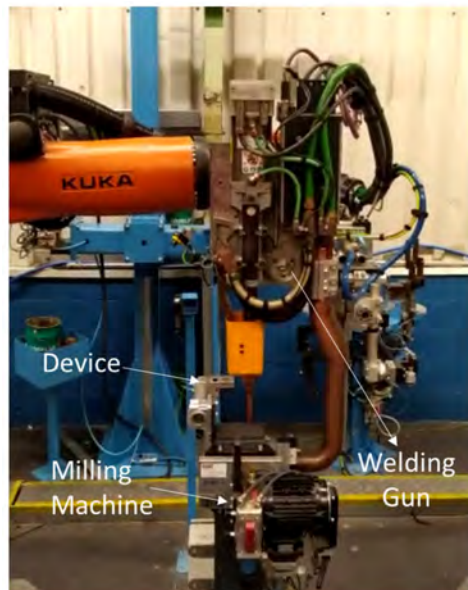


Figure 7. Location of the device in the production line.

To verify a real operation, according to the theory and the simulations carried out in previous investigations [32], an experiment was carried out that modified the alignment of the electrodes. In total, seven different cases of alignment on the x-axis were performed, as shown in Table 1 and Figure 8.

Table 1. Summary of experimental cases based on alignment status.

Case	1	2	3	4	5	6	7
δ (mm)	0	0.9	2.6	4.3	−1.5	−2.4	−3.6

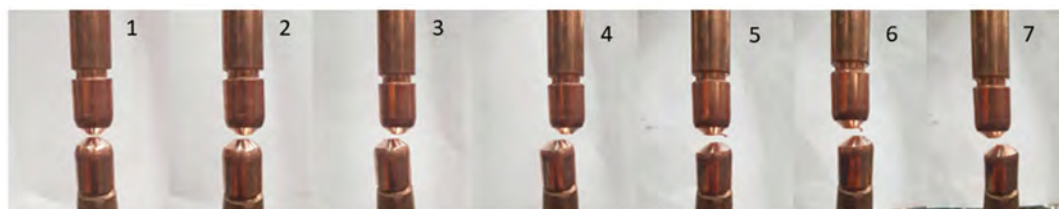


Figure 8. Alignment status for each of the experimental cases.

For each of the cases described above, a series of checks were made to verify that the variations in the magnetic field generated depended on the state of the alignment of the electrodes. As mentioned previously, the misalignment detection device calculated the average magnetic field of each of the sensors for each check and sent the difference between the axes to the welding database. In Figure 9, two different graphs can be seen,

one corresponding with the values of the magnetic field on the x -axis (Figure 9a) and the other corresponding with the values of the magnetic field on the y -axis (Figure 9b).

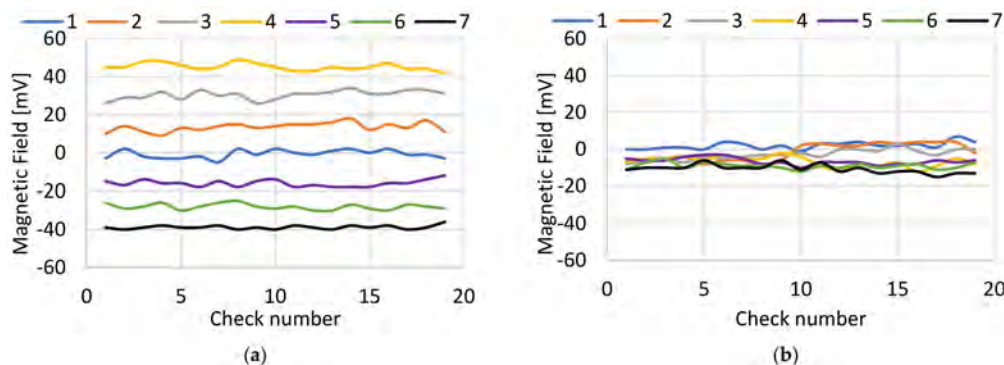


Figure 9. Experimental result: magnetic field generated for each of the cases. (a) Magnetic field measured on the X-axis. (b) Magnetic field measured on the Y-axis.

Figure 9a shows how Case 1 corresponded with the magnetic field data for a few aligned electrodes, with values close to 0 mV due to the initial calibration. If Cases 2, 3 and 4 were compared, as the misalignment on the x -axis increased, the magnetic field values also increased. This was because each time the center of the magnetic field was closer to the measurement sensor located on the $x+$, it was increasingly further away from the measurement sensor located on the x -axis. When Cases 5, 6 and 7 were observed, the misalignment occurred in the reverse direction—that is, in the direction of the measurement sensor located at x - and the absolute value of the magnetic field increased. On the other hand, as shown in Figure 9b, it could be seen that the magnetic field values were very similar, regardless of the case of misalignment.

The global behavior of the generated magnetic field is reflected in Figure 10. This figure shows the values of the magnetic field measured on the X-axis and Y-axis. It could be seen that there was a variation mainly in the values of the magnetic field on the X-axis, varying from the maximum value of 50 mV to the minimum value of about -40 mV. From Figures 8 and 9, it could be concluded that there was a direct relationship between the state of alignment of the electrodes and that this mainly affected the magnetic field measurements taken in the axis in which the misalignment occurred.

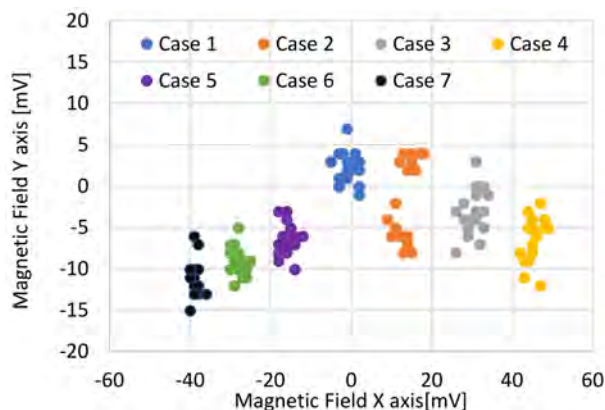


Figure 10. Magnitude of X-Y magnetic field generated by each case.

Several statistical variables such as the mean and the standard deviation could also be obtained from these calculated data. This statistical study allowed the analysis of the behavior of the data and their variability within the same alignment state. These statistical calculations are shown in Table 2.

Table 2. Standard deviation and average for each axis in each experimental case.

Case	1	2	3	4	5	6	7
\bar{x} (mV)	−0.8	13.4	30.7	45.2	−15.7	−28.1	−38.8
\bar{y} (mV)	1.7	−1.8	−2.7	−6.8	−6.5	−9.2	−10.8
σ_x (mV)	2.2	2.5	2.3	1.9	2.2	1.6	1.0
σ_y (mV)	2.2	4.7	2.9	2.7	1.8	1.8	2.4

Two main conclusions could be drawn from Table 2. First, the averages of the values on the x-axis and y-axis served to confirm, once again, that the method was able to detect changes in the alignment of the electrodes; and second, that the dispersion was similar, regardless of the case of the particular study. This guaranteed an acceptable repeatability of the device measurements, thus avoiding false alarms caused by dispersion in the measurements. Despite this, in Case 2, it could be seen that there was a greater variation in the data; this may have been due to variations in the milling characteristics [35].

5. A Real Case Implementation

Once a device capable of detecting the misalignment of electrodes by means of magnetic fields had been designed, and following the objectives sought with this research, a system for the detection of misalignments in high-production lines was designed.

Based on this objective, an acquisition, processing and sending alarm system was designed for the installation of devices in a production line.

For this purpose, the system designed by Garcia et al. [38] for the communication of industrial equipment with an analysis database was followed. In this particular case, the data came from the misalignment detection sensors; these were sent through LoRa to the gateway that provided the data to the PLC. Once the data were in the PLC, they were sent to the database for storage and a subsequent analysis. This is summarized in Figure 11.

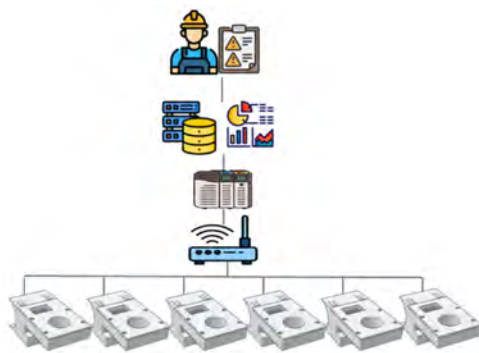


Figure 11. Alarm-sending scheme.

The alarm-sending system followed the following process. First, during the installation of the devices, the state of the alignment of the electrodes was visually checked in such a way that it could be established that the initial measurements corresponded with an electrode in good condition. These values served to eliminate the offset of the measurements in such a way that when the electrodes were aligned, the magnetic field values in x and y were close to zero.

As has been seen throughout the previous sections, the magnitude of the magnetic field depended on the direction in which the misalignment originated. For the validation of the method, it was necessary to independently analyze the x and y components of the magnetic field. However, for the misalignment detection and alarm-sending system, it was only necessary to know when the magnetic field varied regardless of the direction in which the misalignment occurred. This was because the operator would have to repair the condition of the electrodes regardless of the direction of the misalignment. Therefore, the magnitude of the magnetic field vector was calculated from the x and y values, which was the value on which the alarms and pre-alarms were set.

The method of setting the alarms was based on previous experimentation. Figure 12 was obtained from the calculation of the value of the vector for each of the cases. This figure represents the value of the magnitude of the magnetic field vector for each of the misalignments carried out in the Experiment and Results section.

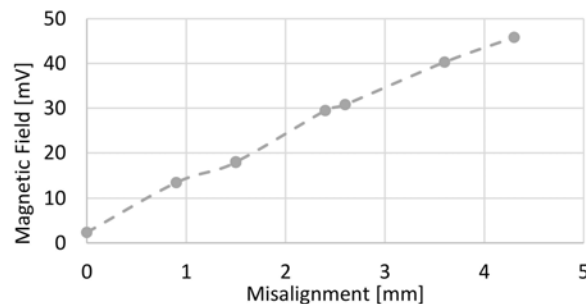


Figure 12. Magnitude of the magnetic field as a function of the misalignment of electrodes.

Based on the values obtained in Figure 12, the alarm and pre-alarm values were established. Assuming that the acceptable misalignment limit was 1 mm, a pre-alarm value could be obtained from the equation of the straight line, giving an approximate result of 13.7 mV. Regarding the alarm, it was considered to be a serious status of misalignment above 2 mm; thus, the alarm value was set at 23.8 mV.

In this first implementation, seven devices were installed within a production line to finally validate the complete system for detecting changes in the alignment of the electrodes (Figure 13). For the start-up of the devices, the initial alignment of the seven welding guns was checked, creating the offset for the start of the alarm system.



Figure 13. Production line device installation.

The welding robot was programmed so that after carrying out the entire process of milling the electrodes, it performed an alignment status check after a certain cycle of points. To carry out the check, the same configuration as in the experimental test was followed, setting the check values at 8 kA for 200 ms.

For the analysis of the alarm system, two different graphs were obtained for each of the devices. Figure 14a shows the magnetic field values of x and y in the coordinate axis during a given period, also showing the pre-alarm threshold in yellow and the alarm threshold in red. Figure 14b shows the series of checks carried out in which temporary trends and behaviors can be observed. The alarm and pre-alarm limits established in the previous section are shown in the same way. As can be seen, during all the checks, the magnetic field values were within the thresholds of good operation in such a way that it could be stated that this welding gun did not suffer from electrode alignment problems.

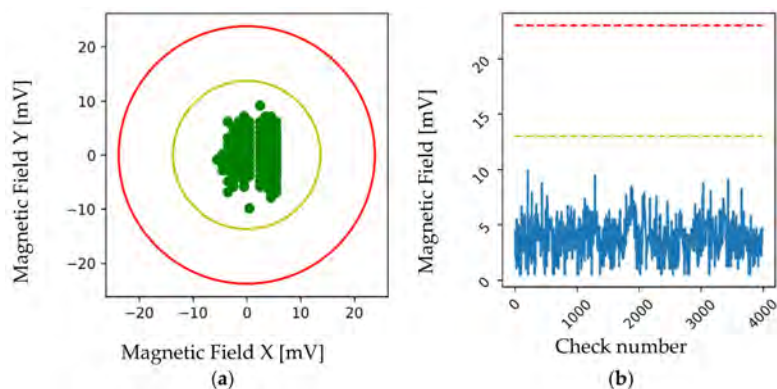


Figure 14. Data obtained from a welding gun in good condition from a production line. (a) Magnetic field axes X and Y . (b) Data series of the magnitude of the magnetic field.

In contrast to the graphs of Figure 14, the data obtained for a welding gun with alignment problems are shown in Figure 15. Figure 15a shows how many of the checks carried out obtained a value greater than the pre-alarm threshold, classified as abnormal behavior. Likewise, a number of points were located above the alarm threshold; these became a critical work area and, therefore, required corrective maintenance actions.

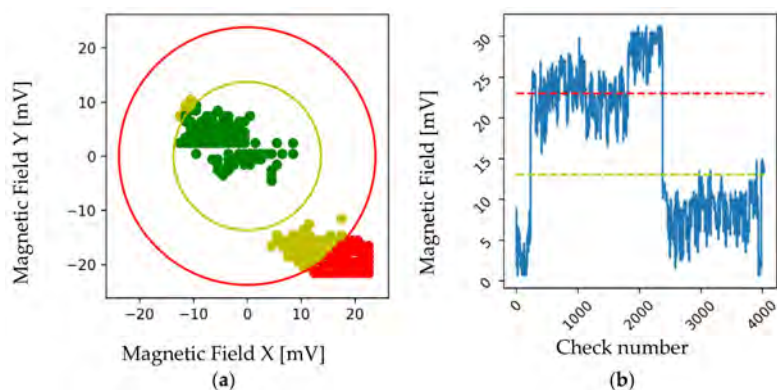


Figure 15. Data obtained from a misaligned welding gun from a production line. (a) Magnetic field axes x and Y . (b) Data series of the magnitude of the magnetic field.

In the same way, observing Figure 15b, at around check 200 there was a significant increase in the values of the magnetic field, exceeding the pre-alarm threshold established at around 13.8 mV. This increase was due to a collision between the robot and the milling machine that ended in a mismatch in the alignment of the electrodes. As the checks continued, at around check 2000 the condition of the electrodes worsened and all the checks were above the alarm threshold. Once the maintenance tasks for the reorientation of the electrodes to their original alignment position had been carried out, at around the 2500 check the magnetic field values were positioned below the pre-alarm and alarm values, thus returning them to normal operating values.

In conclusion, when comparing the behavior of the welding guns in the production lines, it could be determined that this system met the requirements to be implemented in production lines, as it was able to differentiate between the behaviors of perfectly aligned guns, guns with the beginning of a misalignment and totally misaligned guns.

6. Conclusions

This paper investigated the relationship between the alignment of electrodes and the magnetic field generated by welding guns in order to find a reliable method for the detection of this mechanical defect in high-productivity production lines, specifically in the car industry. The main conclusions that were drawn on the basis of the study were:

- (1) The contact area of the electrodes varied when there was a misalignment of the same; this generated a variation in the magnetic field generated when a current flowed through them.
- (2) When measuring the magnetic field always at the same point, the value of the magnetic field changed depending on the amount of misalignment present between both electrodes of the welding gun.
- (3) It was possible to measure the magnetic field of a welding gun with the proposed device, obtaining magnetic field values in the Cartesian axes.
- (4) A reliable protocol for sending alarms was proposed, sending the values through LoRa to the data analysis software. Based on the experimentation, alarm thresholds were established that were capable of determining when a misalignment occurred.

In short, a real solution was given in this paper to the problem of misalignments in production lines, not only presenting a method capable of detecting misalignments in real-time, but also a system that can easily be integrated into high-production lines of the automobile industry, thus presenting real cases of success of the implantation.

Author Contributions: Conceptualization, D.I. and J.M.; methodology, D.I., J.S. and J.M.; software, D.I. and J.M.; validation, D.I.; formal analysis, D.I.; investigation, D.I.; resources, E.G. and J.S.; data curation, D.I.; writing—original draft preparation, D.I.; writing—review and editing, E.G., J.S., J.M.; visualization, D.I.; supervision, E.G., J.S. and J.M.; project administration, E.G., J.S. and J.M.; funding acquisition, E.G. and J.S. All authors have read and agreed to the published version of the manuscript.

Funding: This research received no external funding.

Institutional Review Board Statement: Not applicable.

Informed Consent Statement: Not applicable.

Data Availability Statement: Not applicable.

Acknowledgments: The authors thank Ford España S.A. and in particular to the Almussafes Factory for their support in the present investigation. Likewise, the authors express their greatest gratitude to the “Fundación para el desarrollo y la innovación” (FDI) together with Generalitat Valenciana for supporting this research.

Conflicts of Interest: The authors declare no conflict of interest.

References

- O'Brien, R.L. (Ed.) *Welding Handbook, Welding Processes*, 8th ed.; American Welding Society: Miami, FL, USA, 1991; Volume 2.
- Banga, H.K.; Kalra, P.; Kumar, R.; Singh, S.; Pruncu, C.I. Optimization of the cycle time of robotics resistance spot welding for automotive applications. *J. Adv. Manuf. Process.* **2021**, *3*, e10084. [\[CrossRef\]](#)
- Aravinthan, A.; Nachimani, C. Analysis of Spot Weld Growth on Mild and Stainless Steel. *Weld. J.* **2011**, *90*, 143–147.
- Rajaraman, C.; Sivaraj, P.; Balasubramanian, V. Role of Welding Current on Mechanical Properties and Microstructural Characteristics of Resistance Spot Welded Dual Phase Steel Joints. *Phys. Met. Metallogr.* **2020**, *121*, 1447–1454. [\[CrossRef\]](#)
- Rajaraman, C.; Sivaraj, P.; Sonar, T.; Raja, S.; Mathiazhagan, N. Investigation on microstructural features and tensile shear fracture properties of resistance spot welded advanced high strength dual phase steel sheets in lap joint configuration for automotive frame applications. *J. Mech. Behav. Mater.* **2022**, *31*, 52–63. [\[CrossRef\]](#)
- Zhou, K.; Yao, P. Overview of recent advances of process analysis and quality control in resistance spot welding. *Mech. Syst. Signal Process.* **2019**, *124*, 170–198. [\[CrossRef\]](#)
- Wei, P.S.; Wu, T.H. Electrical contact resistance effect on resistance spot welding. *Int. J. Heat Mass Transf.* **2012**, *55*, 3316–3324, ISSN 0017-9310. [\[CrossRef\]](#)
- Reddy Gillela, P.K.; Jaidi, J.; Gude, V.; Pathak, S.K.; Srivastava, D. A numerical study on contact conditions, dynamic resistance, and nugget size of resistance spot weld joints of AISI 1008 steel sheets. *Numer. Heat Transf. Part A Appl.* **2022**, 1–19. [\[CrossRef\]](#)
- Yusuf, M.N.; Rahaman, W.E.W.A.; Manurung, Y.H.P.; Rafie, M.A.; Reduan, M.S.; Fadhil, M.Z.H. Numerical Analysis and Modelling of Resistance Spot Welded DP600 Steel Sheets. In *Recent Trends in Manufacturing and Materials Towards Industry 4.0*; Lecture Notes in Mechanical Engineering; Osman Zahid, M.N., Abdul Sani, A.S., Mohamad Yasin, M.R., Ismail, Z., Che Lah, N.A., Mohd Turan, F., Eds.; Springer: Singapore, 2021. [\[CrossRef\]](#)
- Chen, Z.; Zhou, Y. Surface modification of resistance welding electrode by electro-spark deposited composite coatings: Part I. Coating characterization. *Surf. Coat. Technol.* **2006**, *201*, 1503–1510, ISSN 0257-8972. [\[CrossRef\]](#)
- Nachi Mani, C. Effects of electrode deformation on carbon steel Weld. *Int. J. Adv. Innov. Thoughts Ideas* **2012**, *1*, 8.
- Parker, J.D.; Williams, N.T.; Holliday, R.J. Mechanisms of electrode degradation when spot welding coated steels. *Sci. Technol. Weld. Join.* **1998**, *3*, 65–74. [\[CrossRef\]](#)
- Peng, J.; Fukumoto, S.; Brown, L.; Zhou, N. Image analysis of electrode degradation in resistance spot welding of aluminium. *Sci. Technol. Weld. Join.* **2004**, *9*, 331–336. [\[CrossRef\]](#)
- Kim, J.W.; Murugan, S.P.; Kang, N.H.; Park, Y.D. Study on the effect of the localized electrode degradation on weldability during an electrode life test in resistance spot welding of ultra-high strength steel. *Korean J. Met. Mater.* **2019**, *57*, 715–725. [\[CrossRef\]](#)
- Kiselev, A.S.; Slobodyan, M.S. Effects of electrode degradation on properties of small-scale resistance spot welded joints of E110 alloy. In *Materials Science Forum*; Trans Tech Publications Ltd.: Bâch, Switzerland, 2019; Volume 970, pp. 227–235.
- Zhang, X.Q.; Chen, G.L.; Zhang, Y.S. Characteristics of electrode wear in resistance spot welding dual-phase steels. *Mater. Des.* **2008**, *29*, 279–283. [\[CrossRef\]](#)
- Shen, J.; Zhang, Y.S.; Lai, X.M. Influence of initial gap on weld expulsion in resistance spot welding of dual phase steel. *Sci. Technol. Weld. Join.* **2010**, *15*, 386–392. [\[CrossRef\]](#)
- Podržaj, P.; Jerman, B.; Simončič, S. Poor fit-up condition in resistance spot welding. *J. Mater. Process. Technol.* **2016**, *230*, 21–25. [\[CrossRef\]](#)
- Hassanifard, S. Analytical and Experimental Investigation of the Effects of Spot Weld Diameter, Gap Distance and Electrode Force on the Mixed Mode of Resistance Spot Welded-Joints. *Modares Mech. Eng.* **2011**, *11*, 39–48.
- Charde, N. Exploring the electrodes alignment and mushrooming effects on weld geometry of dissimilar steels during the spot welding process. *Sadhana* **2014**, *39*, 1563–1572. [\[CrossRef\]](#)
- Moarrefzadeh, A. Study of heat affected zone (HAZ) in resistance welding process. *J. Mech. Eng.* **2012**, *1*, 18–25.
- Senkara, J.; Zhang, H.; Hu, S.J. Expulsion prediction in resistance spot welding. *Welding J. N. Y.* **2004**, *83*, 123–S.
- Summerville, C.D.E.; Adams, D.; Compston, P.; Doolan, M. Process monitoring of resistance spot welding using the dynamic resistance signature. *Weld. J.* **2017**, *11*, 403–412.
- Hlavatý, I.; Hájková, P.; Krejčí, L.; Čep, R. Electric resistance welding of austenitic and galvanized steel sheets. *Teh. Vjesn.* **2018**, *25*, 1274–1277.
- Kaščák, L.; Spišák, E. Evaluation of the influence of the welding current on the surface quality of spot welds. *Int. J. Eng. Sci. IJES* **2016**, *5*, 32–37.
- Chan, K.R.; Scotchmer, N.S. Quality and electrode life improvements to automotive resistance welding of aluminum sheet. In *Proceedings of the Sheet Metal Welding Conference XIII*, Livonia, MI, USA, 14–16 May 2008; pp. 3–5.
- Tang, H.; Hou, W.; Hu, S.J.; Zhang, H.Y.; Feng, Z.; Kimchi, M. Influence of welding machine mechanical characteristics on the resistance spot welding process and weld quality. *Welding J. N. Y.* **2003**, *82*, 116–S.
- Charde, N. Effects of electrode deformation of resistance spot welding on 304 austenitic stainless steel weld geometry. *J. Mech. Eng. Sci.* **2012**, *3*, 261–270. [\[CrossRef\]](#)
- Li, Y.; Tang, G.; Ma, Y.; Shuangyu, L.; Ren, T. An electrode misalignment inspection system for resistance spot welding based on image processing technology. *Measur. Sci. Technol.* **2019**, *30*, 075401. [\[CrossRef\]](#)
- Xing, B.; Yan, S.; Zhou, H.; Chen, H.; Qin, Q.H. Qualitative and quantitative analysis of misaligned electrode degradation when welding galvanized steel. *Int. J. Adv. Manuf. Technol.* **2018**, *97*, 629–640. [\[CrossRef\]](#)

31. Lee, J.; Noh, I.; Jeong, S.I.; Lee, Y.; Lee, S.W. Development of Real-time Diagnosis Framework for Angular Misalignment of Robot Spot-welding System Based on Machine Learning. *Procedia Manuf.* **2020**, *48*, 1009–1019, ISSN 2351-9789. [CrossRef]
32. Ibáñez, D.; García, E.; Martos, J.; Soret, J. Real-time Electrode Misalignment Detection Device for RSW Basing on Magnetic Fields. In Proceedings of the 17th International Conference on Informatics in Control, Automation and Robotics (ICINCO 2020), Paris, France, 7–9 July 2020; pp. 142–149, ISBN 978-989-758-442-8. [CrossRef]
33. Rajaraman, K.C. Ampere’s Magnetic Circuitual Law: A Simple and Rigorous Two-Step Proof. *Int. J. Electr. Eng. Educ.* **2001**, *38*, 246–255. [CrossRef]
34. Sears, F.W. Faraday’s law and Ampere’s law. *Am. J. Phys.* **1963**, *31*, 439–443. [CrossRef]
35. Ibáñez, D.; García, E.; Soret, J.; Martos, J. Influence of Mechanical Failures of the Welding Gun on the Magnetic Field Generated in the Measurement of Misalignment. In *Informatics in Control, Automation and Robotics, Proceedings of the ICINCO 2020, Paris, France, 7–9 July 2020*; Lecture Notes in Electrical Engineering; Gusikhin, O., Madani, K., Zaytoon, J., Eds.; Springer: Cham, Switzerland, 2022; Volume 793. [CrossRef]
36. SS49E Series Linear Position Sensors, Honeywell Inc. Available online: <http://sccatalog.honeywell.com/imc/printfriendly.asp?FAM=solidstate&PN=SS49E> (accessed on 15 September 2022).
37. *DIN EN ISO 5821:2010-04*; Resistance Welding—Spot Welding Electrode Caps (ISO 5821:2009); German Version EN ISO 5821:2009. ISO: Geneva, Switzerland, 2009.
38. García, E.; Montes, N. Mini-term, a novel paradigm for fault detection. *IFAC-Pap.* **2019**, *52*, 165–170. [CrossRef]

Chapter 5. VIRTUAL SENSOR FOR THE DETECTION OF WEAR IN THE SECONDARY CIRCUIT OF THE WELDING GUN

This chapter presents a new method developed for the detection of wear in the secondary circuit of resistance welding guns. This chapter shows the evolution of the investigation to reach a final solution through two papers. In the first place, the first approximation to the detection of wear is shown through the analysis of duty cycle of the power circuit of the welding control. The second article goes further by adding the variables of the secondary resistances by means of a virtual sensor, allowing early detection of wear that occurs in welding guns.

Detection of welding gun secondary wear is critical to maintaining the efficiency and quality of welding operations. The secondary, which is the part that transfers electrical energy from the transformer to the electrode, is subject to constant wear due to the heat and pressure it experiences during the welding process. As a result, detection of secondary wear is essential to avoid potential problems such as increased power consumption, lower quality, and frequent downtime.

One of the main reasons for detecting secondary wear is the impact on power consumption. As the secondary wears, the contact resistance between the electrode and the secondary increases, leading to increased power consumption. This not only increases operating costs, but also affects the environment by producing more carbon emissions. Additionally, secondary wear can lead to poor weld quality,

which can lead to product failure and reputational damage. In addition, frequent downtime due to the replacement of worn secondaries can lead to production delays and financial losses.

During this research, two articles have been developed to explore the importance of detecting wear on the secondary of welding guns. The first article seeks first to emphasize the importance of monitoring secondary wear, highlighting the importance of keeping accurate records of secondary wear and replacing them when necessary to avoid unexpected downtime. This article first shows the correlation between the wear of the secondary with the duty cycle of the power circuit of the welding control by means of the simulation of the electrical circuit. Once this correlation is established, an initial method for the detection of secondary wear is proposed by means of continuous monitoring of the control variable of the IGBTs.

The second article focuses on optimizing the first method so that wear can be detected early, trying to have an early detection of possible wear. In this article we start from the control variable of the IGBTs to implement a virtual sensor of the resistances of the secondary. This allows an analysis of the Mahalanobis distance between both variables. This new method can predict secondary operator wear and alert before any major problem arises. This enhancement can help reduce downtime and costs by predicting when the secondary needs to be replaced.

In conclusion, both articles that are presented below show a real method tested in a production line for the detection of electrode wear in real time, allowing to reduce manufacturing costs, avoiding stops and quality problems.

5.1 SCIENTIFIC CONFERENCE ARTICLE III





Title: A Novel Real-Time Wear Detection System for the Secondary Circuit of Resistance Welding Guns.

Authors: Daniel Ibáñez, Eduardo García, Julio Martos and Jesús Soret.

Published in: Proceedings of the 19th International Conference on Informatics in Control, Automation and Robotics—ICINCO, Lisbon, Portugal. 2022. p. 14-16.

Description: ICINCO, or the International Conference on Informatics in Control, Automation and Robotics, is an annual conference that brings together researchers, engineers, and practitioners in the fields of control, automation, and robotics. The conference provides a forum for sharing new ideas and developments, exchanging information on the latest trends, and discussing challenges faced in these fields. ICINCO2022 was held in Lisbon, Portugal, and featured keynote speeches, technical sessions, and workshops covering a wide range of topics related to informatics in control, automation, and robotics. The conference focused on areas such as intelligent control systems, machine learning and optimization, robotics and automation, and signal processing. The conference attracted participants from around the world, providing a platform for researchers and practitioners to network, exchange ideas, and collaborate on new research.

A novel real-time wear detection system for the secondary circuit of resistance welding guns

D.Ibáñez¹^a, E. García²^b, J.Martos¹^c and J. Soret¹^d

¹ Dept. of Electrical and Electronic Engineering, University of Valencia, Burjassot, Valencia, Spain

² Ford Valencia, 46440, Valencia, Spain

{Daniel.ibanez, Jesus.Soret,Julio.Martos}@uv.es, egarci72@ford.com

Keywords: Resistance Spot welding, predictive maintenance, secondary circuit, welding gun.

Abstract: Currently, many resources are invested in high-production automotive factories to correct quality defects caused in the bodywork due to secondary circuit wear. In the same way, energy losses are generated due to the increase in resistance caused by secondary wear, thus reducing efficiency and increasing the final cost of the product. This happens because, at present, there is no method that allows the predictive detection of problems in the secondary and the arms of the welding gun. Consequently, a solution must be developed to carry out predictive maintenance applicable to the automotive industry to detect this defect. This research provides an answer by proposing a method to detect variations in the state of the secondary of the welding gun using existing data in the welding process, specifically, the evolution of the angle of degassing of the IGBTs of the welding control. To validate the relationship between the control shift angle and the increase in wear, an electronic simulation software was used to simulate the behaviour of the real welding control.

1. INTRODUCTION


The resistance welding process is one of the most widely used in the automotive industry for joining the metal parts of the bodywork, representing around 90% of all welded joints in a bodywork (Koskimäki et al., 2007; Yu et al., 2014; Hwang et al., 2013). As the name of the process indicates, it is the resistance to the current flow of the metals to be welded that causes the localized increase in heat and the formation of the nugget welding. For this process, it is also necessary to exert pressure on the parts to be welded for a specific welding time. Ultimately, therefore, welding is generated by a combination of heat, pressure, and time.


Despite being able to summarize the resistance welding process as the combination of heat, pressure and time, this process is highly complex, since it involves different fields of study such as


electromagnetism, electronics, thermodynamics, materials and mechanics. (Li et al., 2007)


Throughout different investigations, it has been described how the different welding parameters can influence the quality of the welded joint, such as pressure (Zhou et al., 2014; Sun et al., 2007; Ibáñez et al., 2021), the current (Aslanlar et al., 2007; Hwang et al., 2011), the welding time (Aslanlar et al., 2008) or the misalignment of the welding electrodes (Ibáñez et al., 2020). From all these studies it can be concluded that either due to external factors or due to welding parameters, there are many factors that directly or indirectly affect the final quality of the welded joint.

To achieve adequate welding quality, it will therefore be necessary to guarantee that the parameters influencing welding quality remain stable over time. One of the defects that can cause variations in the application of the correct parameters in welding, especially in the application of current, is the mechanical state of the electrical circuit of the

^a <https://orcid.org/0000-0002-3917-9875>

^b <https://orcid.org/0000-0002-4210-9835>

^c <https://orcid.org/0000-0002-8455-6369>

^d <https://orcid.org/0000-0001-8695-6334>

welding gun, specifically, of the secondary circuit of the gun, that is, the arms of the welding gun.

Over time, the way of applying the current to the welding points has been changing to achieve the highest quality with the best possible efficiency and power consumption. If the behavior of a single-phase alternating welding machine is observed, it can be determined that there are inherent losses in the alternating voltage supply (Zhou et al. 2001). For this reason and to guarantee the optimum quality of the welding, three-phase welding machines are used. The three-phase voltage is rectified to convert it from single-phase to direct current. This rectified current results in lower power losses and higher quality welding (Munesada et al.2010).

In this type of converter-based welding machines, the three-phase voltage of the industrial mains line, typically 440V and 50/60Hz, is converted to single-phase direct voltage and stored in a capacitor bank to smooth the voltage.

The capacitor bank is connected to the inverter circuit formed by an IGBTs bridge that modulates the wave at a higher frequency than the line. Usually, to achieve higher welding quality and greater control over the welding current, the wave is modulated at a frequency of 1000Hz, this type of machine being known as mid frequency direct current (MFDC).

The alternating wave produced at the output of the inverter feeds the single-phase transformer of the welding gun. (Salem et al. 2011). This will allow to have a continuous current in the secondary of the transformer. This working mode prevents the welding current from having zero crossings that would cool the part, allowing faster heating of the welding gun. In addition, by working with direct current, inductive power losses or problems with the magnetic material of the machine are avoided (Wei, 2004; Nagasathya et al 2013.).

In MFDC machines, the secondary voltage is determined by the primary voltage, which, as mentioned, is modified by the inverter controlled by the IGBTs. If a constant IGTS control shift angle is maintained, the secondary voltage should remain constant. Starting from this point, it can be stated that the welding current, according to Ohm's law, will be determined by the resistance of the secondary, that is, the resistance of the welding arms and the resistance of the metal to be welded. As the total resistance of the secondary circuit increases, the current flowing between the electrodes decreases (Arslan et al 2020). This makes it essential to guarantee the maintenance of the resistance of the welding arms in such a way that the way in which the current is applied to the metal to be welded is not affected.

2. MFDC MACHINE AND SECONDARY LOAD

The welding current is a fundamental component to achieve optimal welding quality. In the electronic diagram of Figure 1, the stages of the power circuit can be observed differently from the three-phase line of the electrical network to the continuous single-phase line of the welding electrodes.

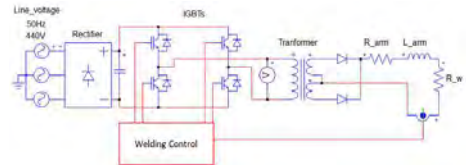


Figure 1. Welding machine electrical schematic

Modern welding machines have a current control system, in such a way that it is guaranteed that the current established by parameters is being applied to the metal to be welded. The welding machine analyzes the secondary current every millisecond and modifies the control shift angle of the IGBTs firing to modify the primary voltage, as it can be seen in the results obtained from the simulation in figure 2 for the different angle s of shot ($\alpha=30^\circ$, $\alpha=80^\circ$ and $\alpha=105^\circ$). As the control angle between the control signals of the IGBTs increases, the effective primary voltage decreases, thus decreasing the secondary voltage and current (Zhou & Cai,2014).

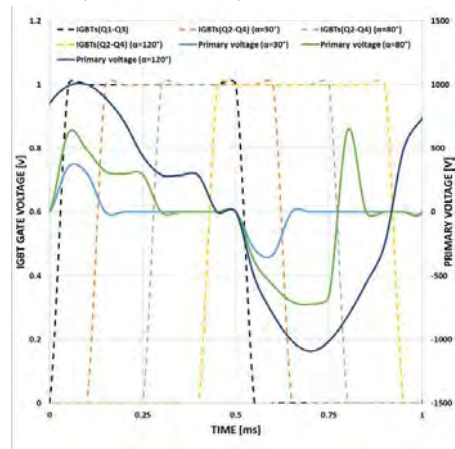


Figure 2. Response of the primary voltage as a function of the control shift angle of the IGBTs

From Figures 1 and 3, the behavior of the IGBT rectifier can be divided into six segments in one period. These six segments can be summarized as:

- State 1: In this state, the IGBTs Q1 and Q4 are conductive, therefore it is in active mode with positive output voltage and output current i.e., the DC side power is converted to the load.
- State 2: At this point Q1 and D3 go on, freewheeling mode with zero and positive output voltage/output current.
- State 3: Diodes D2 and D3 then conduct in feedback mode with negative and positive output voltage and output current. Power from the load is sent back to the DC side.
- State 4: returns to active mode with Q2 and Q3 conducting with negative output voltage and output current. The DC side power is converted to the load. State 5: Return to freewheeling mode with Q2 and D4 conducting with zero and negative output voltage and output current.
- State 6. Finally, Q1 and D4 conduct in feedback mode with positive voltage and negative output current. Power from the load is sent back to the DC side.

According to this description, the output voltage will depend on the period that it is in each of the states, that is, on the control shift angle. Therefore, by adjusting the control shift, the output voltage can be adjusted.

The Fourier series of the output voltage can be obtained as follows:

$$V_{prim} = \sum_{n=1,3,5...} \frac{4V_d}{n\pi} \sin\left(\frac{n\alpha}{2}\right) \cos(n\omega t) \quad (1)$$

Where V_d represents the output voltage at the rectifier and α is the control shift.

In this way, the secondary voltage can also be related to the control shift angle of the IGBTs, as the welding control increases the control shift angle between the signals, the secondary voltage is reduced. In a similar way and due to the power conservation law, the secondary current will also be influenced by the primary power, therefore, as the control shift angle between the control signals increases, the welding current decreases, considering constant resistance, can be obtained from the simulation figure 3, in which the relationship between the control shift angle and the final welding current is observed.

Following Ohm's law, the welding current is determined not only by the secondary voltage but will also be influenced by the resistance of the secondary circuit. This resistance of the circuit can be divided into two blocks: The first load can be defined as those elements that do not directly participate in welding,

that is, joints between the copper elements of the gun, cooled braids, welding arms, etc. If the welding gun is in an optimal state of maintenance, this resistance should remain constant. In the second load block are those elements that have an active role in welding, that is, this resistance is made up of the electrode holders, the electrodes, the connection between the electrode and the metal, the resistance of the metal and the resistance of the union between the metals to be welded. This resistance will depend on the type of material, the type of electrodes and the wear of the electrodes.

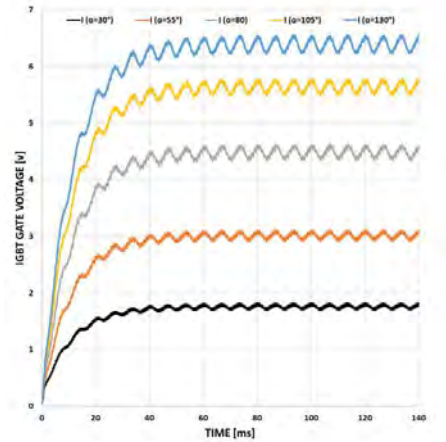


Figure 3. Response of the secondary current as a function of the control shift angle of the IGBTs

Due to this variability of the welding points and to guarantee the energy supplied to the joint and therefore the quality of the joints, the welding machines regulate the control shift angle of the IGBTs in such a way that the current supplied does not depend on resistance, but this will depend solely on the control of the welding machine.

3. SECONDARY CIRCUIT WEAR

Eventually, mainly due to the erosion caused by the fatigue of the work cycles of the welding guns, the secondary circuit begins to show wear. Specifically, these wears appear in the first block of the load defined in the previous section.

The wear that can appear in the secondary is very diverse, since, based on the definition of this load block, it is made up of different components and

joints, as shown in figure 4. The main worn elements that can occur in a secondary are:

- Corrosion on welding arms caused by water leaks at welding gun joints or caused by changing electrodes.
- Transformer pins worn or fired due to poor cooling or lime scale.
- Cracked arms caused by metal fatigue over time.
- Clogged refrigerated braids.
- Cracked or missing weld strips.

All these wears contribute notably to the increase in the resistance of the first load-bearing block. This first block does not initially have a direct influence on the weld if the welding machine control can reach the optimum welding current. However, as these wears become more noticeable, typical welding problems begin to appear, such as sparks, inconsistent weld joints, or even missing welds.

On the other hand, an increase in secondary resistance means an increase in the power consumed during welding. If this increase in resistance is caused by wear, the power supplied to the welding point will be the same, however, the power consumed during the process will increase, causing greater energy consumption.



Figure 4. Real cases of wear in the secondary circuit

Figure 5 shows the control shift angle necessary to reach each of the currents. Each of the curves represents a parasitic resistance value of the secondary corresponding to the simulated resistance value of the first block, keeping the second block with a constant load. In this way, it can be verified that as the resistance of the secondary caused by wear increases, the angle necessary to achieve the desired current also increases, that is, the voltage of the

primary increases and therefore the energy consumed during welding.

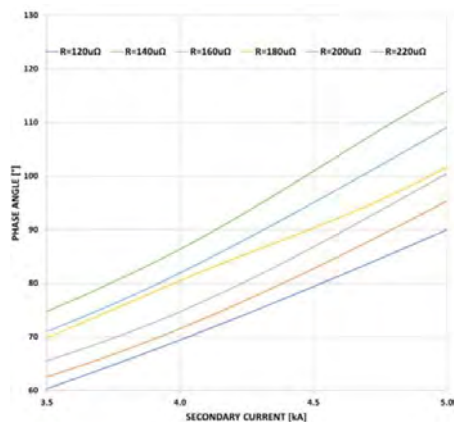


Figure 5. Evolution of the control shift angle depending on the resistance of the secondary.

4. SECONDARY WEAR DETECTION

Due to the implications of this defect in both welding quality and energy consumption, its early detection is essential.

Specifically, a method is presented for the predictive detection of secondary circuit wear by monitoring the control shift angle of the IGBTs. The method bases its operation on the collection of welding data in real time from the welding guns during their normal work cycle.

The welding cycle of a welding gun in a real welding line can be described as: the new electrodes are placed on the electrode holder and welding points begin to be made on the metal to be welded, in the specific case of the manufacture of the car body, the characteristics of the metals to be welded vary depending on the piece, so each specific welding joint needs its own parameterization to achieve the required welding quality. After making a series of welding points, usually between 150-200 joints, the electrodes are milled to return them to their initial geometry and remove any dirt that might remain attached.

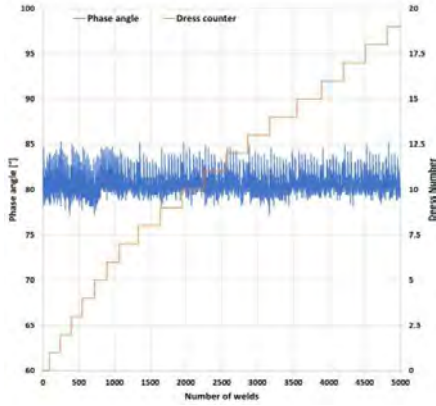


Figure 6. Control shift angle along the electrode life.

Within this work cycle, there is a variation of the welding current and the control shift angle of the IGBTs. This variation is given both by the differences in the metal to be welded and by the degradation of the electrode. It can be considered that this variation remains constant when passing from one duty cycle to another, so if the entire cycle is reduced to a single value, it could be stated that the average current and the control shift angle should remain constant.

Figure 5 shows the control shift degrees for a welding gun together with the evolution of the number of joints made. It can be seen how despite the variation between each of the points represented, the trend remains stable.

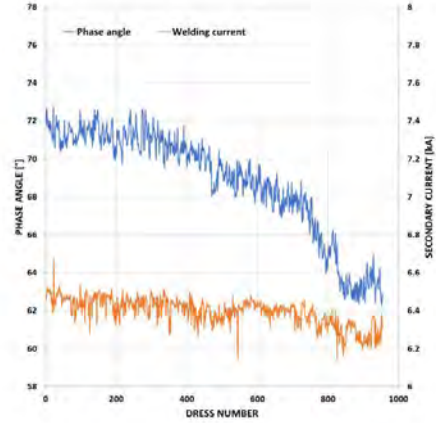
After observing that the usual behaviour of the work cycle between milling is stable, the hypothesis can be raised since when the secondary circuit begins to show wear, a distortion will be observed in the wear data due to the correction of the welding machine to guarantee the desired current.

Figure 6 shows the actual data of a welding gun that shows a beginning of degradation. In this case, it is observed how it goes from a stable behaviour to a behaviour with a downward trend. This means that for the same welding current, the welding machine needs a higher electrical consumption and therefore the parasitic resistance of the secondary circuit has increased.

From the comparison of figures 6 and 7, it can be determined that by carrying out continuous monitoring of the control shift angle of the IGBTs, it is possible to detect changes in the parasitic resistance of the secondary circuit. In other words, the hypothesis of the analysis of the evolution of the control shift angle for the determination of the

increase in wear in the secondary circuit of the welding machine is confirmed.

Figure 7. Evolution of the control shift angle with the wear



of the secondary circuit

5. REAL-TIME MONITORING SYSTEM

This method is designed to be applied in real welding lines, specifically, for this study, ARO type C and X welding guns controlled by means of the BOS6000 welding timer have been analysed.

First, a protocol is established for the acquisition of welding data in real time. This first step notably reduces the amount of data that is handled, since, as shown in the previous sections, each of the control shifts of each welding point is not analysed, but rather it is analysed based on the average control shift of all weld joints made throughout a milling cycle.

Therefore, this first step collects the data from the welding database, performs the average by cycles and indexes the data in the database on which the alarms are generated.

$$W = Q_3 + 1.5IQR \quad (2)$$

For the generation of alarms, a simple method of detecting changes in behaviour is established. As shown in equation 1, the warning limit is established by calculating the sum of the third quartile plus 1.5 times the interquartile of the data series. Similarly, the alarm level is established as the sum of the third quartile plus 3 times the interquartile as describe in equation 3.

$$A = Q_3 + 3IQR \quad (3)$$

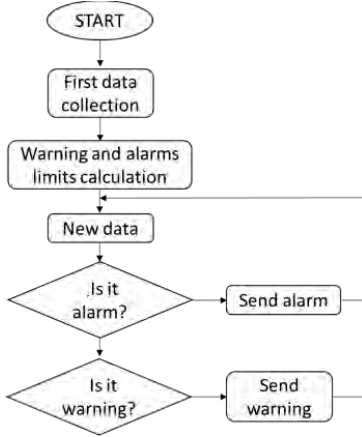


Figure 8. Alarm system.

Therefore, initially, an initial amount of data is needed to calculate the quartiles and thus establishing the warning and alarm limits, that is, an amount of data is needed to make an initial calibration.

In this way, when new data arrives from a specific welding gun, the data is labelled according to whether it is within the established warning and alarm thresholds. When a welding gun begins to show wear, the data will go from being in the good working group to the warning or alarm group, thus being able to carry out the necessary actions to reduce and minimize the quality problems associated with this defect.

In short, this entire system can be described according to the flow chart in Figure 8.

This programming has been carried out for validation on 450 welding guns installed on a real welding line. Usually, a welding gun installed on a high production line can do around 10,000 welding points per day, which would mean working with around 450,000 data per day. With the simplification of the average between milling cycles, this amount of data can be reduced to about 2500 daily data, which significantly reduces the number of resources needed for their management and analysis.

Figures 9 and 10 show two real graphs of behaviour for two different welding guns in a period of two months.

Figure 9, corresponding to what has been called gun A, shows the behaviour for a welding gun in good condition. The offset angle data oscillates within a range of two degrees but rarely reaches the warning threshold, so it is not necessary to carry out any maintenance on the welding gun.

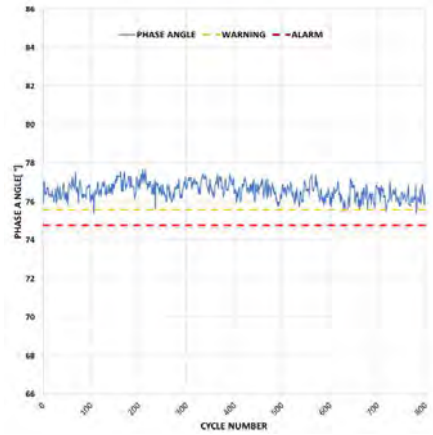


Figure 9. Evolution of the control shift angle gun A.

However, looking at Figure 10, the data shown presents three behaviour zones. In the first zone, or initial zone, the data is above the warning threshold but shows a variable behaviour. In the second zone, the data exceeds the warning threshold, and the value remains stable over a certain time, finally, and as no maintenance action is performed, the offset angle data increases significantly, which means that the resistance of the secondary is increasing exponentially.

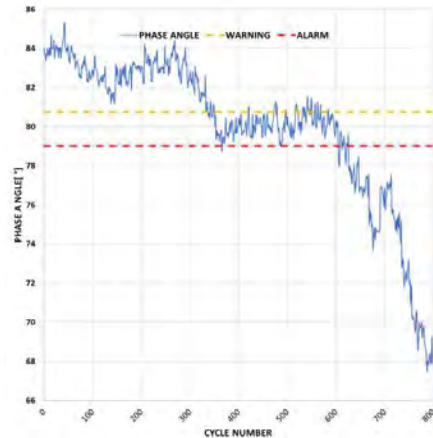


Figure 10. Evolution of the control shift angle gun B.

Similarly, comparing both figures it can be seen how the energy consumption, as described in the previous sections, remains constant over time for gun A, however, to perform the same welding cycle gun

B needs each time a greater contribution of energy, which is lost in the parasitic resistance of the secondary.

In short, from the comparison of figures 9 and 10 it can be determined that the method chosen for setting the warning and alarm thresholds seems to be the right one to carry out predictive maintenance.

CONCLUSION

Throughout this paper, an effective method for detecting wear in the secondary circuit of resistance welding guns has been shown. This defect causes a decrease in welding quality and also an increase in energy consumption in resistance welding processes. Electronic simulation has shown how the relationship between current and control shift angle is easily demonstrable. From this relationship it has been assumed that if an analysis of the history of the data is carried out, an increase in the wear of the secondary welding circuit can be determined.

This method has been applied in a real factory, adapting the study for data reduction, and simplifying the analysis and sending of alarms to those responsible for maintenance.

From the real data acquired in the production lines, it has been possible to validate that this method is viable and reliable for the detection of wear problems in the welding lines through the analysis of the shift angle control.

ACKNOWLEDGEMENTS

This study was supported by the Universitat de València, Ford Spain S.L. and Fundación para el Desarrollo y la Innovación (FDI), Spain, which the authors gratefully acknowledge.

REFERENCES

- Koskimäki, P. Laurinen, E. Haapalainen, L. Tuovinen, and M. Juha Rönning, "Application of the extended knn method to resistance spot welding process identification and the benefits of process information," *IEEE Trans. Indus. Electron.* 54(5), 2823–2830 (2007).
- J. Yu, D. Choi, and S. Rhee, "Improvement of weldability of 1 GPa grade twin-induced plasticity steel," *Welding J.* 93(3), 78s–84s (2014).
- G. Hwang, P. Podrzaj, and H. Hashimoto, "Note: Resistance spot welding using a microgripper," *Rev. Sci. Instrum.* 84(10), 106105-1–3 (2013).
- Y. B. Li, Z. Q. Lin, S. J. Hu, and G. L. Chen, "Numerical analysis of magnetic fluid dynamics behaviors during resistance spot welding," *J. Appl. Phys.* 101(05), 053506 (2007).
- Zhou, Kang, and Lilong Cai. "Study on effect of electrode force on resistance spot welding process." *Journal of applied physics* 116.8 (2014): 084902.
- Sun, H. T., et al. "Effect of variable electrode force on weld quality in resistance spot welding." *Science and Technology of Welding and Joining* 12.8 (2007): 718-724.
- Ibáñez, D.; García, E.; Martos, J. and Soret, J. (2021). A Novel Method for the Real-time Force Losses Detection in Servo Welding Guns. In *Proceedings of the 18th International Conference on Informatics in Control, Automation and Robotics - ICINCO*, ISBN 978-989-758-522-7; ISSN 2184-2809, pages 669-676. DOI: 10.5220/0010549006690676 (2021)
- Saleem, Jawad & Majid, Abdul & Haller, Stefan & Bertilsson, Kent. (2011). A study of IGBT rupture phenomenon in medium frequency resistance welding machine. 236-239. 10.1109/ACEMP.2011.6490602.
- Aslanlar, Salim, et al. "Effect of welding current on mechanical properties of galvanized chromided steel sheets in electrical resistance spot welding." *Materials & Design* 28.1 (2007): 2-7
- Hwang, In Sung, Mun Jin Kang, and Dong Cheol Kim. "Expulsion reduction in resistance spot welding by controlling of welding current waveform." *Procedia Engineering* 10 (2011): 2775-2781.
- Aslanlar, S., et al. "Welding time effect on mechanical properties of automotive sheets in electrical resistance spot welding." *Materials & Design* 29.7 (2008): 1427-1431.
- Ibáñez, D.; García, E.; Martos, J. and Soret, J. (2020). Real-time Electrode Misalignment Detection Device for RSW Basing on Magnetic Fields. In *Proceedings of the 17th International Conference on Informatics in Control, Automation and Robotics - ICINCO*, ISBN 978-989-758-442-8; ISSN 2184-2809, pages 142-149. DOI: 10.5220/0009820801420149
- Y. ZHOU, S. J. DONG and K. J. ELY, "Weldability of Thin Sheet Metals by Small-Scale Resistance Spot Welding using High-Frequency Inverter and Capacitor-Discharge Power Supplies," in *Journal of Electronic Materials*, Vol. 30, No. 8, 2001.
- T. Munesada, Y. Takasaki, T. Sonada "Spot Welding current control with a frequency controlled inverter power supply," 16th International Conference on Electrical Engineering" July 11-14, 2010 Busan Korea
- Li, Wei .Energy consumption in AC and MFDC resistance spot welding, XI the Sheet Metal Welding Conference, Heights, Michigan. p. 1-12. 2004.
- Nagasathya N., Boopathy S. R., Santhakumari A. MFDC- An energy efficient adaptive technology for welding of thin sheets, IEEE Energy Efficient Technologies for Sustainability Conference (ICEETS), 2013, Nagercoil, India, p. 901-906.
- Arslan, Serdal & Tarimer, İlhan & Güven, Mehmet & Oy, Sibel. (2020). A medium frequency transformer design

for spot welding machine using sizing equation and finite element analysis. Engineering review. 40. 42-51. 10.30765/er.40.3.05.

- Zhou, K. and Cai, L. (2014), Study of safety operation of AC resistance spot welding system. IET Power Electronics, 7: 141-147. <https://doi.org/10.1049/iet-pel.2013.0094>
- Gao, David (Zhiwei) (2016). Electric Renewable Energy Systems || DC-AC inverters. , (), 354–381. doi:10.1016/B978-0-12-804448-3.00016-5

5.2 SCIENTIFIC ARTICLE III

Title: Incipient Wear Detection of Welding Gun Secondary Circuit by Virtual Resistance Sensor Using Mahalanobis Distance.

Authors: Daniel Ibáñez, Eduardo García, Julio Martos and Jesús Soret.

Published in: *Sensors* 2023, 23(2), 94; Special Issue: Virtual Sensors for Industry 4.0 Era <https://doi.org/10.3390/s23020894>

Impact factor: 3.847 (2021). Quartile (category: "Instruments & Instrumentation"): Q2 (2021)

Citations: 1 (accessed on March 2022).

Description: *Sensors* is a leading peer-reviewed, open access journal that focuses on the science and technology of sensors. It is published semi-monthly online by MDPI and is affiliated with several societies related to the field of sensors. The journal offers high visibility and is indexed in various databases, including Scopus, SCIE, PubMed, and MEDLINE. It has a Q2 ranking in Instruments & Instrumentation and a Q1 ranking in Instrumentation according to JCR and CiteScore, respectively.

Sensors is important as it provides a platform for researchers and scientists to publish their findings and advancements related to sensors. It promotes interdisciplinary research, which is crucial for the development of innovative sensor technologies. With its open access policy, *Sensors* ensures that research findings are accessible to a wider audience, which can lead to more collaborations and further advancements.

The special issue of *Sensors* named "Virtual Sensors for Industry 4.0 Era" focuses on the use of Industry 4.0 technologies, such as Digital Twin or industrial Big Data, to define virtual sensors that allow measuring parameters of industrial lines. The aim is to

provide an alternative to the installation of a large number of sensors or to measure parameters that are otherwise impossible to measure. The issue highlights the possibilities offered by Industry 4.0 and how virtual sensors can be utilized to carry out predictive maintenance, improve the quality of parts, and reduce costs.

Article

Incipient Wear Detection of Welding Gun Secondary Circuit by Virtual Resistance Sensor Using Mahalanobis Distance

Daniel Ibáñez ^{1,*}, Eduardo Garcia ², Jesús Soret ¹ and Julio Martos ¹

¹ Department of Electronic Engineering, Campus de Burjassot, Universidad de Valencia, 46100 Valencia, Spain

² Ford Spain, Poligono Industrial Ford S/N, 46440 Almussafes, Spain

* Correspondence: daniel.ibanez@uv.es; Tel.: +34-961-791-543

Abstract: Wear of the secondary of the welding gun, caused by mechanical fatigue or due to a bad parameterization of the welding points, causes an increase in quality problems such as non-existent welds or a reduced weld nugget size. In addition to quality problems, this defect causes production stoppages that affect the final cost of the manufactured part. Different studies have focused on evaluating the importance of different welding parameters, such as current, in the final quality of the welding nugget. However, few studies have focused on preventing weld command parameters from degrading or changing. This investigation seeks to determine the wear of the secondary circuit to avoid variability in the current supplied to the welding point caused by this defect and the increase in circuit resistance, especially in industrial environments. In this work, a virtual sensor is developed to estimate the resistance of the welding arm based on previous research, which has shown the possibility of detecting secondary wear by analysing the duty cycle of the power circuit. From the data of the virtual sensor, an anomaly detection method based on the Mahalanobis distance is developed. Finally, an integral system for detecting secondary wear of welding guns in real production lines is presented. This system establishes performance thresholds based on the analysis of the Mahalanobis distance distribution, allowing monitoring of the secondary circuit wear condition after each welding cycle. The results obtained show how the system can detect incipient wear in welding guns, regardless of which part of the secondary the wear occurs, improving decision-making and reducing quality problems.

Keywords: MFDC welding; wear monitoring; virtual sensor; Mahalanobis distance



Citation: Ibáñez, D.; Garcia, E.; Soret, J.; Martos, J. Incipient Wear Detection of Welding Gun Secondary Circuit by Virtual Resistance Sensor Using Mahalanobis Distance. *Sensors* **2023**, *23*, 894. <https://doi.org/10.3390/s23020894>

Academic Editor: Songling Huang

Received: 15 December 2022

Revised: 5 January 2023

Accepted: 8 January 2023

Published: 12 January 2023



Copyright: © 2023 by the authors. Licensee MDPI, Basel, Switzerland. This article is an open access article distributed under the terms and conditions of the Creative Commons Attribution (CC BY) license (<https://creativecommons.org/licenses/by/4.0/>).

1. Introduction

Resistance spot welding (RSW) is widely used for joining metal sheets without extra material input. This is due to it being possibly the fastest, cheapest, and most efficient joining method. These advantages make this method one of the most used technologies for joining metals in industries such as aerospace or automotive industries [1,2]. For example, currently, over 90% of assembly work in a car body is completed by RSW, a vital joining process for automotive production [3].

In the resistance spot welding process, two or more sheets of metal are pressed by means of the electrodes of the welding gun; this action can be carried out by a pneumatic cylinder or by a servomotor, depending on the type of welding. Once the necessary pressure is reached, the welding timer circulates the welding current through the contact metal sheets, generating the necessary energy to melt the metals. This energy generates following the basic Joule heat generation equation (Equation (1)):

$$Q = I^2 \cdot R \cdot t \quad (1)$$

Despite the simplicity of the heat generation equation, resistance spot welding is a complex process, as it involves different fields of study such as electromagnetism, electronics, thermodynamics, materials, and mechanics [4]. Therefore, due to the complexity

of the process, there are many parameters that influence the final quality of the welding joint. The different parameters and influences on the final quality have been studied by different authors, highlighting the importance of pressure, current, electrode wear, welding shunt effect, or electrode misalignment [5–8]. Therefore, it is essential for the industry to guarantee the stability of the process to avoid the variations in the parameters that have an impact on welding. One of the defects in welding guns that causes production problems is the wear of the power circuit. Within this circuit, elements such as disparate screws, copper/aluminium arms of welding guns, diodes, and transformers are included.

MFDC Welding

In resistance spot welding, there are two prevalent types of power sources responsible for controlling the way power is delivered to the load: three-phase medium-frequency DC power source and single-phase AC power source, both having different characteristics that generate a different effect in the way the nugget is formed [9]. First, in a single-phase AC power supply, two thyristors are connected in parallel, which allows current to pass during the positive semicycle through one of them, while in the negative semicycle, it passes through the other [10]. In this type of welding machine, the welding timer establishes the adjustment of the firing angle for each of the thyristors in each control cycle, starting from 0° to 180° . This firing angle control allows the welding timer to control the energy supplied to the welding point. The main characteristic of this type of welding is that in certain periods, the current is zero, which allows the welding nugget to cool, thus losing energy efficiency [11].

On the other hand, the medium-frequency three-phase DC power supply can be mentioned. This type of power supply is more complex, having four functional blocks: a three-phase AC power supply, a rectifier, an IGBT H-bridge inverter, and, finally, the welding transformer, as shown in Figure 1.

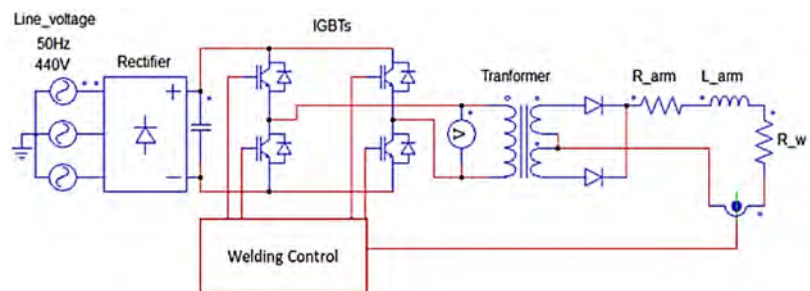


Figure 1. Schematics of MFDC Welder.

Figure 1 shows the three-phase network voltage rectified to an approximate DC single-phase voltage, U_{dc} . This DC voltage is chopped at the H-bridge, in such a way that the primary voltage of the transformer depends on the state of the IGBTs. When IGBTs Q1 and Q4 are on, the voltage in the primary of the welding transformer is $+U_{dc}$, while when Q2 and Q3 are in conduction, the voltage in the primary is $-U_{dc}$. However, when the parallel IGBTs are on simultaneously, the output voltage will be equal to 0. The conduction states of the IGBTs are controlled by the welding timer. This control is based on an SMPS (phase-shifted full-bridge); therefore, to control the energy supplied to the welding point, the welding timer modifies the duty cycle of the SMPS [12,13].

Compared with the previous type of single-phase AC power supply, this type of welding power supply supplies a continuous current to the welding point, which allows heat to be supplied to the metal sheets during the entire process. The MFDC welder usually works at frequencies close to 1000 Hz, which allows greater control over the output current, adjusting it throughout the process based on the energy supplied. For these reasons, this type of power supply has a higher energy efficiency than the single-phase AC power

supply. Due to this fact, this type of power supply is usually used in industries with a high production of welded joints, such as the automobile industry, as it favours lower energy consumption and greater control over the welded joints [14].

In both types of power supply, the electrical current of the secondary circuit depends on the primary voltage, either through the control of the IGBTs for the MFDC or through the phase shift of the thyristors firing in single-phase AC, and on the secondary resistance. Consequently, variations in the resistances of the secondary circuit cause variations in the current applied to the weld. It is, therefore, essential to guarantee the correct performance of the different elements that make up this power circuit.

The wear that occurs in the power circuit, specifically that of the secondary circuit, has a very diverse origin and nature, as it occurs in different elements of the welding gun, as shown in Figure 2. The different wears that may occur are corrosion of the welding arms due to cooling water leaks, worn transformer pins, poor cooling or limescale, cracked arms caused by metal fatigue, clogged chilled braids, or thermal strip lamination breakage. All these types of wear cause both quality problems due to the instability of the process and production problems due to production stoppages caused by the need to repair the worn elements.



Figure 2. Typical wear in secondary circuit [15].

The detection of tool wear in different machinery and processes has been widely studied, as manufacturing industries tend to be increasingly automated, which makes it essential to detect events that may appear throughout the machinery process. These studies could be classified into two groups: those that use equipment additional to that of the production process and those that are based solely on the data acquired from the machine. As an example of the sensor-based tool wear monitoring, Gonçalves et al. [16] proposed a wear detection method in CNC machines by means of image analysis acquired during the production process. Similarly, Zhixiong et al. [17] showed a method for tool wear detection using audio signals together with machine learning, showing promising results for its real application in production lines. However, the main disadvantage of these methods is the need to purchase and install the additional equipment necessary to perform wear monitoring.

Second, due to the increasing availability of production data in the industry, new research is focused on sensorless wear monitoring. This type of monitoring usually requires greater knowledge of the process and a higher cost of data processing. For example, Zhang et al. [18] showed a complete analysis of the operation of the milling machine and, based on the monitoring of the physical model, showed a method of detecting wear and tear of the machine. In the same way and from the knowledge of the production lines, Garcia et al. [19] presented a method for the detection of wear of mechanical elements of the production lines by means of the analysis of the time used by the mechanical element to carry out the assigned task.

However, despite the growing demand for solutions for real-time detection of machinery wear in the industry, the different studies carried out in the field of resistance welding do not propose a real solution for the detection of wear in welding guns. As previously mentioned, many studies show the influence of the parameters on the final quality of welding. Similarly, many studies focus on the influence of mechanical problems and weld

quality. In relation to the wear of the machine, the different studies have focused on the detection of the wear of the electrodes as these are a fundamental piece in the application of pressure and current to the welding point [20,21]. Nevertheless, at this time, there is no research that focuses its study on the detection of wear not only of the electrodes but of all the elements involved in the secondary circuit of the resistance welding gun.

Due to the absence of research on the determination of secondary wear in resistance welding guns, this gun variable cannot currently be monitored in real time. Consequently, for wear detection, welding guns are periodically inspected for signs of wear or damage. This can be performed visually, by looking for cracks, chips, or other signs of damage to the gun's components. Additionally, the gun's performance can be monitored over time to detect any changes that may indicate wear, such as a decrease in welding speed or accuracy, that is, once a consequence has already occurred in production. In some cases, it may be necessary to disassemble the gun and inspect its components more closely to detect wear.

Therefore, the main problem resides in the non-existence of an adequate method for the detection of wear in the secondary in the production lines, showing excessively high costs associated with its detection-repair. This leads to focusing the research on the search for a method capable of performing this monitoring of secondary wear automatically and efficiently.

2. Background and Objectives

In this section, studies carried out previously for the detection of secondary wear are presented first. These studies serve as a useful context and will serve as a starting point for this research. The objectives set out in our own research are presented below. These objectives are based on the research carried out previously and seek to solve the drawbacks of the previous solutions identified in these studies. In summary, this section addresses both the background of the research and the objectives that have been established in our study.

2.1. Previous Research

In previous investigations, a method for detecting problems in the secondary circuit of the welding guns was investigated by analysing the existing data in the welding timer (see [5]).

Starting from the existing data in the welding timer, it was verified that an increase in the variation in the wear conditions of the secondary had an influence on the control values of the welding timer. Specifically, the SMPS duty cycle history was analysed.

Based on the duty cycle analysis, it was observed that as the welding arm wear increased, the welding timer corrected the IGBT control signal values. Figure 3 shows the evolution of the duty cycle in a pistol that presents secondary wear problems. In the first period from weld point 0 to the point 350 approximately, the duty cycle values are stable. From this moment on, the value of the duty cycle tends to increase up to the welding point 550 where the fault occurs. After carrying out the repair, the value of the duty cycle decreases and returns to behaving stable. Therefore, it was determined that by analysing these values, it is possible to detect wear in the welding arms. After establishing this relationship, an initial alarm detection system based solely on real-time monitoring of the SMPS duty cycle was established. This alarm system bases detection on the interquartile range rule [22].

Consequently, the above methods fail to fully respond to the existing problem, leaving out of detection those cases in which the resistance that wears out is much lower than the global resistance of the secondary. This makes it necessary to continue these lines of research to improve the previous methods in order to achieve a total detection of secondary wear.

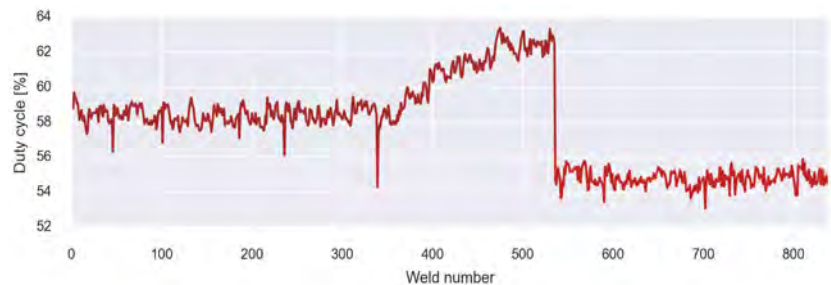


Figure 3. Analysis of secondary wear through duty cycle. The main problem with this method is that not all elements that wear cause a drastic increase in the overall resistance of the secondary, but sometimes, if the resistance of the arm is high, an increase in wear in a low-resistance element does not cause a noticeable increase in duty cycle, being difficult to detect it with the initial method.

2.2. Research Objectives

The main objective of this research is to improve the initial method for the early and effective detection of the wear of the secondary power circuit's elements of the welding guns.

As mentioned, as the secondary resistance increases, the duty cycle increases to correct the current reduction in the welding tips, but sometimes, the resistance of the welding arm is much greater than the welding resistance. This means that when severe wear is generated within the elements that are part of the welding resistance, this will not cause a drastic increase in the total resistance of the secondary. As a consequence, the duty cycle will not increase considerably, thus making it difficult to detect wear using the alarm method described above.

As a result, the objective of this research is to improve the wear detection system based on the theoretical basis of the previous investigation, assuming that when wear exists, the resistance of the element in poor condition increases. To do this, and in accordance with the disadvantages of the previous system, the analysis will no longer start from the duty cycle but from the circuit's own resistances, estimating them from the existing data in the welding timer, that is, from a virtual sensor of the resistances of the secondary.

3. Materials and Methods

3.1. Virtual Sensors for Resistance Estimation

A sensor can be defined as a device capable of measuring a physical magnitude and converting it into a signal that can be processed by the observer or instrument. Sensors can be divided into two categories: physical sensors and virtual sensors. Virtual sensors, also known as smart sensors or estimators, take readings from real physical sensors and calculate the outputs using some process models. This type of sensor is used due to the fact that they are flexible, cheap, and can perform measurements on elements that are difficult to measure due to their complexity [23].

In this particular case, the estimation of the resistance of the secondary circuit of the welding gun is sought by means of the existing data in the welding control, such as the current, the voltage of the electrodes, and the duty cycle of the IGBTs, as can be seen in Figure 4.

The secondary circuit can be schematically reduced into two resistances, one corresponding to the resistance of the welding gun arm and the different elements that compose it, and another corresponding to the resistance of the electrode. The electrode resistance can be easily obtained from Ohm's law, as the values of current and voltage drop are available in the welding timer. However, to obtain the resistance of the arm, only the value of the current that passes through the arm is available in the welding timer. Therefore, to obtain the value of the resistance of the welding gun arm, it is necessary to obtain first the other

variables necessary for the calculation, specifically, the value of the voltage drop in the welding arm.

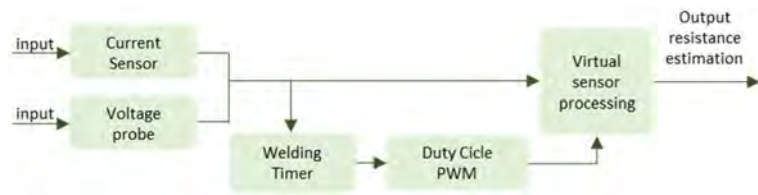


Figure 4. Conceptual summary of the virtual sensor for the estimation of the resistance of the secondary.

The secondary voltage can be calculated by decomposing the circuit in Figure 1 [24]. First, the rectifier converts the three-phase AC into a single-phase DC according to Equation (2):

$$V_{rectifier} = \frac{1}{\pi} \int_{\frac{\pi}{3}}^{\frac{2\pi}{3}} V_{line} \sin(\omega t) d(\omega t) = \frac{3}{\pi} V_{line} \quad (2)$$

Then, starting from the behaviour equations of the SMPS and together with Equation (2), the secondary voltage can be expressed as a function of the duty cycle as:

$$V_{sec} = 2 \left(\frac{N_s}{N_p} \right) V_{rectifier} \cdot D_{cycle} = \frac{6}{\pi} V_{line} \frac{D_{cycle}}{N} \quad (3)$$

Consequently, and starting from the variables obtained by the welding timer throughout the welding process, the value of the resistance of the welding arm can be estimated from Equation (4). This value of the resistance is estimated as it is assumed in this investigation that the power factors, the reactance, and the circuit losses that cause an error in the calculation of the resistance value remain stable within each particular welder. Therefore, it is considered unnecessary to calculate the exact value of the resistance.

$$R_{arm} = \frac{V_{arm}}{I_{sec}} = \left(\frac{\frac{6}{\pi} V_{line} \frac{D_{cycle}}{N} - V_{weld}}{I_{sec}} \right) \quad (4)$$

Summarizing, from the schematic of Figure 4 and Equation (4), Figure 5 of the operation of the virtual sensor is obtained. In Figure 5, it can be seen as a summary that the output signal of the system, that is, the resistance of the arm and the welding resistance, is calculated from the existing variables in the welding timer, current, welding voltage, and duty cycle.

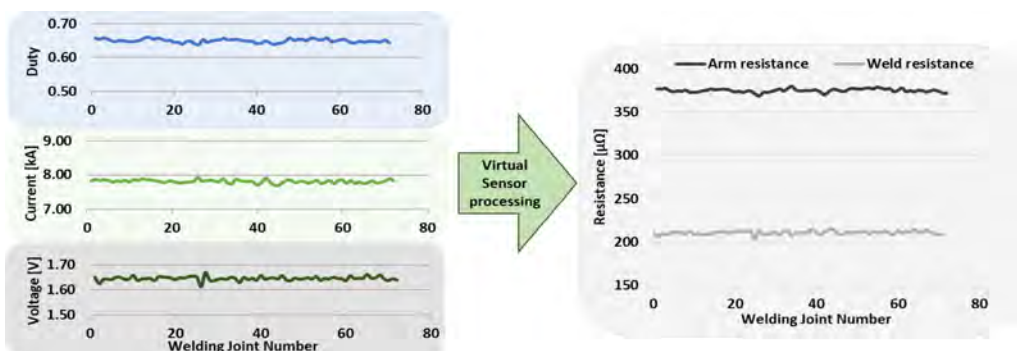


Figure 5. Virtual sensor operation. Input and output signals.

3.2. Incipient Wear Detection

Once the variables of the virtual sensor on which the analysis is going to be carried out have been obtained, a method for the detection of incipient wear for resistance welding guns is proposed.

In this case, it is intended to detect anomalies in the resistance data to detect incipient wear of the secondary circuit. An anomaly is defined as data that deviate from the normal behaviour of a series of data and, in this research, it is decided to use the analysis of the Mahalanobis distance for the detection of anomalies and, therefore, for the detection of wear in the secondary circuit.

The Mahalanobis distance (MD) is the measure of the effective distance between a point and a distribution [25], being effective in multivariate data. These result due to the use of the covariance matrix of variables to find the distance between data points and the centre, according to Equation (5). That is, Mahalanobis calculates the distance between point “P₁” and point “P₂” considering the standard deviation. MD, therefore, provides good results with outliers being considered multivariate. To find these outliers by MD, the distance between each point and the centre in n-dimensional data is calculated and outliers are found considering these distances. MD detects outliers based on the distribution pattern of data points [26,27].

$$D^2 = (X_{p1} - X_{p2})^T \cdot C^{-1} \cdot (X_{p1} - X_{p2}) \quad (5)$$

where C is the covariance matrix and X_{pn} represents coordinates of observations in n-dimensional space.

$$d(p, q) = \sqrt{(p_1 - q_1)^2 + (p_2 - q_2)^2 + \dots + (p_n - q_n)^2} \quad (6)$$

Euclidean distance, d , Equation (6), is also commonly used to find the distance between two points (p and q) in two- or higher-dimensional spaces [28]. However, MD uses the covariance matrix unlike Euclidean. This means that MD can be used with correlated variables even if the points do not have the same scale.

Figure 6 shows the resistance data of the arm and the welding obtained from the virtual sensor for a welding gun of a production line. These data are used to calculate both the Mahalanobis distance and the Euclidean distance. Once the distances have been calculated, pre-alarm and alarm thresholds are established. These anomaly thresholds are established bearing in mind the distribution of the calculated distance according to Equation (7).

$$\begin{aligned} Th_{pre-alarm} &= Q3 + 1.5 \cdot IDR \\ Th_{alarm} &= Q3 + 3 \cdot IDR \end{aligned} \quad (7)$$

where $Q3$ represents the value of the third quartile and IDR the difference between the first decile and the ninth decile.

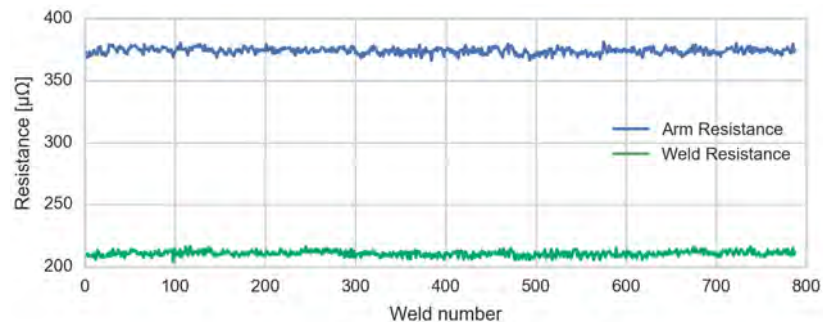


Figure 6. Virtual Sensor Resistance Output Values.

Figure 7 shows the calculated thresholds using the Euclidean distance (a) and the Mahalanobis distance (b). Comparing both results, in the case of the Euclidean distance, the thresholds are set in a circle, causing a poor fit with the data dispersion. However, using the Mahalanobis distance, and therefore, the correlation between both variables, the thresholds are set elliptically, which allows further adjustment of the thresholds to the correlated behaviour of the data [29].

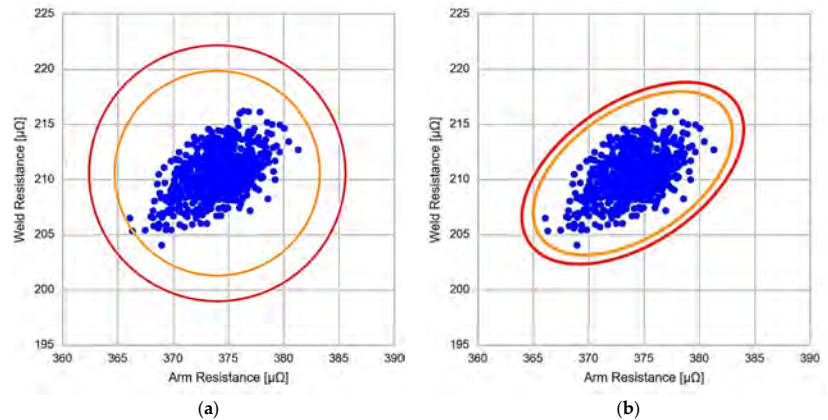


Figure 7. Threshold comparison. (a) Euclidean distance. (b) Mahalanobis distance.

Considering the result obtained from the thresholds, it is considered that for this study in which there is a correlation or linearity between both variables, the most appropriate method for detecting anomalies is MD. However, to validate this statement, the same welding gun in which an anomaly begins to appear is evaluated.

Figure 8 shows the previous data (blue dots) together with the new data corresponding to the appearance of wear in some mechanical element of the secondary circuit (brown dots).

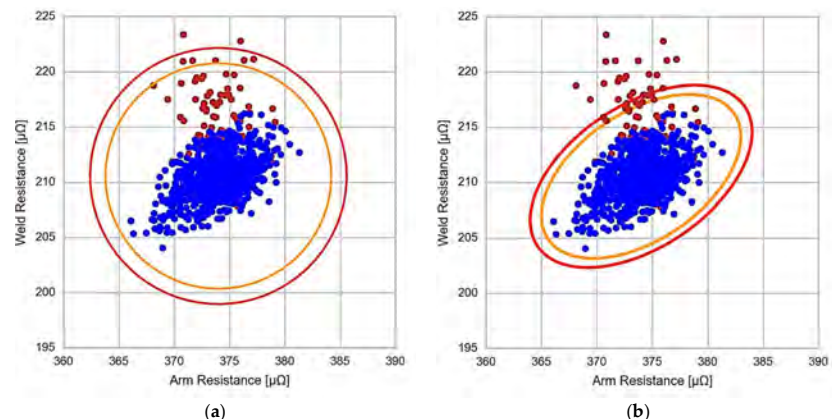


Figure 8. Incipient wear detection. (a) Euclidean distance. (b) Mahalanobis distance.

Analysing the data obtained in Figure 8, some conclusions can be drawn. First, in Figure 8a, which corresponds to the detection of anomalies by means of the Euclidean distance, despite the existence of anomalies, many of the data corresponding to the anomaly, brown points, are within the thresholds alarm and pre-alarm. However, a small number of points are above the thresholds. Therefore, this method is valid to detect anomalies but not in an incipient way, as it is not capable of detecting the first initial values of the anomaly.

On the other hand, Figure 8b shows the anomaly detection results using the Mahalanobis distance. From the results, it can be seen that many points are located outside the alarm and pre-alarm thresholds compared to the previous case. This behaviour suggests that the Mahalanobis distance method would be better for early anomaly detection. To conclude with the analysis of both methods, Figure 9 represents the average of minimum distances from each point with its closest alarm threshold for each of the methods and as a function of the multiplying factor of the inter-decile range of Equation (7). This value is used to determine which of the methods finds the anomaly earlier, or what is the same as the incipient wear of the secondary circuit.

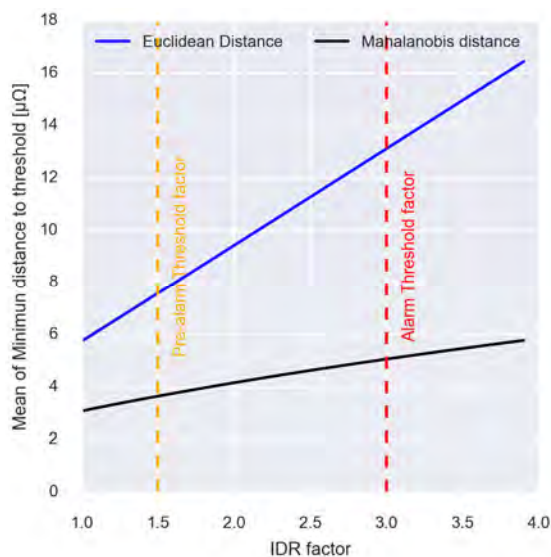


Figure 9. Comparison of the average minimum distance between the points and the closest threshold for the Euclidean distance and the Mahalanobis distance.

Several conclusions can be drawn from Figure 9. Throughout the different IDR multiplication factors that can be set for the calculation of the thresholds, the average minimum distance to the nearest threshold is lower by the Mahalanobis distance, which, therefore, results in a better fit of the thresholds to the existing data population. In the same way, it is observed that if an increase in the IDR multiplying factor is necessary to that established in Equation (7) to avoid false positives, in the case of the Euclidean distance, the values of the average minimum distance increase almost linearly with the increase in the factor, which increases the difficulty of early detection of the abnormality. Consequently, it is established that the most adequate method for the incipient detection of secondary wear is the one based on the Mahalanobis distance between the resistance of the welding arm and the welding resistance.

3.3. Wear Detection System

Once the method used for the detection of incipient wear has been established, a system is designed to apply the method autonomously not only to a welding gun but also to an indeterminate number of them. The detection system is mainly divided into three stages: calibration and obtaining of initial threshold, analysis of new incoming data, and recalibration.

Then, Algorithm 1 is followed for calibration. Current, voltage, and duty cycle values are obtained to calculate the arm resistance and welding resistance. Once the resistance values are obtained, the Mahalanobis distance is calculated, and the alarm and pre-alarm

thresholds are established by the Mahalanobis distance distribution (Figure 10) and according to Equation (7). These alarm and pre-alarm values are stored to be used in the analysis stage.

Algorithm 1: Threshold Calibration.

Input:

V_{weld} , I_{sec} and D_{cycle}

Output:

Al (Alarm Thershold), Pr (Prealarm Threshold), C

1. Calculate R_{arm} and R_{weld} resistance according to Equation (4).
 2. Calculation of the inverse covariance matrix of R_{arm} and R_{weld} .

$$C = \begin{bmatrix} Var(R_{arm}) & Cov(R_{arm}, R_{weld}) \\ Cov(R_{weld}, R_{arm}) & Var(R_{weld}) \end{bmatrix}$$
 3. Calculation of the Mahalanobis distance according to Equation (5).
 4. Determination of the alarm and pre-alarm thresholds based on the Mahalanobis distance distribution.
-

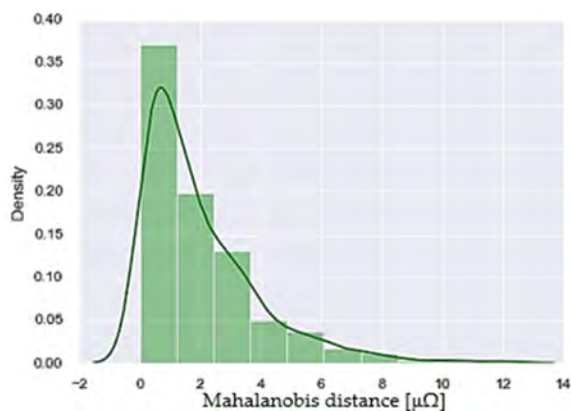


Figure 10. Mahalanobis distance distribution.

After establishing the pre-alarm and alarm values for each welding gun, Algorithm 2 is carried out for the analysis of anomalies for the new incoming data collected from the production line. This algorithm calculates the resistance values again and the Mahalanobis distance between both variables starting from the covariance matrix calculated by Algorithm 1 for each welding gun. Once the distance has been calculated, each of the welding points is evaluated with the alarm and pre-alarm thresholds.

Algorithm 2: Analysis of new incoming data.

Input:

$V_{weldnew}$, I_{secnew} , $D_{cyclenew}$, Al, Pr and C

Output:

Alarm/Prealarm warning

1. Calculate R_{arm} and R_{weld} resistance according to Equation (4).
 2. Calculation of the Mahalanobis distance (D) according to Equation (5) using the old covariance matrix (C).
 3. Determination of alarm/pre-alarm status:
 - If $D > Al$ then “Alarm”
 - If $D > Pr$ and $D < Al$ then “Pre-alarm”
-

Finally, to improve the detection method, a recalibration process is carried out after correcting the mechanical failure that caused the alarm of a certain welding gun. In addition, Algorithm 3 is executed periodically so that if the new data present thresholds lower than those previously calculated, they are updated. This makes it possible to better adjust the thresholds and detect wear earlier.

Algorithm 3: Recalibration after alarm.

Input:

$V_{\text{weld_after_alarm}}$, $I_{\text{sec_after_alarm}}$, $D_{\text{cycle_after_alarm}}$, Al , Pr and C

Output:

Al , Wn , C

1. Calculate R_{arm} and R_{weld} resistance according to Equation (4).
2. Calculation of the Mahalanobis distance (D) according to Equation (5) using the new covariance matrix (C).
3. Determination of the alarm and pre-alarm thresholds based on the Mahalanobis distance distribution,
4. Comparison between new and old threshold:

If $Al_{\text{new}} < Al$ and $Pr_{\text{new}} < Wn$ then:

$Al = Al_{\text{new}}$

$Pr = Pr_{\text{new}}$

As a summary, Figure 11 shows the operation of the algorithms mentioned above. Figure 11a shows the resistance values of the arm and the weld, while Figure 11b shows the values of the Mahalanobis distance between both variables. In the first place, the initial data are used to calculate the covariance matrix and the alarm thresholds (Algorithm 1). The data show a normal behaviour, without detecting any anomaly until approximately weld number 200. From this moment on, the data begin to experience a growing anomaly. This anomaly is detected by the system using Algorithm 2. After executing the appropriate maintenance operations, approximately at weld number 300, the alarm system is recalibrated with the new data, calculating the new covariance matrix and the new detection thresholds (Algorithm 3).

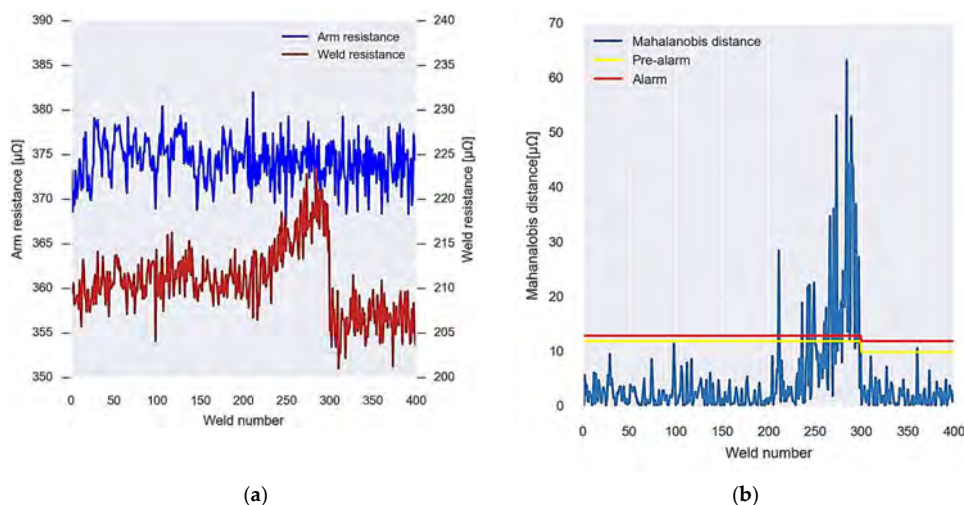


Figure 11. Graphic summary of the operation of the wear detection system algorithms. (a) Resistances obtained from the virtual sensor. (b) Calculated Mahalanobis distance and alarm and pre-alarm thresholds.

4. Results

The results section shows the results of the application of the proposed system in a real factory. This section presents the block diagram of the data collection system within a real factory, together with three success stories in which the virtual sensor and the proposed algorithms have been used to detect different types of anomalies in the processes of the factory. Each of these cases demonstrates the effectiveness of the system in detecting anomalies and its ability to be used in real production lines.

This system is designed to be implemented in the manufacturing industry, specifically, its operation is tested in an automotive production factory. The data collection system is presented in the block diagram of Figure 12. Each of the welding guns collects current, welding voltage, and duty cycle for each weld joint made, and these data are sent to the base welding data.

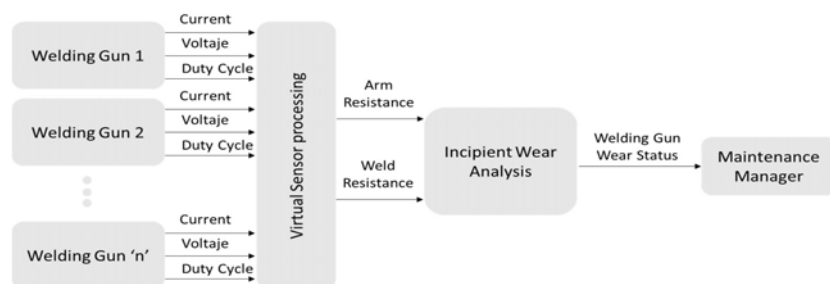


Figure 12. Flow diagram of the operation of the incipient wear detection system in welding guns.

The data from the welding database goes through the virtual sensor processing in order to obtain the resistance values. Once the resistances are calculated, they are stored in the analysis database. To reduce the number of data stored in the database, the average resistance data between milling cycles are analysed.

The data from the analysis database are used to calculate the alarm and pre-alarm thresholds, as shown in the previous section. Finally, once the thresholds have been established, the new data are analysed, the wear status of the secondary of each of the welding guns is labelled, and an alert message is sent to the operator in charge of each of the analysed equipment.

In total, this system has been tested on six hundred and fifty different welding guns. The welding guns analysed are of the MFDC type, differing in two types of pressure application, either by a pneumatic cylinder or by a servomotor.

The results shown below are extracted from the six hundred and fifty welding guns analysed; specifically, three real cases of welding guns installed in production lines that have detected wear are presented. These three results show the total number of patterns that can occur in welding guns: increase in welding arm resistance, increase in welding resistance, and increase in both resistances.

4.1. Gun 1: Welding Arm Wear

In this section, the results of the calibration of welding gun 1 are presented following the first calibration algorithm shown in the previous section. Figure 13 shows the resistance data of the arm and the welding of the gun used for calibration; in total, 200 welding points made by that welding gun are used. In this way, the dynamic behaviour of the process is considered, as well as the own variations due to the wear of the capsules and the change of the same. The resistance of the arm has an average value of $340\ \mu\Omega$, while the resistance of the weld has an average value of $160\ \mu\Omega$.

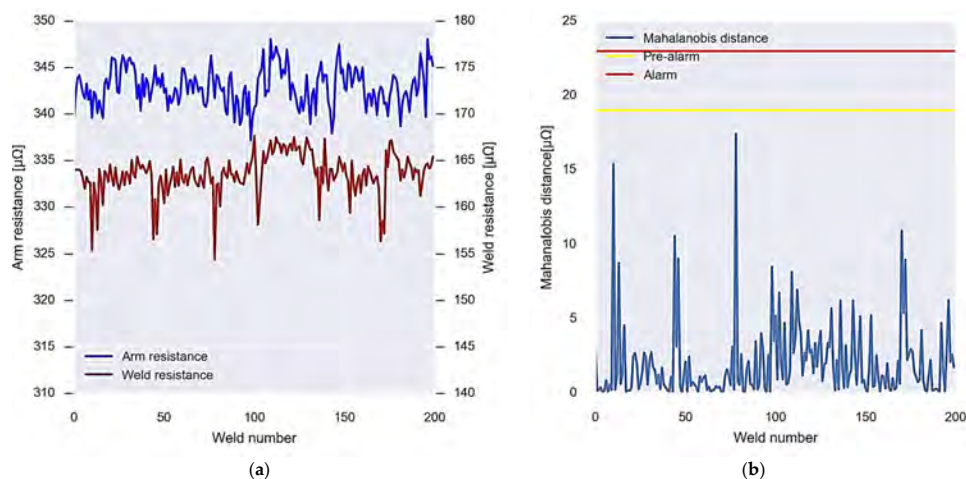


Figure 13. Operation of the initial calibration algorithm for gun 1. (a) Data of the resistances used for the calibration. (b) Calibration result, Mahalanobis distance, and alarm thresholds.

Finally, Figure 13 shows the thresholds obtained by means of the calibration algorithm as a function of the Mahalanobis distance between the two resistors. If the data are within the thresholds, the calibration is considered to have been successful. Otherwise, a new calibration must be performed.

Once the alarm and pre-alarm thresholds for gun 1 have been set, the new data coming from the welding gun virtual sensor are analysed in real time. Figure 14a shows the values of each of these arm and weld resistance data.

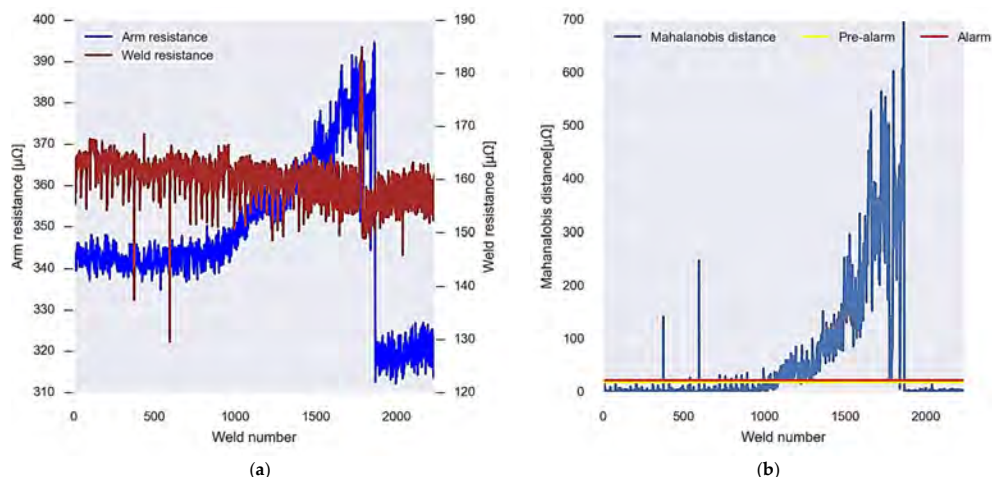


Figure 14. Gun 1 alarm system operation. (a) New incoming resistance data. (b) Analysis and recalibration of alarms.

For these data, the Mahalanobis distance is calculated considering the covariance matrix obtained in the calibration. Once the Mahalanobis distance is calculated, it is evaluated together with the set thresholds, and it is figured out whether it is an alarm or not. In this case, an alarm is experienced up to weld point 1800, where the values drop, and a recalibration is performed using Algorithm 3.

4.2. Gun 2: Welding Resistance Wear

As in the case of gun one, for gun two, a first calibration is carried out with 200 values. Figure 15a shows the resistance values of both the arm and the welding of the gun. The arm resistance has an average value of $350\ \mu\Omega$, while the welding resistance is $230\ \mu\Omega$.

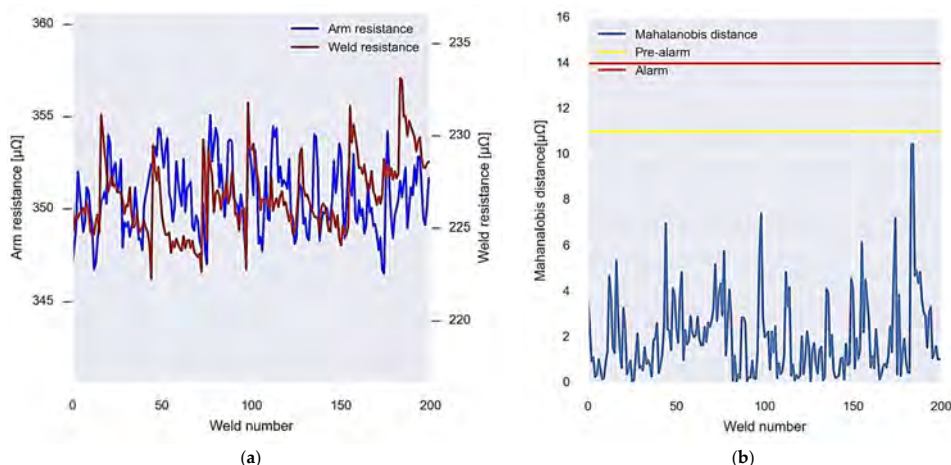


Figure 15. Operation of the first calibration algorithm for gun 2. (a) Data of the resistances used for the calibration. (b) Calibration result, Mahalanobis distance, and alarm thresholds.

As in the previous case, the Mahalanobis distance between the arm and weld resistance data is calculated and evaluated together with the alarm and pre-alarm thresholds set during calibration. In this case, no point is above the established thresholds, writing down that the calibration has been successful and that the gun is in good condition (Figure 15b).

In Figure 16a, the data can be seen in real time after the first calibration of welding gun 2. In this case, it can be seen how the resistance data have greater variability, but despite this, the Mahalanobis distance remains below the alarm thresholds up to the point where the alarm occurs (Figure 16b). In the same way as in the previous case, after the alarm period has elapsed, the recalibration of the algorithm is carried out.

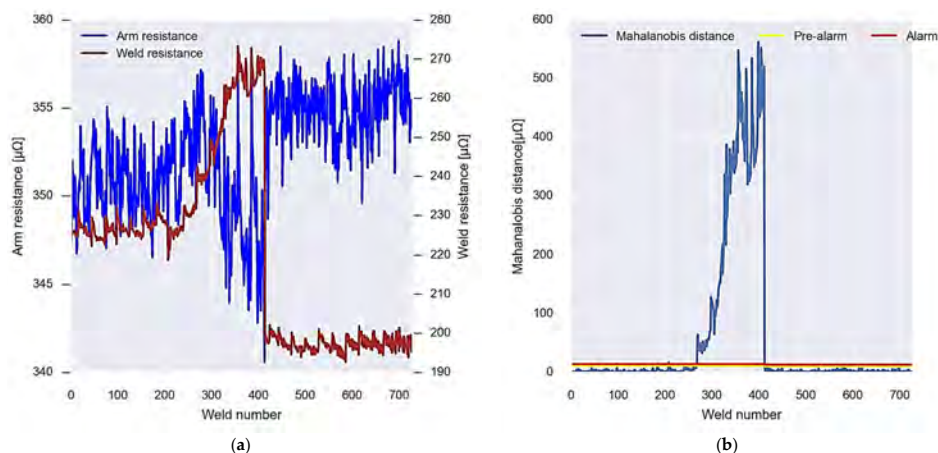


Figure 16. Gun 2 alarm system operation. (a) New incoming resistance data. (b) Analysis and re-calibration of alarms.

4.3. Gun 3: Welding Resistance and Arm Resistance Wear

Lastly, for gun 3, the same calibration is carried out as in the two previous cases, taking the initial 200 values of resistance of the arm and welding (Figure 17a). These values allow you to calculate your covariance matrix and the alarm and pre-alarm thresholds (Figure 17b).

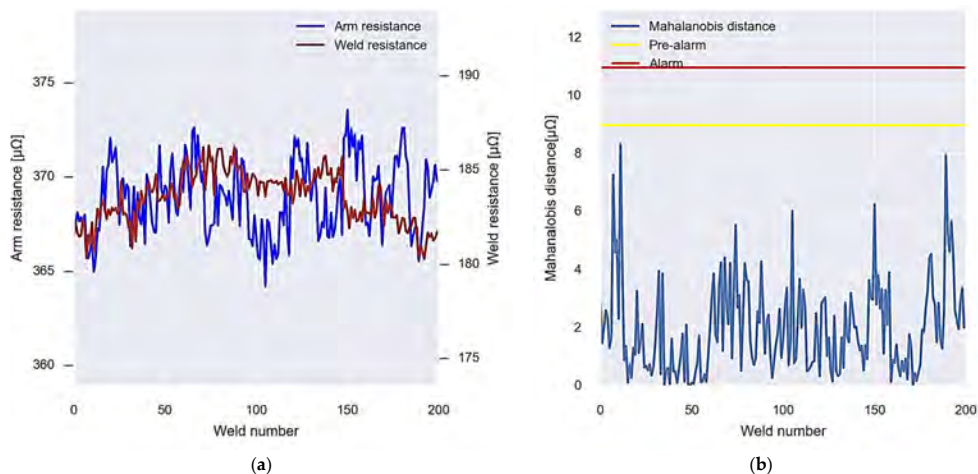


Figure 17. Operation of the first calibration algorithm for gun 3. (a) Data of the resistances used for the calibration. (b) Calibration result, Mahalanobis distance, and alarm thresholds.

In the same way, this welding gun presents an evolution in which the Mahalanobis distance data between the resistors exceed the thresholds defined by the calibration. Figure 18a shows the evolution of the resistance values of the arm and welding resistance after carrying out the initial calibration. In this case, around weld point 250, it is first exceeded; once the fault is repaired, the Mahalanobis distance is recalibrated to return to values above the alarm thresholds; after weld point 100, the alarm threshold is exceeded again, without observing any type of repair (Figure 18b).

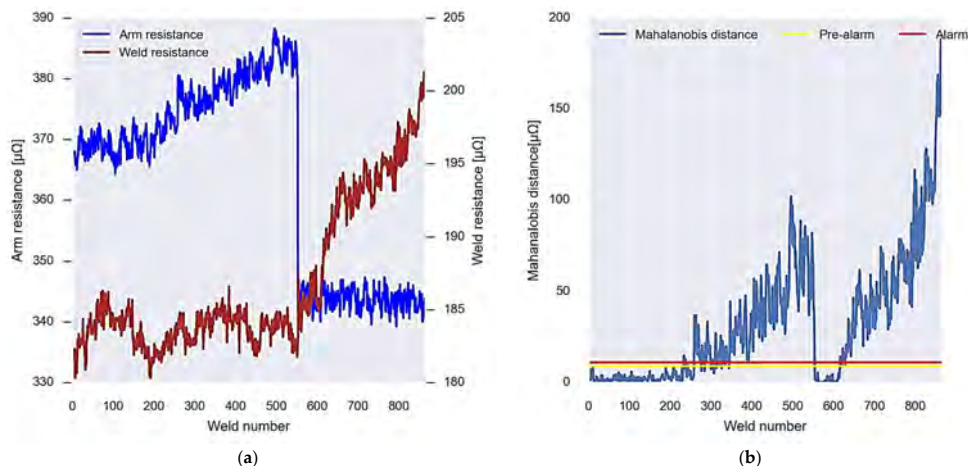


Figure 18. Gun 3 alarm system operation. (a) New incoming resistance data. (b) Analysis and recalibration of alarms.

5. Analysis and Discussion of Results

The data obtained by the virtual sensor for gun 1 show that after having performed the calibration based on the Mahalanobis distance and setting the behaviour thresholds, an alarm is produced around point 1000 as the data exceed the established thresholds, both alarm and pre-alarm. The distance between the arm strength data and the weld continues to increase until the defect repair is performed around weld point 1800 (Figure 14).

After the repair, Algorithm 3 is carried out, which recalculates the covariance matrix and the new alarm and pre-alarm thresholds. Observing the evolution of the resistance of the arm and the resistance of the welding in the figure, it can be determined that this alarm is caused by the resistance of the welding arm and, therefore, wear will occur in the copper strips, in the connections of the transformer, or in the connecting bolts of the arms.

After the system sent the alarm and in order to repair the existing defect, the operators carried out a visual inspection of the welding gun to carry out the repair and verified that the copper strip was in poor condition. The strapping pins were burned, and the sheets had started to break, causing an exponential increase in resistance (Figure 19). This explains the increase in the Mahalanobis distance seen in the data and the generation of the alarm.



Figure 19. Real case of detection-worn copper strip. Cut sheets.

If the data obtained for gun 2 is observed (Figure 16), it can be seen that an alarm occurs at weld point 250. This is because the Mahalanobis distance data exceed the established thresholds. This situation is maintained until weld point 400, where a repair of the defect is performed. Analysing Figure 16, it can be seen that the increase in Mahalanobis distance is related to the increase in weld resistance. This suggests that the worn items are the electrodes, electrode holders, or hardware in this section of the welding gun. Therefore, repair should focus on these components to correct wear and reduce the Mahalanobis distance. After the repair of the worn element, a recalibration of the welding gun wear detection algorithm is performed to adjust and reduce the Mahalanobis distance. As a result, the data return to values below the alarm and pre-alarm thresholds.

Finally, the case of gun 3 (Figure 17) shows two different types of alarm. In the first place, it is observed that from weld point 250 to 550, the Mahalanobis distance data are above the alarm and pre-alarm thresholds due to the increase in the resistance of the arms. After this, a recalibration of the wear detection algorithm is performed and the data return to normal. However, around weld point 650, the Mahalanobis distance again exceeds the thresholds, but this time due to weld resistance. In this case, it is seen that the data continue to continuously increase without any repair or recalibration of the algorithm being performed.

In summary, the three cases analysed show the effectiveness of the welding gun wear detection system in real time. In the case of gun 1, the alarm occurs due to the increase in the resistance of the arms, which indicates that the wear occurs in the arms, the copper straps, the screws, the transformer terminals, etc. In the case of gun 2, an alarm occurs due to increased welding resistance, indicating that wear is occurring on the electrodes, electrode holders, or hardware in this section of the welding gun. In the case of gun 3, two different alarms are produced due to different causes of wear, both on the arm and on the

welding resistance. In short, these cases prove the system's ability to detect incipient wear in welding guns and to send alarms to operators so that they can intervene promptly and prevent welding gun failures and weld quality problems.

6. Conclusions

This article presents a system to detect the incipient wear of welding guns in real time. The main objective of this system is to improve efficiency and quality in the welding process by detecting early wear on the welding guns and allowing operators to intervene in a timely manner.

To achieve this goal, the system uses a virtual sensor that converts current, voltage, and duty cycle signals into arm resistance and weld resistance values. Then, the Mahalanobis distance between both resistors is calculated and, based on those values, sends alarms to the operators.

The system was tested in a real study in a car manufacturing factory in which 650 welding guns were tested. The results showed that the system is capable of accurately and opportunely detecting incipient wear both in the arms of the gun and in the part in charge of welding (electrodes, electrode holders, etc.).

Furthermore, the system has several advantages compared to other wear detection methods. In the first place, it is not based on visual inspections or on measurements carried out by operators, so it is not necessary to have personnel in charge of carrying out these actions. In addition, it is based on accessible data, which makes it easier to implement in factories. Secondly, it makes it possible to detect wear in real time, which makes it possible to intervene before failures occur in the welding gun, unlike current systems based on periodic maintenance.

The main disadvantage present in the proposed method is the need to have to recalculate the covariance matrices for each welding gun for both Algorithm 1 and Algorithm 3. This increases the computational cost and increases the probability of system execution failure due to, for example, the covariance matrix not being reversible. In this research, a comparison has been made between two different methods for calculating the distances between the resistors; however, it would be necessary to make a comparison with other, different methods to establish to a greater extent which ones present a more adequate behaviour for the detection of the secondary wear.

In short, this innovative system is an efficient and accurate way to detect incipient wear on welding guns. It can improve efficiency and quality in the welding process and has several advantages compared to other wear detection methods.

Author Contributions: Conceptualization, D.I.; methodology, D.I., J.S. and J.M.; software, D.I.; validation, D.I. and E.G.; formal analysis, D.I., J.S. and J.M.; investigation, D.I.; resources, E.G., J.S. and J.M.; data curation, D.I.; writing—original draft preparation, D.I.; writing—review and editing, D.I., E.G., J.S. and J.M.; visualization, D.I.; supervision, E.G., J.S. and J.M.; project administration, E.G., J.S. and J.M.; funding acquisition, E.G., J.S. and J.M. All authors have read and agreed to the published version of the manuscript.

Funding: This research received no external funding.

Institutional Review Board Statement: Not applicable.

Informed Consent Statement: Not applicable.

Data Availability Statement: Not applicable.

Acknowledgments: The authors thank Ford España S.A. and, in particular, the Almussafes Factory for their support in the present investigation. Likewise, the authors express their greatest gratitude to the “Fundación para el desarrollo y la innovación” (FDI) together with Generalitat Valenciana for supporting this research.

Conflicts of Interest: The authors declare no conflict of interest.

References

1. RWMA. *Resistance Welding Manual*, 4th ed.; Resistance Welder Manufacturer's Association: Philadelphia, PA, USA, 1989.
2. Banga, H.K.; Kalra, P.; Kumar, R.; Singh, S.; Pruncu, C.I. Optimization of the cycle time of robotics resistance spot welding for automotive applications. *J. Adv. Manuf. Process.* **2021**, *3*, e10084. [\[CrossRef\]](#)
3. Su, Z.W.; Xia, Y.J.; Shen, Y.; Li, Y.B. A novel real-time measurement method for dynamic resistance signal in medium frequency DC resistance spot welding. *Meas. Sci. Technol.* **2020**, *31*, 055011. [\[CrossRef\]](#)
4. Li, Y.B.; Lin, Z.; Hu, S.; Chen, G.L. Numerical analysis of magnetic fluid dynamics behaviors during resistance spot welding. *J. Appl. Phys.* **2007**, *101*, 053506. [\[CrossRef\]](#)
5. Wohner, M.; Mitzschke, N.; Jüttner, S. Resistance spot welding with variable electrode force—Development and benefit of a force profile to extend the weldability of 22MnB5+AS150. *Weld. World* **2020**, *65*, 105–117. [\[CrossRef\]](#)
6. Yu, J. Adaptive resistance spot welding process that reduces the shunting effect for automotive high-strength steels. *Metals* **2018**, *8*, 775. [\[CrossRef\]](#)
7. Xing, B.; Yan, S.; Zhou, H.; Chen, H.; Qin, Q.H. Qualitative and quantitative analysis of misaligned electrode degradation when welding galvanized steel. *Int. J. Adv. Manuf. Technol.* **2018**, *97*, 629–640. [\[CrossRef\]](#)
8. Wang, L.; Rong, Y. Review on processing stability, weld defects, finite element analysis, and field assisted welding of ultra-high-power laser (≥ 10 kW) welding. *Int. J. Hydromechatron.* **2022**, *5*, 167–190. [\[CrossRef\]](#)
9. Yu, J. New methods of resistance spot welding using reference waveforms of welding power. *Int. J. Precis. Eng. Manuf.* **2016**, *17*, 1313–1321. [\[CrossRef\]](#)
10. Zhou, K.; Cai, L. Online measuring power factor in AC resistance spot welding. *IEEE Trans. Ind. Electron.* **2014**, *61*, 575–582. [\[CrossRef\]](#)
11. Nagasathya, N.; Boopathy, S.R.; Santhakumari, A. MFDC—An energy efficient adaptive technology for welding of thin sheets. In Proceedings of the 2013 International Conference on Energy Efficient Technologies for Sustainability, Nagercoil, India, 10–12 April 2013; IEEE: Toulouse, France, 2013; pp. 901–906.
12. Zhou, K.; Yao, P. Review of Application of the Electrical Structure in Resistance Spot Welding. *IEEE Access* **2017**, *5*, 25741–25749. [\[CrossRef\]](#)
13. Arslan, S.; Tarimer, İ.; Güven, M.; Oy, S. A medium frequency transformer design for spot welding machine using sizing equation and finite element analysis. *Eng. Rev.* **2020**, *40*, 42–51. [\[CrossRef\]](#)
14. Hidoğlu, M.; Kahraman, U.; Kahraman, N. The effect of AC and MFDC resistance spot welding technology on mechanical properties of new generation automotive steels. *Pamukkale Üniversitesi Mühendislik Bilim. Derg.* **2021**, *27*, 465–471.
15. Ibáñez, D.; García, E.; Martos, J.; Soret, J. A Novel Real-Time Wear Detection System for the Secondary Circuit of Resistance Welding Guns. In Proceedings of the 19th International Conference on Informatics in Control, Automation and Robotics—ICINCO, Lisbon, Portugal, 14–16 July 2022; pp. 185–192, ISBN 978-989-758-585-2. ISSN 2184-2809. [\[CrossRef\]](#)
16. Lins, R.G.; de Araujo, P.R.M.; Corazzim, M. In-process machine vision monitoring of tool wear for Cyber-Physical Production Systems. *Robot. Comput. Integr. Manuf.* **2020**, *61*, 101859, ISSN 0736-5845. [\[CrossRef\]](#)
17. Li, Z.; Liu, R.; Wu, D. Data-driven smart manufacturing: Tool wear monitoring with audio signals and machine learning. *J. Manuf. Process.* **2019**, *48*, 66–76, ISSN 1526-6125. [\[CrossRef\]](#)
18. Zhang, X.; Gao, Y.; Guo, Z.; Zhang, W.; Yin, J.; Zhao, W. Physical model-based tool wear and breakage monitoring in milling process. *Mech. Syst. Signal Process.* **2023**, *184*, 109641. [\[CrossRef\]](#)
19. Garcia, E.; Montés, N.; Llopis, J.; Lacasa, A. Miniterm, a Novel Virtual Sensor for Predictive Maintenance for the Industry 4.0 Era. *Sensors* **2022**, *22*, 6222. [\[CrossRef\]](#) [\[PubMed\]](#)
20. Mathisizik, C.; Köberlin, D.; Heilmann, S.; Zschetzsch, J.; Füssel, U. General Approach for Inline Electrode Wear Monitoring at Resistance Spot Welding. *Processes* **2021**, *9*, 685. [\[CrossRef\]](#)
21. Panza, L.; De Maddis, M.; Spena, P.R. Use of electrode displacement signals for electrode degradation assessment in resistance spot welding. *J. Manuf. Process.* **2022**, *76*, 93–105. [\[CrossRef\]](#)
22. Vinutha, H.P.; Poornima, B.; Sagar, B.M. Detection of outliers using interquartile range technique from intrusion dataset. In *Information and Decision Sciences*; Springer: Singapore, 2018; pp. 511–518.
23. Liu, L.; Kuo, S.; Zhou, M. Virtual sensing techniques and their applications. In Proceedings of the 2009 International Conference on Networking, Sensing and Control, Okayama, Japan, 26–29 March 2009; pp. 31–36. [\[CrossRef\]](#)
24. Lee, Y.-S.; Martin, H.L. Chow, 7—Diode Rectifiers. In *Power Electronics Handbook*, 4th ed.; Rashid, M.H., Ed.; Butterworth-Heinemann: Woburn, MA, USA, 2018; pp. 177–208. ISBN 9780128114070. [\[CrossRef\]](#)
25. Mahalanobis, P.C. On the Generalised Distance in Statistics. *Proc. Natl. Inst. Sci. India* **1936**, *12*, 49–55.
26. De Maesschalck, R.; Jouan-Rimbaud, D.; Massart, D.L. The mahalanobis distance. *Chemom. Intell. Lab. Syst.* **2000**, *50*, 1–18. [\[CrossRef\]](#)
27. Ghorbani, H. Mahalanobis distance and its application for detecting multivariate outliers. *Facta Univ. Ser. Math. Inform.* **2019**, *34*, 583–595. [\[CrossRef\]](#)

28. Gower, J.C. Properties of Euclidean and non-Euclidean distance matrices. *Linear Algebra Its Appl.* **1985**, *67*, 81–97. [[CrossRef](#)]
29. Ahn, J.; Park, M.; Lee, H.-S.; Ahn, S.J.; Ji, S.-H.; Song, K.; Son, B.-S. Covariance effect analysis of similarity measurement methods for early construction cost estimation using case-based reasoning. *Autom. Constr.* **2017**, *81*, 254–266, ISSN 0926-5805. [[CrossRef](#)]

Disclaimer/Publisher’s Note: The statements, opinions and data contained in all publications are solely those of the individual author(s) and contributor(s) and not of MDPI and/or the editor(s). MDPI and/or the editor(s) disclaim responsibility for any injury to people or property resulting from any ideas, methods, instructions or products referred to in the content.

Chapter 6. CONCLUSION AND FUTURE WORKS

This chapter shows the conclusions derived from the lines of research carried out throughout this Ph.D. study. Subsequently, the possible lines of future research that arise from the findings obtained during this Ph.D. study are introduced.

6.1 CONCLUSION

Throughout this Ph.D. study, different lines of research have been developed, focused on the continuous monitoring of the different parameters that could affect the quality of welding. Specifically, the premise was that in production processes, a variation in machine conditions leads to an increase in problems with the quality of the final product. In the case of resistance welding, the welding guns are responsible for performing the welded joint. Therefore, the studies carried out focused on detecting and reducing variability in the process, avoiding wear, and detecting anomalies in behavior.

During the Ph.D. study, mainly three lines of research were developed to achieve the set goal of optimizing the resistance welding process. **Chapter 3** presents the first line of research, which focuses on reducing the variability that exists in the milling process, mainly causing problems in the quality of the weld point. This research presents a novel method for detecting milling problems and electrode wear using unsupervised clustering methods. Throughout the article, the relationship between the resistance data in series and the variation of the mechanical properties of the electrodes is described. Despite working with time series, feature extraction was carried out to reduce dimensionality, allowing for the reduction of the number of inputs for the clustering

algorithm. This also made it possible to scale the input data so that they were not influenced by the existing resistance differences in each welding gun. The main advances obtained from this research are: a method for detecting the relationship between welding variables and the milling state, an alarm system that establishes pre-alarm states and correct operation according to the clustering algorithm's output, providing a satisfactory response to the **S.O2**, and a data collection system on a welding line that allows real-time data analysis, both for this research and for the following lines of research. This line of research also allowed the first publication in high-impact scientific journals, as shown in the chapter.

The second line of research, presented in **Chapter 4**, also focused on detecting mechanical problems that generate quality problems and stops in the welding lines. Specifically, the second line of research aimed to detect the electrode alignment. Throughout the three articles presented in this chapter, the evolution of both the method and the device capable of applying the method in a real hard-welding line is seen. The three articles show the process followed from the initial idea to the final solution implemented in a real welding line.

This line of research succeeded in relating the alignment of the electrodes and the magnetic field generated by welding guns to detect mechanical defects in production lines of welded joints by resistance welding. The study found that electrode misalignment caused variations in the contact area and the magnetic field, which could be measured by a device capable of measuring the magnetic field. A reliable protocol was also proposed to send alarms through LoRa to the data analysis software, with alarm thresholds established to determine misalignment.

Overall, the article presents a real solution to the problem of misalignments in production lines, with a method for real-time detection and easy integration into the automotive industry, by fulfilling goals **S.O3** and **S.O4**.

. Additionally, it is highlighted that this proposed detection method represents an improvement over those currently based on vision, whether through observation by operators themselves or using artificial vision systems. This is because the proposed detection method has a lower implementation cost and is not influenced by the environmental dirt typical of the welding line. This makes this method more accurate and reliable, as it is based on the direct measurement of the magnetic field generated by the welding guns.

Finally, **Chapter 5** shows the last of the research lines, which seeks to detect another mechanical problem such as wear on the secondary circuit of the welding guns, i.e., wear on the arms of the welding gun. This line of research was divided into two phases, represented in the two published articles. In the first article, an effective method is presented for detecting wear on the secondary circuit of resistance welding guns, which can cause a decrease in weld quality and an increase in energy consumption in resistance welding processes. It has been demonstrated through electronic simulation how the relationship between current and control angle change is easily demonstrable. From this relationship, it has been assumed that if a history analysis of the data is carried out, an increase in wear on the welding circuit can be determined. This method has been applied in a real factory, adapting the study for data reduction and simplifying the analysis and sending of alarms to maintenance personnel. From the real data acquired on the production lines, it has been validated that this method is viable and reliable for detecting wear problems in welding lines through the analysis of the control of the change angle. As a continuation of this first article, the second article is presented as an improvement over the first. This article shows a system that uses a virtual sensor that converts current, voltage, and duty cycle signals into welding arm and resistance values. Then, the Mahalanobis distance between both resistances is calculated, and alarms are sent to the operators based on those values.

The system was tested in a real study in an automobile factory in which 650 welding guns were tested. The results showed that the system is capable of detecting incipient wear precisely and timely in both the arms of the gun and the part responsible for welding (electrodes, electrode holders, etc.), which allows to achieve the objective **S.O5**.

The main advantages obtained from this line of research presented in **Chapter 5** are that, in comparison with other wear detection methods, this method does not rely on visual inspections or measurements carried out by operators, so there is no need to have personnel responsible for carrying out these actions. Additionally, it is based on accessible data, which facilitates its implementation in factories. Secondly, it allows for real-time wear detection, which allows for intervention before welding gun failures occur, unlike current systems based on periodic maintenance.

In conclusion, this Ph.D. study presents three lines of research aimed at optimizing the resistance welding process by reducing variability and detecting mechanical problems that affect the quality of the final product. The first line of research focuses on reducing variability in the milling process by detecting milling problems and electrode wear using unsupervised clustering methods. The second line of research aims to detect electrode misalignment, and the third line of research focuses on detecting wear on the secondary circuit of resistance welding guns.

The main contributions of this Ph.D. study are the development of novel methods for detecting mechanical problems and reducing variability in the resistance welding process. These methods have been successfully applied in real-world settings and have resulted in improved quality of welded joints, reduced energy consumption, and increased efficiency. The proposed methods are based on accessible data, allowing for easy implementation in factories, and allow for real-time detection of mechanical problems, enabling intervention before welding gun failures occur. Overall, this Ph.D. study makes significant contributions to the field

of resistance welding and provides practical solutions to improve the quality and efficiency of production lines.

6.2 FUTURE WORKS

Similarly to conclusions, the future research stemming from this Ph.D. study can be split into the three research lines that have been conducted in this Ph.D. study.

Firstly, the research line presented in **Chapter 3** provides a method for condition monitoring of the milling process and weld wear based on existing data in real production lines. The proposed approach uses unsupervised clustering methods to group electrode wear by analyzing current and resistance data. This method has shown great potential in detecting milling defects and electrode wear, reducing quality problems, and providing a system for sending alarms based on the behavior of welding variables. However, there is still room for improvement in this research.

One of the limitations of this research is that the system is not yet capable of differentiating between types of faults. Different mechanical factors influence milling problems, such as worn blades, transformer secondary circuit problems, etc. Therefore, in future work, the objective should be to go from the cataloging of faults as alarm, pre-alarm, and correct status to a fault labeling system based on behavior pattern. This could help in the early detection of specific faults, which could then be addressed to improve the quality of welded joints.

Additionally, this investigation has used unsupervised learning methods due to the characteristics of the sample. However, in future work, it would be interesting to experiment with other analysis methods that could improve the detection system. Furthermore, it is necessary to continue evaluating the proposed system in real production lines to test its

effectiveness under different conditions. The system proposed offers an alarm system that establishes pre-alarm status and correct operation according to the output of the clustering algorithm. Nevertheless, future work should focus on developing a fault labeling system based on behavior pattern and experimenting with other analysis methods that could further improve the detection system.

In the second line of research, **Chapter 4**, promising results have been shown for detecting incipient wear of welding guns in real-time. However, there are still some areas for improvement that could be addressed in future work. One limitation of this system is that it assumes the welding gun is functioning correctly at the start of the welding process. However, sometimes the guns are already worn before the start of the process, which affects the system's accuracy. Investigating alternative ways of detecting the initial wear of welding guns, such as using additional sensors to measure the voltage across the gun, would be interesting for future work.

In this line of research, multivariable analysis has been conducted using the electrode resistance and arm resistance variables for wear detection. As future work, it would be interesting to separate the study of both resistances to focus on whether secondary wear occurs in the first or second resistance. This would reduce the maintenance time employed.

Lastly, while the system presented in this article is effective in detecting wear and anomalies in real-time, there is still room for improvement in terms of data analysis and management. For example, the system currently generates a high volume of data and requires significant computation, such as the need to calculate the covariance matrix for each case, which can be challenging to manage and analyze in real-time. Developing more advanced algorithms for analyzing and interpreting the data generated by the system could help operators make more informed decisions and prevent potential quality issues in the manufacturing process.

Regarding the third and final line of research described in **Chapter 5**, there are several future works based on the obtained results. The first one would be the validation and final implementation on a series of welding guns in production. This would allow to verify the final robustness of the method and begin with the analysis of the results.

From the magnetic field data obtained, it is expected to obtain not only whether it is misaligned or not, but also the degree and direction of misalignment. To achieve this, new algorithms will have to be developed that can perform this function.

Furthermore, since research shows in **Chapter 3** and **Chapter 4** have allowed for the collection of new data from the production process, a future research line would be to investigate whether an external sensor is necessary for measuring misalignment, as proposed in this research line , or if it is possible to use welding process variables together with misalignment sensor values to identify process variables that reflect the misalignment state, in order to develop a virtual misalignment sensor based on the variables obtained during the welding process.

Finally, all lines of research have been focused on obtaining the mechanical state of the welding gun to avoid an increase in quality problems. Each of these lines has made it possible to break down the barriers to obtaining and handling data from the welding process of welding controls. Therefore, it is considered that with the outputs obtained from each one of the lines and the data obtained from the welding process, it is possible to continue with an approach more focused on determining changes in the welding quality, since the state of the welding has been monitored, welding gun and the result of the welding variables after performing the spot welding.

REFERENCE

1. Hou, Z.; Kim, I.-S.; Wang, Y.; Li, C.; Chen, C. Finite element analysis for the mechanical features of resistance spot welding process. *J. Mater. Process. Technol.* 2007, 185, 160–165.
2. Huh, H.; Kang, W. Electrothermal analysis of electric resistance spot welding processes by a 3-D finite element method. *J. Mater. Process. Technol.* 1997, 63, 672–677.
3. Aravinthan, A.; Nachimani, C. Analysis of SpotWeld Growth on Mild and Stainless Steel. *Weld. J.* 2011, 90, 143–147.
4. Ighodaro, O.L.R., Biro, E. & Zhou, Y.N. Study and Applications of Dynamic Resistance Profiles During Resistance Spot Welding of Coated Hot-Stamping Steels. *Metall Mater Trans A* 48, 745–758 (2017).
5. Zhang, H., & Senkara, J. (2011). Resistance welding: fundamentals and applications. CRC press.
6. Podrżaj P., Polajnar J.D.I., and Kariz Z.: ‘Overview of resistance spot welding control’, *Sci. Technol. Welding Joining*, 2008, 13, (3), pp. 215–224
7. Nagasathya, N.; Boopathy, S.R.; Santhakumari, A. MFDC-An energy efficient adaptive technology for welding of thin sheets. In *Proceedings of the 2013 International Conference on Energy Efficient Technologies for Sustainability*, Nagercoil, India, 10–12 April 2013; IEEE: Toulouse, France, 2013; pp. 901–906.
8. Arslan, S.; Tarimer, İ.; Güven, M.; Oy, S. A medium frequency transformer design for spot welding machine using sizing equation and finite element analysis. *Eng. Rev.* 2020, 40, 42–51.
9. Wohnner, M., Mitzschke, N. & Jüttner, S. Resistance spot welding with variable electrode force—development and benefit of a force profile to extend the weldability of 22MnB5+AS150. *Weld World* 65, 105–117 (2021).
10. H.T. Sun, X.M. Lai, Y.S. Zhang & J. Shen (2007) Effect of variable electrode force on weld quality in resistance spot welding, *Science and Technology of Welding and Joining*, 12:8, 718-724,
11. Tang H, Hou W, Hu SJ. Forging force in resistance spot welding. *Proceedings of the Institution of Mechanical Engineers, Part B: Journal of Engineering Manufacture.* 2002;216(7):957-968.
12. Zhang, Y. S., Wang, H., Chen, G. L., & Zhang, X. Q. (2007). Monitoring and intelligent control of electrode wear based on a measured electrode displacement curve in resistance spot welding. *Measurement Science and Technology*, 18(3), 867.

13. Chen, Z., & Zhou, Y. H. (2006). Surface modification of resistance welding electrode by electro-spark deposited composite coatings: Part I. Coating characterization. *Surface and coatings technology*, 201(3-4), 1503-1510.
14. X.Q. Zhang, G.L. Chen, Y.S. Zhang, Characteristics of electrode wear in resistance spot welding dual-phase steels, *Materials & Design*, Volume 29, Issue 1, 2008, Pages 279-283, ISSN 0261-3069.
15. Panza, L., De Maddis, M., & Spena, P. R. (2022). Use of electrode displacement signals for electrode degradation assessment in resistance spot welding. *Journal of Manufacturing Processes*, 76, 93-105.
16. Nielsen, C. V., Zhang, W., Perret, W., Martins, P. A., & Bay, N. (2015). Three-dimensional simulations of resistance spot welding. *Proceedings of the Institution of Mechanical Engineers, Part D: Journal of Automobile Engineering*, 229(7), 885-897.
17. Charde, N. (2012). Effects of Electrode Deformation on Carbon Steel Weld Geometry of Resistance Spot Welding. *Original Research Journal*, 1(5), 5-12.
18. Charde, N. (2014). Exploring the electrodes alignment and mushrooming effects on weld geometry of dissimilar steels during the spot welding process. *Sadhana*, 39(6), 1563-1572.
19. Li, Y., Tang, G., Ma, Y., Shuangyu, L., & Ren, T. (2019). An electrode misalignment inspection system for resistance spot welding based on image processing technology. *Measur. Sci. Technol*, 30, 075401.
20. Xing, B., Yan, S., Zhou, H., Chen, H., & Qin, Q. H. (2018). Qualitative and quantitative analysis of misaligned electrode degradation when welding galvanized steel. *The International Journal of Advanced Manufacturing Technology*, 97, 629-640.
21. Zhao, D., Bezgans, Y., Wang, Y., Du, W., & Vdonin, N. (2021). Research on the correlation between dynamic resistance and quality estimation of resistance spot welding. *Measurement*, 168, 108299.
22. Zhou, B., Pychynski, T., Reischl, M., Kharlamov, E., & Mikut, R. (2022). Machine learning with domain knowledge for predictive quality monitoring in resistance spot welding. *Journal of Intelligent Manufacturing*, 33(4), 1139-1163.
23. Dai, W., Li, D., Zheng, Y., Wang, D., Tang, D., Wang, H., & Peng, Y. (2022). Online quality inspection of resistance spot welding for automotive production lines. *Journal of Manufacturing Systems*, 63, 354-369.
24. Stavropoulos, P., Sabatakakis, K., Papacharalampopoulos, A., & Mourtzis, D. (2021). Infrared (IR) quality assessment of robotized resistance spot welding based on machine learning. *The International*

- Journal of Advanced Manufacturing Technology*, 1-22
25. Jiuping Xu, Lei Xu, Chapter Eight - Maintenance Decision Support, Editor(s): Jiuping Xu, Lei Xu, Integrated System Health Management, Academic Press, 2017, Pages 377-432, ISBN 9780128122075, <https://doi.org/10.1016/B978-0-12-812207-5.00008-0>.
 26. De Jonge, B., & Scarf, P. A. (2020). A review on maintenance optimization. *European journal of operational research*, 285(3), 805-824.
 27. Zonta, T., Da Costa, C. A., da Rosa Righi, R., de Lima, M. J., da Trindade, E. S., & Li, G. P. (2020). Predictive maintenance in the Industry 4.0: A systematic literature review. *Computers & Industrial Engineering*, 150, 106889.
 28. Silvestri, L., Forcina, A., Introna, V., Santolamazza, A., & Cesarotti, V. (2020). Maintenance transformation through Industry 4.0 technologies: A systematic literature review. *Computers in Industry*, 123, 103335.
 29. Pinciroli, L., Baraldi, P., & Zio, E. (2023). Maintenance optimization in Industry 4.0. *Reliability Engineering & System Safety*, 109204.
 30. Pichika, S. N., Yadav, R., Rajasekharan, S. G., Praveen, H. M., & Inturi, V. (2022). Optimal sensor placement for identifying multi-component failures in a wind turbine gearbox using integrated condition monitoring scheme. *Applied Acoustics*, 187, 108505.
 31. Wu, J., Zi, Y., Ma, H., Wu, Y., & Xue, X. (2022). Optimal Placement of Sensors Based on Data Fusion for Condition Monitoring of Pulley Group under Speed Variation Condition. *Machines*, 10(2), 148.
 32. Sharma, A., Verma, P., Choudhary, A., Mathew, L., & Chatterji, S. (2021). Application of wavelet analysis in condition monitoring of induction motors. In *Advances in Electromechanical Technologies: Select Proceedings of TEMT 2019* (pp. 795-807). Springer Singapore.
 33. Janssen, L. A. L., & Arteaga, I. L. (2020). Data processing and augmentation of acoustic array signals for fault detection with machine learning. *Journal of Sound and Vibration*, 483, 115483.
 34. Alqatawneh, I. (2021). Automatic Data Processing Framework Based Deep Neural Network for Condition Monitoring (Doctoral dissertation, University of Huddersfield).
 35. Kudelina, K., Asad, B., Vaimann, T., Rassölkin, A., Kallaste, A., & Khang, H. V. (2021). Methods of condition monitoring and fault detection for electrical machines. *Energies*, 14(22), 7459.
 36. Singh, L., Alam, A., Kumar, K. V., Kumar, D., Kumar, P., & Jaffery, Z. A. (2021). Design of thermal imaging-based health condition monitoring and early fault detection technique for porcelain insulators using Machine learning. *Environmental Technology & Innovation*, 24, 102000.

-
37. Mawson, V. J., & Hughes, B. R. (2020). Deep learning techniques for energy forecasting and condition monitoring in the manufacturing sector. *Energy and Buildings*, 217, 109966.
 38. Mohanraj, T., Yerchuru, J., Krishnan, H., Aravind, R. N., & Yameni, R. (2021). Development of tool condition monitoring system in end milling process using wavelet features and Hoelder's exponent with machine learning algorithms. *Measurement*, 173, 108671.